Study on Catalytic Depolymerization of Lignin Using Ionic Liquid and Solid Acid -Supported Metal Catalysts

2020.3

Graduate School of Bio-Applications and Systems Engineering

Tokyo University of Agriculture and Technology

Xiuhui Wang

Contents

Chapter 1

General Introduction

1.1 General overview

With the depletion of non-renewable fossil resources and the growing interest in renewable resources, the research of using renewable biomass materials to replace petrochemical products has attracted wide attention in the past decades [1]. Most of the researches are devoted to the conversion of cellulose and hemicellulose into sugar to produce biofuel [2]. However, as the second major component of biomass for sustainable utilization, the most common way to utilize lignin is to burn directly to obtain heat source or to utilize it directly without any treatment. Compared with cellulose and hemicellulose, lignin is the most abundant renewable resource containing aromatic rings, which is highly crosslinked by three monomers (coumaryl, coniferyl and sinapyl alcohols) [3]. Therefore, the conversion of lignin into aromatic ring chemicals provides a great possibility for the efficient utilization of lignin.

In order to improve the utilization of biomass, it generally utilized by degradation or hydrolysis, such as the preparation of hexose and pentose from cellulose and hemicellulose [4-5]. Similarly, due to the complex structure of lignin, to make better use of its aromatic ring structures, it is necessary to effectively degrade lignin, such as acidolysis, pyrolysis, photodegradation, microbial degradation and so on, to obtain low molecular aromatic chemicals and biomass oils [6-8]. However, most of the degradation methods of lignin are harsh, which is not conducive to environmental protection, and the research on the reaction medium, catalyst selection and mechanism of lignin degradation is still immature. Therefore, how to degrade lignin efficiently in a mild and environmentally friendly way has become the key to value application of lignin.

1.2 Physicochemical properties and structure of lignin

1.2.1 Physicochemical properties of lignin

Lignin, as one of the most promising renewable sources to obtain phenolic molecules in nature, is a typical amorphous polymer. The glass transition temperature (T_g) of lignin is not easy to measure due to its chemical structure non-uniformity and the broad molecular weight distribution caused by the separation method. In general, the T_g of lignin depends on its molecular weight, in addition, it is also affected by the degree of condensation (carbon-carbon bond number), the content of casein radical and methoxy (syringyl). Generally, the T_g of hardwood lignin is usually lower than that of softwood lignin [9], which may be due to the softwood lignin has more condensate structure and higher phenolic hydroxyl content than those of in hardwood, which limits the molecular movement through strong intermolecular hydrogen bonds [10].

The lignin macromolecules form a large number of intramolecular and intermolecular amino bonds due to the presence of hydroxyl groups. The solubility of lignin in solvents is related to the properties of lignin and the solubility parameters and hydrogen bond energy of the solvents used [11]. In addition, the difference of lignin solubility is also related to its separation method.

The molecular weight of lignin has a wide range, which is caused by different plant species and separation methods. For example, the molecular weight of sulfate lignin extracted by Dong et al. [12] was as high as 42900. Liang et al. [13] obtained a molecular weight of only 450-2250 from lignin extracted from wood. In addition, the molecular weight of lignin is also related to the determination methods (such as size exclusion chromatography, gel permeation chromatography, light scattering method).

1.2.2 The structure of lignin

Lignin was first discovered by agronomist P. Payen in 1838, and later successfully separated from plants by F. Schulze and named Lignin. In the world, lignin reserves are very high, and about 150 billion tons of lignin are formed by plants every year [14]. Like cellulose and hemicellulose, lignin, accounting for 15-35 wt. %, is a major component of lignocellulosic biomass [15]. Specifically, lignin is a highly complicated cross-linked three-dimensional amorphous resin that surrounds the outer layer of polysaccharide fibers, protecting the inside carbohydrates and proteins from microbial attack and water damage while providing structural integrity and rigidity [16,17]. Typically, three monomers are present in lignin, namely, *p*-coumaryl alcohol, coniferyl alcohol, and sinapyl alcohol as shown in Figure 1.1. These monolignols further generate corresponding phenyl paranoids, *p*-hydroxyphenyl (H), guaiacyl (G), and syringyl (S) lignin subunits, in which they are incorporated into lignin macromolecules [18].During the biosynthesis of lignin, various cross-linkages (e.g., β-O-4, α-O-4, 4-O-5) and C−C interunit linkages (e.g., β-1, β-5, β-β, 5-5) are formed. Among them, the β-O-4 linkage represents the most abundant one, constituting approximately 50−65 % of the structure as shown in Figures 1.2 and 1.3 [19,20].

Table 1.1 lists the proportion of main links between phenylpropane units in softwood and hardwood lignin. As the table 1.1 shows that the phenylpropane units mainly linked by β-O-4 bonds in both softwood and hardwood lignin. This particular type of link accounts for about 48 % - 60 % of the total links in lignin. In addition, about 10 % - 15 % of the ether bonds exist in a type of α-O-4 and 4-O-5 linkages. Since the lignin of softwood is mainly composed of guaiacyl phenylpropane unit (Figure. 1.1) [21], and there are no substituents at the 5th position of benzene ring in guaiacyl phenylpropane unit, it will be polymerized with adjacent phenylpropane unit through the 5th position, resulting in the formation of β-5 and 5-5 type links. Hardwood lignin contains more

syringyl phenylpropane units, and the 3 and 5 positions of the benzene ring in the phenylpropane unit are replaced by methoxy groups, which reduces the formation of β-5 and 5-5 linkages, which explains why the content of β-5 and 5-5 type links in hardwood lignin is lower than that in softwood lignin. Due to hardwood lignin is relatively lack of multi-branched chain structure caused by 5-5 type linkage, hardwood lignin has better linear structure [21]. Based on the above discussion, if the various linkages widely existing between the lignin phenylpropane units can be broken, especially the β-O-4 type chain which accounts for a large proportion, lignin can be effectively depolymerized. And lignin with higher molecular weight could be converted into aromatic compounds with smaller molecular weight, and also release cellulose and hemicellulose components in lignocellulose, which can be used as raw materials for biomass processing [22].

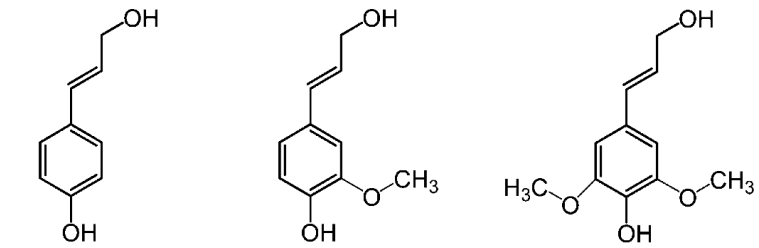

Figure 1.1. Chemical structures of the three monolignols of lignin.

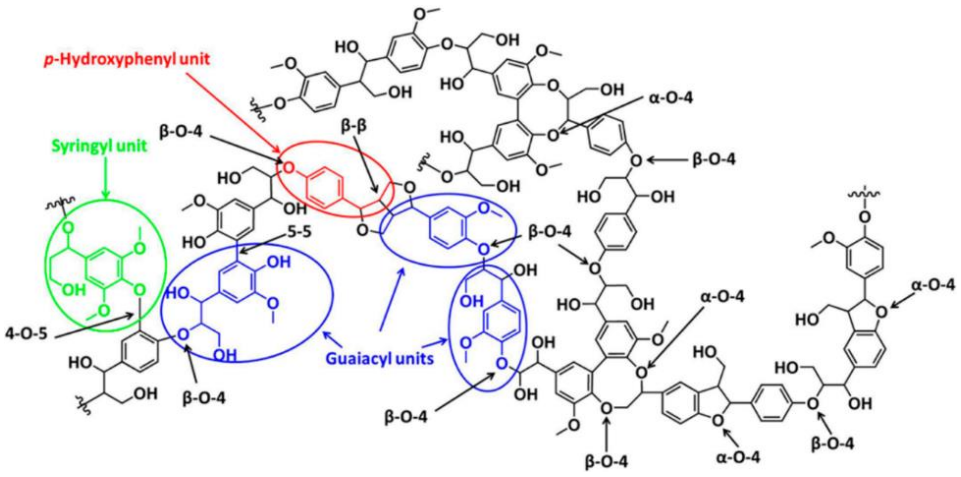

Figure 1.2. Representative structure models of lignin [23].

Table 1.1. Proportion of major linkages between phenylpropane units of lignin [22-28].

Linkage type	Approximate percentage (%)	
	Softwood	Harwood
β-O-4	48	60
α-O-4	6-8	6-8
4-O-5	3.5-4	6.5
β-5	9-12	6
5-5	9.5-11	4.5
β-1	7	7
β-β	2	3

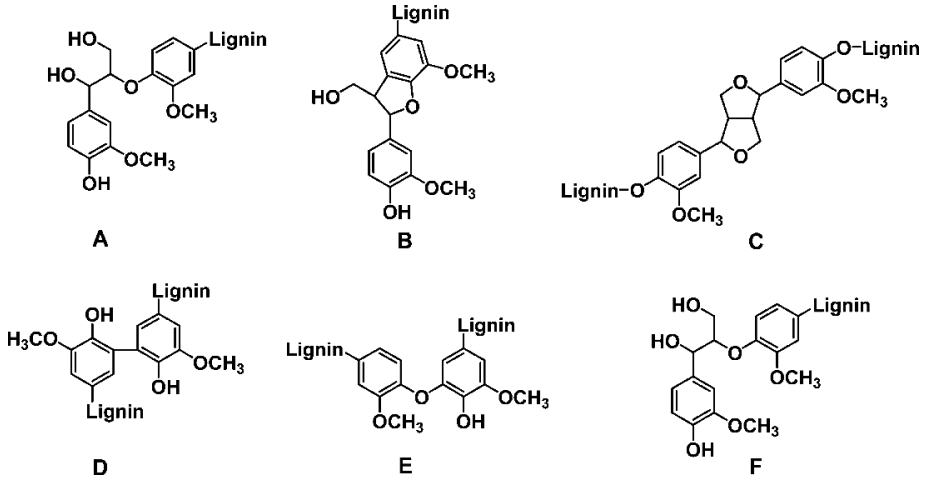

Figure 1.3. Common linkages found in lignin: A : β-O-4, B : β-5, C : β-β′, D : 5-5′, E : 4-O-5, F : β-1′ [16].

Table 1.2 shows the content of functional groups per 100 C_9 units in softwood lignin. It can be seen that lignin mainly contains methoxyl, aliphatic hydroxyl, phenolic hydroxyl and carbonyl [24]. Methoxy groups mainly present in the form of substituents on benzene rings in guaiacyl and syringyl phenylpropane units. As mentioned above, about 90 % of softwood lignin is composed of guaiacyl phenylpropane units, and each of these units contains one methoxy group on the benzene ring, which explains that 90 -95 methoxy groups are contained in every 100 C_9 units in Table 1.2 [21, 24]. As shown in Figure 1.2, in the phenylpropane unit of cork lignin, each propyl group at position α

and γ may have hydroxyl groups, which may explain why the aliphatic hydroxyl groups are more abundant in softwood lignin. In the process of lignin formation, phenolic free radicals usually undergo random radical coupling reaction, which results in relatively low phenolic hydroxyl content. Carbonyl groups usually appear at the end of the molecular structure of lignin and exist in the form of aldehydes.

Table 1.2. Content of functional groups in softwood lignin (per 100 C_9 units) [24].

Functional group	Content
Methoxyl	90-95
Phenolic hydroxyl	20-30
Aliphatic hydroxyl	115-120
Carbonyl	20

1.3 Modification of lignin

Lignin is a macromolecule material, due to its complex structure, low reactivity and poor solubility, high value utilization of lignin has become a major challenge. Researchers mainly modified lignin by introducing other functional groups or changing the spatial structure of molecules through cross-linking and condensation reactions, such as amination, epoxidation, phenolation, hydroxymethylation, oxidation and polyesterification etc. The modification is carried out to improve the reactivity of lignin and expand its application in the field of materials.

Yuan et al. [29] succeeded in obtaining esterification products by using ionic liquid 1-butyl-3-methylimidazolium chloride ([Bmim]C1) as solvent and octanol chloride modified wood powder at 130 °C. Oxygenation reagents such as H_2O_2 and ClO_2 were often used in the oxidation modification of lignin, Yang et al. [30] found that lignin was oxidized by H_2O_2 to produce a stable but highly pyrolytic modified structure, and the content of ortho-disubstituted phenols in lignin macromolecule increased, which expanded its application. Li et al. [31] used phenol phenolation to modify lignin, and further epoxidized lignin with epichlorohydrin to obtain lignin-based epoxy resin.

Lignin macromolecules contain a wide variety of functional groups, which provides various possibilities for the modification of lignin. The modified lignin has certain functional polymer materials and has great application in materials, petroleum, mining, agriculture and medicine.

1.4 Progress in lignin depolymerization

In order to make better use of lignin, which contains abundant aromatic ring structure, it is necessary to convert lignin into low molecule weight products for the preparation of value-added chemicals. At present, the main methods of lignin depolymerization are biological method [32,33], physical method [34,35], and chemical method [36,37]. Among them, the biological method mainly uses microorganisms such as fungi, bacteria and enzymes which can degrade lignin. This method is environmentally friendly, but it has poor controllability, slow degradation speed, long time-consuming and low efficiency. Physical methods mainly use microwave, ultrasonic, steam explosion and other means to promote the cleavage of the ether bond or the carbon-carbon bond of lignin. However, they are usually combined with other depolymerization methods. The main chemical methods used for lignin depolymerization are pyrolysis, hydro-reduction, acid catalytic depolymerization, alkali catalytic depolymerization, and metal catalytic depolymerization. Chemical methods are efficient and time-consuming, but harmful to the environment. Compared with the characteristics of different depolymerization methods, chemical method is a relatively mature method suitable for lignin depolymerization, and the following discussion are mainly on the common chemical methods for lignin depolymerization.

1.4.1 Pyrolysis process

The process of pyrolysis, also known as thermochemical treatment, which refers to in the absence of oxygen, lignin was heated and caused the breakage, isomerization and small molecule polymerization of lignin macromolecule to produce solid coke, non-condensable gas and liquid fuel [38,39]. Recently, this method has been regarded as an efficient biomass energy conversion and utilization technology, and has become one of the priority technologies in the field of biomass utilization. The pyrolysis process of

lignin is more suitable for industrial large-scale production because of its short time-consuming and large processing capacity, and has received extensive attention. According to the phase of lignin pyrolysis, pyrolysis can be divided into pyrolysis reaction in gas phase and in liquid phase. Generally speaking, the pyrolysis temperature of lignin in liquid phase is relatively low, but with relatively high pressure.

The rapid pyrolysis process of lignin in gas phase was specially studied by the international research organization of the United Kingdom, the Netherlands and the Republic of Germany [40], in the laboratory scale and a pilot plant was set up, with reaction temperature of 400-700 ℃ and the reaction residence time is 0.3-15 s by using fluidized bed or airflow reactor with continuous feeding and intermittent feeding. The results showed that the yields of liquid products, coke and non-condensable gases are 30-50 %, 30-50 % and 6-40 %, respectively. However, due to the low melting point of lignin solid particles, the lignin melted at the feed of reactor which caused the feed of lignin material was unstable in the process. Moreover, the molten lignin easily caused the fluidized bed to lose fluidization, resulting in the reactor not being able to continue to operate. Compared to pyrolysis process of lignin in gas phase, in liquid phase the reaction temperature, the coke and gas yield were lower. Lavoie et al. [41] studied the pyrolysis of lignin in alkaline aqueous solution with reaction temperature of 300-330 ℃. The reaction conditions were milder than those of rapid pyrolysis. The results showed that the yield of liquid products could reach about 60 %, but the solid yield was still about 30 %.

From the current research, the gas phase pyrolysis process is still very immature, but liquid phase pyrolysis can improve the yield of small molecular substances, which is a relatively promising method.

1.4.2 Hydro-reduction process

The research on the preparation of phenolic compounds by hydrogenation reduction of alkali lignin was very attractive. The mechanism of hydro-reduction was that methyl-aryl ether bonds and unsaturated bonds in side chains of alkali lignin were attacked by hydrogen atoms, resulting in depolymerization of lignin macromolecules. According to the different catalysts, lignin hydro-reduction reaction can be divided into homogeneous catalytic oxygenation reaction and heterogeneous catalytic hydrogenation reaction.

At present, many homogeneous catalysts cannot be used for lignin hydrogenation reduction, mainly due to expensive synthesis and the low recovery. Hu et al. [42] studied the homogeneous catalytic hydrogenation reduction of lignin model compounds using water-soluble ruthenium complexes as catalysts. The results showed that carbonyl groups in the molecular structure of lignin could be hydrogenated to alcoholic hydroxyl groups or methyl groups. Robinson et al. [43] studied the preparation of biofuel by heterogeneous catalytic hydrogenation of lignin with cationic Rh/C as catalyst. The results showed that the reduction effect was satisfactory. Pepper et al. [44] used Raney nickel catalyst for catalytic hydrogenation, the yield of phenols reached 55.2 %, and the H/C ratio of the product was also significantly improved.

1.4.3 Acid catalytic depolymerization

The first report on acid-catalyzed of lignin was in 1924, Hägglund and Björkman [45] used 12 % hydrochloric acid to hydrolyze lignin to thiobarbituric acid, phloroglucinol and barbituric acid. In recent years, different types of inorganic acids, Lewis acids, zeolites, organic acids and acidic ionic liquids have been used to depolymerized lignin and its model compounds. It was found that when $FeCl_3$, $ZnCl_2$, Fe $(OAc)_2$, $Cu(OAc)_2$ and $Ni(OAc)_2$ were used as catalysts to degrade lignin, Brønsted acid was formed by the reaction of Lewis acid with water or alcohol. Therefore, Lewis acid was usually used

for the depolymerization of lignin in water or low molecular alcohol. However, due to the repolymerization of lignin, the product was mainly solid residue, and the bio-oil with low yield [46]. Zhao et al. [47] studied the depolymerization of different kinds of lignin catalyzed by phosphorus-aluminum-vanadium heteropoly acid ($H_5PMo_{10}V_2O_{40}$). It was found that 65.21 % of lignin was efficiency depolymerized, and the liquefaction products were mainly small aromatic organic compounds and methyl succinic acid. In addition, it has been found that solid acid catalyst ZSM-5 had the best catalytic effect in pyrolysis of softwood lignin with the highest yield of aromatic products obtained [48,49]. Riaz et al. [50] found that in supercritical ethanol/formic acid mixed systems, when lignin was hydrolyzed at 350 °C using concentrated sulfuric acid, the conversion of lignin was 92 %. Generally, due to solvent effects, inorganic acids catalyzed lignin depolymerization more efficiently in phenolic or alcoholic systems than in water systems. However, due to the phenol solvent can undergo a nucleophilic substitution reaction with a cation to form a corresponding phenolic by-product, it is prudent to select the solvent [51]. Otherwise, the hydrolysis rate of each functional group in lignin was different, and the hydrolysis rate of 4-methoxy group was higher than that of 3,4-dimethoxy group and 3,4,5-Trimethoxy group [52]. In addition, in acidic system, the α-aryl ether bond was destroyed earlier than the β-aryl ether bond, resulted in the hydrolysis rate of α-aryl ether was much faster than that of β-aryl ether, moreover, the hydrolysis of phenolic α-ether was faster than that of non-phenolic [53]. Ionic liquids are good solvents for lignin and are conducive to the formation of carbon cation reactions. Some ionic liquids are inherently acidic, and they have been used for lignin depolymerization. It has been found that the relative acidity is not proportional to the ability of ionic liquids to catalyze the hydrolysis of lignin β-O-4 bond. This is because besides acidity, the properties of anions and cations of ionic liquids and their ability to form hydrogen bonds with lignin (model compounds) also affect the hydrolysis [54].

1.4.4 Alkali catalytic depolymerization

Alkali catalytic depolymerization of lignin is an effective method to obtain aromatic chemicals under mild conditions. Since aryl alkyl ether bonds (including β-O-4 bonds) are the most easily broken bonds in lignin, ether bond breaking is the main reaction of alkali-catalyzed lignin depolymerization [55,56]. Some scholars had found that in the reaction of alkali catalytic depolymerization of lignin, the selectivity and yield of degradation products particularly depend on the reaction pressure, temperature, time, alkali concentration and lignin to solvent mass ratio [55,57]. Higher reaction temperature and longer reaction time were beneficial to the formation of monomers, but the solid residue increased due to the repolymerization of the products or intermediates, and strong alkali was beneficial to the improvement of lignin conversion [58]. Recently, organic alkaloids were used in lignin depolymerization with better results [59,60]. Alkali catalysts were also used combined with different catalysts, Long et al. [61] studied the depolymerization of lignin NaOH and Ru/C, from which lignin was firstly depolymerized into monomer phenols and their oligomers, and then the oligomers were further converted into more stable aliphatic alcohols. The conversion of lignin was 92.5 % and compared with the effect of single catalyst, the yield of solid residue was greatly reduced. In the case of alkali catalytic depolymerization of lignin, the yield of biomass oil was generally limited to 20 % [62,63] due to the repolymerization of intermediate products of lignin depolymerization. Some scholars found that the use of phenolic end-capping agents was conducive to the formation of phenolic compounds and could inhibit the occurrence of repolymerization [64]. In addition, acidic substances would be formed in the process of lignin depolymerization, and the deactivation of the catalyst may be caused by the neutralization of acid and alkali.

1.4.5 Metal catalytic depolymerization

In metal catalytic depolymerization of lignin, the commonly used catalysts are noble metal catalysts, nickel-based catalysts, copper-chromium oxide catalysts, sulfide metal catalysts, homogeneous catalysts and amorphous alloy catalysts. Some scholars have used the supported metal catalysts (such as Pt, Ru, Ni, Pd and Cu) to catalyze lignin depolymerization, and found that aliphatic ether bonds and aromatic ether bonds were not broken at the same time, and selective hydrogenation of aliphatic ether bonds was more likely to occur. The cleavage of the aryl ether bond required a very high temperature or pressure, and the conditions were more severe [65]. In addition, some scholars found that with the increase of the amount of Pt/C catalyst, the total yield of monomeric phenol decreased due to the side reaction, but the yield of the target product alkylphenol increased [66]. Sergeev et al. [67] investigated the reaction of aryl ethers catalyzed by Ni catalyst, and found that the stability of the ether bonds containing aryl rings was aryl-aryl ether bond, aryl-alkyl ether bond and nodal-alkyl ether bond in turn. Ji et al. [68] considered the low catalytic activity of FeS_2 for aromatic ring hydrogenation, and supported FeS_2 on activated carbon, SBA-15, SiO_2 and $A1_2O_3$ to catalyze the selective hydrogenation of dibenzyl ether and toluene to achieve a high yield of 100 %. Some scholars used PW/C catalyst to catalyze alkali lignin depolymerization, and the yield of phenolic substances reached 67 mg/g lignin [69]. Compared with single metal catalysts, the use of bimetallic catalysts made it possible to optimize the performance of catalysts and improved the selectivity of catalysts. For example, CoMo catalysts were superior to nickel catalyst because of its low hydrogenation ability and the ability of maintain the integrity of aromatic rings [70]. In addition, bifunctional catalysts contained metal and acid components, which could effectively solve the problem of deactivation of traditional sulfides. Zhao et al. [71] reported that bifunctional combinations of Pd/C, Pt/C, Ru/C or Rh/C and phosphoric acid could selectively catalyze the conversion of

phenolic substances to cycloalkanes and methanol. Zhang et al. [72] found that lignin mainly undergo cleavage of β-O-4 bond and methoxy group during depolymerization, SO_4^{2-}/ZrO_2 mainly caused the cleavage of β-O-4 bond, while CuO mainly caused the removal of methoxy group from benzene ring. Crestini et al. [73] found that MTO (methyltrioxorhenium) could degrade lignin effectively combined with H_2O_2. Recently, the chalcopyrite ($CuFeS_2$) and hydrogen peroxide were used to oxidize lignin and its model compounds, the reactants could be oxidized to dicarboxylic acid with high selectivity [74] which was attributed to the oxidative cracking of β-β bond. Ouyang [75] and Wu [76] oxidized lignin with H_2O_2, CuO and $Fe_2(SO_4)_3$, it was found that the addition of Cu^{2+} could effectively promote the production of phenoxy free radicals, thereby increasing the rate of free radical oxidation reaction, and promoting the breaking of side chains and ether bonds; while Fe^{3+} could improve the oxidation ability of H_2O_2 and contribute to the increase of the yield of phenolic compounds.

In the process of chemical catalytic depolymerization of lignin, another important condition is the reaction medium. It not only has a significant impact on the efficiency of lignin depolymerization, but also is an important factor in measuring the environmental friendliness of the reaction process.

1.5 Ionic liquid and application in lignin

1.5.1 Structure of ionic liquid

Ionic liquid (IL) is generally a molten salt which is composed of an organic cation containing nitrogen or phosphorus and an organic or inorganic anion which is in a liquid state below 100 °C [77]. Depending on the different cations, it is classified into imidazole-, pyridine-, pyrroline-based ionic liquids, etc. as shown in Figure 1.4, and the anions in IL are mainly Cl^-, Br^-, I^-, BF_4^-, CH_3COO^-, NO_3^-, HSO_4^-, and so on. According to the solubility of ILs in water, they can be divided into hydrophilic and hydrophobic ILs. For example, most ILs such as [Bmim]Cl, [Bmim]Ac, [Bmim]BF_4 are hydrophilic, while [Bmim]PF_6 and [BPy]PF_6 are hydrophobic ILs. In addition, according to the acidity and basicity of ILs, they can also be divided into acidic, basic and neutral ILs, among which acidic ILs include Lewis acidic and Brønsted acidic ILs.

Compared with other solvents, ILs have many unique properties, such as, the low melting point and they are liquid at room temperature. ILs have very low vapor pressures and generally do not evaporate or boil, so they can be used in a wide temperature range [78]. In addition, ILs are non-volatile, non-flammable and non-explosive, and have excellent chemical stability. Moreover, its solubility is also very strong which can various substances including inorganic substances, organic substances and even polymers. As a solvent, the ionic liquid can partially or completely dissolve the reactants, but has poor solubility to the product, making it easier to separate it from the product [79]. Finally, ILs are designed solvents whose polarity and hydrophilicity can be changed by the combination of different anions and cations [80].

1.5.2 IL application in lignin dissolution and extraction

A large number of intramolecular and intermolecular hydrogen bonds have been

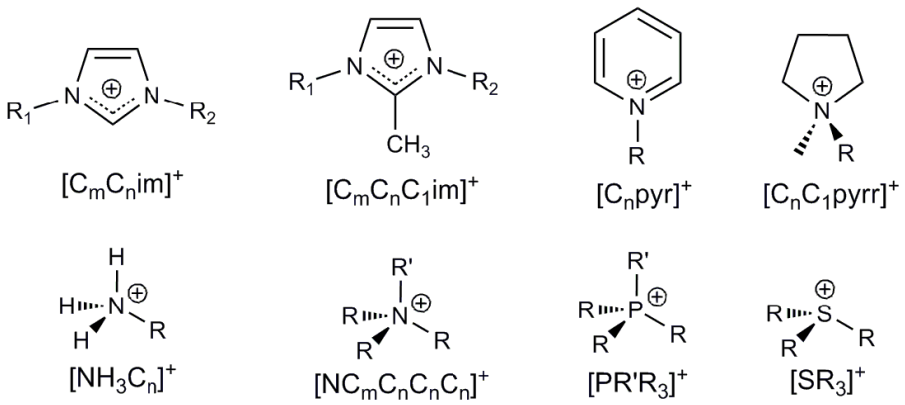

Figure 1.4. Common cations of ionic liquids.

formed in lignin macromolecules due to the presence of hydroxyl groups. The solubility of lignin in solvents is related to the properties of lignin, the solubility parameters and hydrogen bond energies of the solvents used [81]. It has been found that ionic liquids are good solvents for lignin. By comparing the Hildebrand solubility parameters of lignin and ionic liquids, the solvent for lignin can be found reasonably. The Hildebrand solubility parameter of lignin is 24.6. If the Hildebrand solubility parameter of ionic liquids is close to this value, it can dissolve lignin [82,83].

In 2002, Rogers et al. [84] found that 1-methyl-3-butylimidazolium chloride ([Bmim]Cl) could dissolved cellulose with the solubility of 25 % under microwave irradiation. Subsequently, ILs were also found to have better solubility of lignin and biomass [85,86]. Among them, 1-methyl-3-ethylimidazolium acetate ([Emim]OAc), 1-methyl-3-butylimidazolium acetate ([Bmim]OAc), 1-methyl-3-ethylimidazolium chloride ([Emim]Cl) and 1-methyl-3-butylimidazolium chloride ([Bmim]Cl) had the high solubility efficiency for lignin and biomass. Furthermore, phosphite ionic liquids are easy to dissolve cellulose, while methanesulfonate and amino acid based ionic liquids are more soluble for lignin dissolution [87-91]. Pu et al. [85] found that ionic liquids containing methyl sulfate and trifluorosulfonic acid had excellent solubility for lignin extracted from southern pine kraft pulp. And the solubility of lignin in [Hmim]CF_3SO_3,

[Mmim]$MeSO_4$, [Bmim]$MeSO_4$ ILs exceeded 20 wt. %, among which the methyl sulfate ionic liquid [Mmim]$MeSO_4$ had the strongest lignin solubility, while ionic liquids with large anion volume and no coordination capacity, such as [Bmim]PF_6, were almost insoluble to lignin. Lee et al. [92] studied the extraction of lignin from wood powder by ionic liquid [Emim]OAc with a separation of 40 %, and the crystallinity of cellulose can be reduced to less than 45. The cellulose obtained by this process could be hydrolyzed by Trichoderma cellulase with a conversion of more than 90%. Kilpeläinen et al. [93] showed the cations of ionic liquids contain unsaturated double bonds or benzene ring structure are beneficial to lignin dissolution, because they could form strong π-π interaction with aromatic rings in lignin, thus promoting lignin dissolution. In addition, Muhammad [94] and Zavrel [95] found that the unsaturated bonds of cationic side chains in ionic liquids could form π-π interaction, thus promoting lignin dissolution. Janesko [96] also verified the obvious π accumulation and hydrogen bonding between imidazole cations and lignin model compounds by using the dispersion correction density functional theory.

According to the results of the literature, ionic liquids with high lignin solubility should have the following characteristics: anions have small volume and high coordination capacity such as Cl^-, which could interact with lignin to form hydrogen bonds; cations or their side chains should be linked with unsaturated double bonds or unsaturated functional groups such as benzene rings, so as to form π-π stacking between lignin benzene rings and promote lignin dissolution.

1.5.3 IL application in lignin depolymerization

Ionic liquids can be used as a reaction medium in lignin depolymerization, which are more prone to form carbon cations; on the other hand, lignin shows high solubility in ionic liquids [97]. In addition, the special properties of ionic liquids, such as the high

concentration of anions can reduce the depolymerization temperature and promote the cleavage of lignin ether bonds lignin, also promote lignin depolymerization [98].

Boovanahalli et al. [99] used highly nucleophilic brominated ionic liquids for ether decomposition of lignin, using 2-methoxynaphthalene as a model compound to demethylate in a mixed solution of 1-butyl-3-methylimidazolium bromide ([Bmim] Br) and p-toluene sulfonic acid and obtained 2-naphthol with a high yield (97 %). In addition, protonic acids such as hydrochloric acid and sulfuric acid were used as catalysts, which obtained the same effect. Some scholars [100] used heteropoly acid, as a new kind of solid acid catalysts, in exploring solid catalysts suitable for dealkylation of lignin model compounds in ILs. It was found that eugenol was converted into target products with high conversion rate and no other by-products were formed. In addition, Stark et al. [101] used different metal catalysts to oxidize lignin in different ILs and found that $Mn(NO_3)_2$ combined with 1-ethyl-3-methyl-mymitrifluoromethanesulfonate ([Emim]CF_3SO_3) showed high conversion of lignin about 66.3 %.

At present, the study of lignin depolymerization in ionic liquids is still in the preliminary stage. Due to the complexity of lignin structure, most of the studies are carried out with model materials, and the depolymerization of practical lignin as raw material is rare. Moreover, the influence of catalyst and reaction medium on lignin depolymerization needs to be further studied.

1.6 Purpose of this study

Lignin is a complex aromatic biopolymer and a potentially valuable source of aromatic compounds, an efficient means of extracting and depolymerizing are required for the utilization of lignin. However, the traditional extraction and depolymerization methods have several disadvantages including high energy inputs and potential pollutants under harsh conditions, which were seriously impediment to their application. Therefore, develop a novel process to extract lignin from biomass as the feedstock and a continuous flow fixed-bed reaction system for lignin depolymerization are necessary to produce high value-added chemicals.

Firstly, due to the complex structure, low reactivity and poor solubility of lignin, it is difficult to directly utilize lignin, so high performance on lignin-based materials need to be prepared by modification. In recent years, it has been found that ionic liquids composed of cations and anions are new green solvents for lignin dissolution. However, the processes typically require either high temperature processing (≥100 °C) or long processing time (>12 h), with a relatively low yield of lignin extracted from the biomass. To separate lignin efficiently, a solvent system consisting of ionic liquids and antisolvents should be developed.

Secondly, many approaches have been employed to convert lignin into value added products, however, most of process operated at either higher temperature (≥ 250 °C) or pressure (> 2.5 MPa) with hydrogen or oxygen in batch reactors with low yields of phenols by using different model compounds. Therefore, it is indispensable to develop a continuous flow system for efficient catalytic depolymerization of actual lignin into value-added aromatic products at low temperature without external hydrogen or oxygen.

Thirdly, the catalysts for the depolymerization process are classified into homogeneous catalysts and heterogeneous catalysts. The former is difficult to be separated from the product and difficult to recover which limited in practical

applications. The latter is difficult to contact with lignin macromolecules and often needs to be carried out under harsh conditions. Moreover, the yield and selectivity of phenolic products are low. So, it is important to construct a new catalytic system to achieve efficient and highly selective depolymerization of lignin.

Finally, in comparison with noble metal supported catalysts, Pt-based catalysts show great attraction because of their highly efficient in lignin depolymerization. Although several studies have reported on lignin depolymerization by using ionic liquids combined with different catalysts, but the reaction mechanism is still unclear. Therefore, according to the studies of different model compounds, which can help us to understand the synergistic effect of ionic liquid and catalysts, and propose the mechanism of lignin depolymerization.

Consequently, the purpose of this study is to develop a novel process to extract lignin from biomass as the feedstock by using ionic liquids and antisolvents efficiently, and a continuous flow fix-bed reaction system for efficient catalytic depolymerization of actual lignin with metal-supported solid acid catalysts to produce phenolic compounds. First, different types of ionic liquids were used as the extraction solvent to separate lignin from red pine, combined with methanol, water and acetonitrile as antisolvents to and extraction process is shown in Figure 1.5. Then three kinds of catalysts, including SO_4^{2-}/ZrO_2, Pt-SO_4^{2-}/ZrO_2 and Pt-La_2O_3-SO_4^{2-}/ZrO_2, under the synergy of [Apy]Cl were studied for lignin depolymerization. Due to the remarkable properties of La_2O_3 which has a special electronic structure and acidic properties, furthermore, it is able to decrease the size of the Pt domain and stabilize Pt dispersion. These properties indicate that Pt supported on La_2O_3-SO_4^{2-}/ZrO_2 is a rather considerable system for lignin depolymerization. And according to previous research, self-assemble core-shell structure catalysts (Pt-SO_4^{2-}/ZrO_2 and Pt-La_2O_3-SO_4^{2-}/ZrO_2,) were prepared, the possible structure is shown in Figure 1.6.

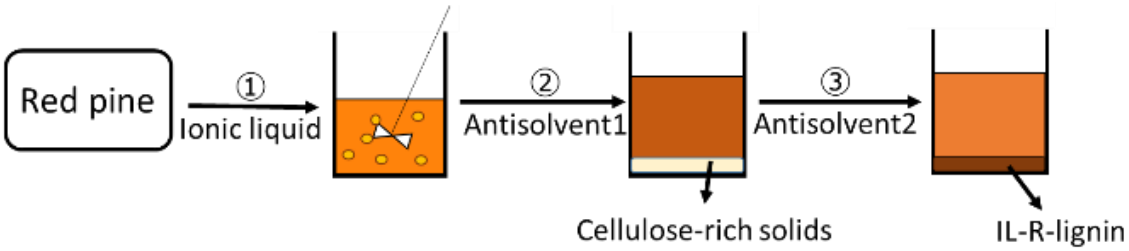

Figure 1.5. Extraction process of lignin from red pine.

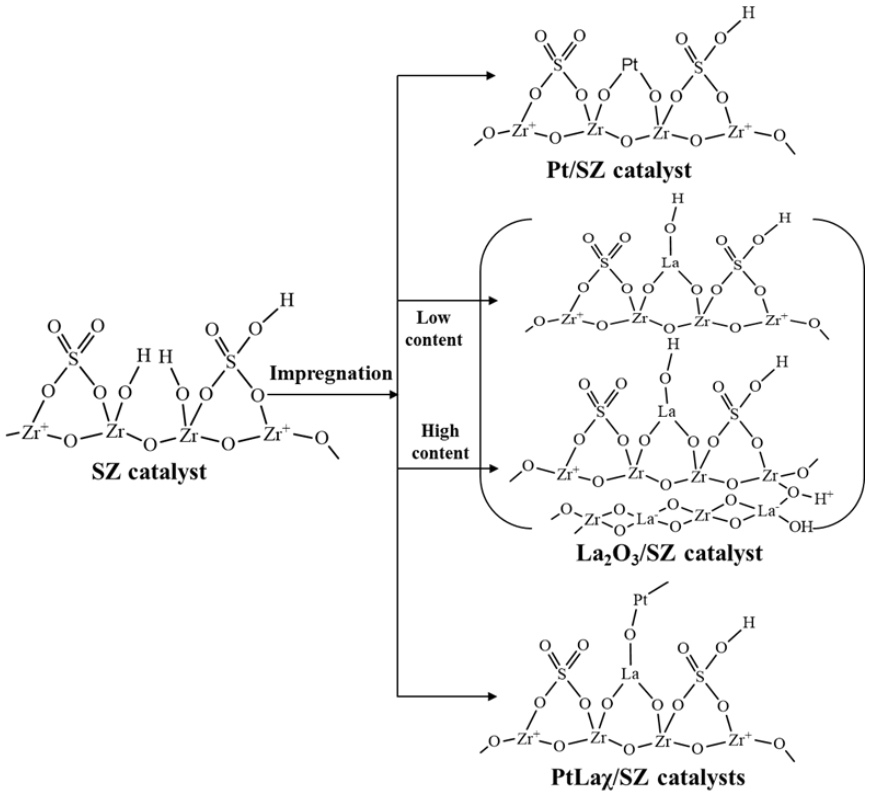

Figure 1.6. Possible mechanism of addition of Pt and La into sulfated zirconia and structure of the Pt/SZ and PtLaχ/SZ catalysts.

The detailed works in this research are introduced as below:

In Chapter 2, a novel process to extract lignin from biomass as the feedstock was developed, the extraction of lignin from lignin/cellulose/xylan mixture and red pine were evaluated with different kinds of ionic liquids and antisolvents. Comparing the catalytic activity for lignin depolymerization and the mild modification effect on the structure of alkali lignin among the used ILs, N-allyl-pyridinium chloride ([Apy]Cl) was chosen as the promising ionic liquid, moreover, methanol, water and acetonitrile

were chosen as antisolvents. Furthermore, based on results of three model compounds in [Apy]Cl pretreatment, the effect of ionic liquid was also elucidated and a hypothetical mechanism of lignin dissolution in ionic liquid was proposed.

In Chapter 3, to evaluate the feasibility of ionic liquid-solid acid catalysts system, the effect of reaction temperature and the addition of platinum to the ZrO_2/SO_4^{2-} on the yields (carbon-based) of total products and phenolic compounds were studied. Based on the above results and previous reports, the proposed mechanism of lignin depolymerization under catalysis of ZrO_2/SO_4^{2-} and Pt-ZrO_2/SO_4^{2-} after [Apy]Cl pretreatment was studied in a continuous flow fix-bed reaction system.

In Chapter 4, to further improve the catalytic performance, effects of lanthanum oxide addition to the support on the performance of Pt-La_2O_3-SO_4^{2-}/ZrO_2, where La/Pt atomic ratio was 1, 3, 6, were investigated. By adding La_2O_3 the number of Lewis acid sites increased, less Pt oxide species and better Pt dispersion on surface and/or in the mesopores of the support (La_2O_3-SO_4^{2-}/ZrO_2) especially with the La/Pt atomic ratio was 3, which showed the high yields of the carbon-based products and phenolic compounds. Simultaneously, through the study of model compounds and products distribution the reaction pathways of lignin depolymerization were proposed.

References

[1]. H. S. Kheshgi, R. C. Prince, G. Marland. The potential of biomass fuels in the context of global climate change: focus on transportation fuels. Annual Review of Energy and the Environment, 2000, 25: 199-244.

[2]. D. Pornlada, V. Nawin, L. Navadol. Effects of kraft lignin on hydrolysis/dehydration of sugars, cellulosic and lignocellulosic biomass under hot compressed water. Bioresource Technology, 2013, 144: 504-512.

[3]. A. P. Karmanov, Y. B. Monakov. Hydrodynamic properties and structure of lignin. International Journal of Polymeric Materials and Polymeric Biomaterials, 2000, 48: 151-175.

[4]. T. Farid, M. Moein, R. Mostafa. Ethanol production from steam exploded rapeseed straw and the process simulation using artificial neural networks. Biotechnology and Bioprocess Engineering, 2015, 20: 139-147.

[5]. J. M. Gallo, D. M. Alonso, M. A. Mellmer, et al. Production of furfural from lignocellulosic biomass using Beta zeolite and biomass-serived solvent. Topics in Catalysis, 2013, 56: 1775-1781.

[6]. X. H. Wen, Y. N. Jia, J. X. Li. Degradation of tetracycline and oxytetracycline by crude lignin peroxidase prepared from Phanerochaete chrysosporium: a white rot fungus. Chemosphere, 2009, 75: 1003−1007.

[7]. W. Holger, A. Nora, R. R. Philipp. Lignin oxidation studies in a continuous two-phase flow microreactor. Chemical Engineering and Processing, 2013, 73: 29-37.

[8]. B. Giovanni, B. Carlo, D. Maurizio, et al. Degradation of steam-exploded lignin from beech by using Fenton's reagent. Biomass and Bioenergy, 2003, 24: 233-238.

[9]. W. O. S. Doherty, P. Mousavioun, C. M. Fellows. Value-adding to cellulosic ethanol lignin polymers. Industrial Crops and Products, 2011, 33: 259-276.

[10]. Y. Chung, J. V. Olsson, R. J. Li. A renewable lignin-lactide copolymer and application in biobased composites. ACS Sustainable Chemistry & Engineering, 2013, 1: 1231-1238.

[11]. A. Casas, J. Palomar, M. V. Alonso, et al. Comparison of lignin and cellulose solubilities in ionic liquids by COSMO-RS analysis and experimental validation. Industrial Crops and Products, 2012, 37: 155-163.

[12]. D. Dong, A. L. Fricke. Investigation of optical effect of lignin solution and determination of Mw of kraft lignin by LALLS. Journal of Applied Polymer Science, 1993, 50: 1131-1140.

[13]. X. C. Liang, J. Liu, Y. Fu. Influence of anti-solvents on lignin fractionation of eucalyptus globulus via green solvent system pretreatment. Separation and Purification Technology, 2016, 163: 258-266.

[14]. Y. Chen, F. Wang, Y. Jia, N. Yang, X. Zhang. One-step ethanolysis of lignin into small-molecular aromatic hydrocarbons over nano-SiC catalyst. Bioresource

technology, 2017, 226, 145-149.
[15]. F. Monteil-Rivera, M. Phuong, M. W. Ye. Isolation and characterization of herbaceous lignins for applications in biomaterials. Industrial Crops and Products, 2013, 41:356-364.
[16]. B. M. Upton, A. M. Kasko. Strategies for the conversion of lignin to high-value polymeric materials: Review and perspective. Chemical Reviews, 2016, 116, 2275-2306.
[17]. S. Dutta, K. C. W. Wu, B. Saha. Emerging strategies for breaking the 3D amorphous network of lignin. Catalysis Science & Technology, 2014, 4, 3785-3799.
[18]. A. J. Ragauskas, G. T. Beckham, M. J. Biddy, R. Chandra, F. Chen, M. F. Davis, B. H. Davison, R. A. Dixon, P. Gilna, M. Keller, P. Langan, A. K. Naskar, J. N. Saddler, T. J. Tschaplinski, G. A. Tuskan, C. E. Wyman. Lignin valorization: Improving lignin processing in the biorefinery. Science 2014, 344, 6185.
[19]. S. Dutta, K. C. W. Wu, B. Saha. Emerging strategies for breaking the 3D amorphous network of lignin. Catalysis Science & Technology, 2014, 4, 3785−3799.
[20]. B. Lochab, S. Shukla, I. K. Varma. Naturally occurring phenolic sources: monomers and polymers. RSC Advance. 2014, 4, 21712-21752.
[21]. J. Zakzeski, P. C. A. Bruijnincx, A. L. Jongerius. The catalytic valorization of lignin for the production of renewable chemicals. Chemical Reviews, 2010, 110: 3552-3599.
[22]. J. Zakzeski, B. M. Weckhuysen. Lignin solubilization and aqueous phase reforming for the production of aromatic chemicals and hydrogen. ChemSusChem, 2011, 4: 369-378.
[23]. C. Li, X. Zhao, A. Wang, G. W. Huber, T. Zhang. Catalytic transformation of lignin for the production of chemicals and fuels. Chemical Reviews, 2015, 115, 11559−11624.
[24]. F. S. Chakar, A. J. Ragauskas. Review of current and future softwood kraft lignin process chemistry. Industrial Crops and Products，2004, 20: 131−141.
[25]. E. Adler. Lignin chemistry-past, present and future. Wood Science and Technology, 1977, 11:169-218.
[26]. M. P. Pandey, C. S. Kim. Lignin depolymerization and methods. Chemical Engineering & Technology, 2011，34: 29-41.
[27]. P. C. R. Pinto, E. A. B. D. Silva, A. E. Rodrigues. Insights into oxidative conversion high-added-value phenolic aldehydes. Industrial & Engineering Chemistry Research, 2011, 50: 741-748.
[28]. D. K. Shen, S. Gu, K. H. Luo. The pyrolytic degradation of wood-derived lignin process. Bioresource Technology, 2010, 101: 6136-6146.
[29]. T. Q. Yuan, S. N. Sun, F. Xu. Hom esterification of poplar wood in an ionic liquid under mild conditions: characterization and properties. Journal of Agricultural & Food Chemistry, 2010, 58 (21):11302-I 1310.

[30]. Z. Yang，M. Chen，Z. Luan，W. Zhang．Solubility of alkali lignin in dilute solutions of [bmim]c1 at room temperature．Asian Journal of Chemistry, 2014，26(6) 1707-1710．
[31]. W. T. Li et al., Synthesis of Lignin-Based Epoxy Resin in Ionic Liquid [BMIm]Cl, Applied Mechanics and Materials, 2015, 740, 51-54.
[32]. L. T. M. Pham, Y. H. Kim. Discovery and characterization of new O-methyltransferase from the genome of the lignin-degrading fungus Phanerochaete chrysosporium for enhanced lignin degradation. Enzyme and Microbial Technology, 2016, 82: 66-73.
[33]. S. Yadav, R. Chandra. Syntrophic co-culture of Bacillus subtilis and Klebsiella pneumonia for degradation of kraft lignin discharged from rayon grade pulp industry. Journal of Environmental Sciences, 2015, 33: 229-238.
[34]. D. K. Shen, N. N. Liu, C. J. Dong, et al. Catalytic solvolysis of lignin with the modified HUSYs in formic acid assisted by microwave heating. Chemical Engineering Journal, 2015, 270: 641-647.
[35]. X. P. Ouyang, G. D. Zhu, X. Z. Huang, et al. Microwave assisted liquefaction of wheat straw alkali lignin for the production of monophenolic compounds. Journal of Energy Chemistry, 2015, 24: 72-76.
[36]. Z. Fang, T. Sato, R. L. Smith Jr, et al. Reaction chemistry and phase behavior of lignin in high-temperature and supercritical water. Bioresource Technology, 2008, 99: 3424-3430.
[37]. J. Y. Pan, J. Fu, S. G. Deng, et al. Distribution coefficient of products from lignin oxidative degradation in organic-water systems. Fuel Processing Technology, 2015, 140: 262-266.
[38]. S. Czernik, A.V. Bridgwatert. Overview of Applications of Biomass Fast Pyrolysis Oil. Energy & Fuels, 2004, 18(2):590-598.
[39]. G. W. Huber, A. Sara Iborra, A. Corma. Synthesis of Transportation Fuels from Biomass: Chemistry, Catalysts, and Engineering. Chemical Reviews, 2006, 37(9):4044.
[40]. D. J. Nowakowski, A. V. Bridgwater, D. C. Elliott, et al. Lignin fast pyrolysis: Results from an international collaboration. Journal of Analytical & Applied Pyrolysis, 2010, 88(1):53-72.
[41]. J. M. Lavoie, W. Bare, M. Bilodeau. Depolymerization of steam-treated lignin for the production of green chemicals. Bioresource Technology, 2011, 102 (7):4917-4920.
[42]. T. Q. Hu, G. Leary, D. Wong. A New Approach Towards the Yellowing Inhibition of Mechanical Pulps. Part I: Selective Removal of α Hydroxyl and a-Carbonyl Groups in Lignin Model Compounds. Holzforschung, 1999, 53(1):43-48.
[43]. J. M. Robinson, C. E. Burgess, M. A. Bently, et al. The use of catalytic hydrogenation to intercept carbohydrates in a dilute acid hydrolysis of biomass to effect a clean separation from lignin. Biomass & Bioenergy, 2004, 26(5):473-483.

[44]. J. M. Pepper, W. Steck. The effect of time and temperature on the hydrogenation of aspen lignin. Canadian Journal of Chemistry, 2011, 41(11):2867-2875.
[45]. E. Hägglund, C. B. Björkman,. Lignin Hydrochloride. Biochemistry, 1924, 147: 74.
[46]. B. Guvenatam, E. H. J. Heeres, E. A. Pidko, et al. Lewis-acid catalyzed depolymerization of protobind lignin in supercritical water and ethanol. Catalysis Today, 2016, 259: 460-466.
[47]. Y. Zhao, Q. Xu, T. Pan, et al. Depolymerization of lignin by catalytic oxidation with aqueous polyoxometalates. Applied Catalysis A: General, 2013, 467: 504-508.
[48]. K. G. Kalogiannis, S. D. Stefanidis, C. M. Michailof. Pyrolysis of lignin with 2DGC quantification of lignin oil: effect of lignin type, process temperature and ZSM-5 in situ upgrading. Journal of Analytical and Applied Pyrolysis, 2015, 115: 410-418.
[49]. Y. Q. Yu, X. Y. Li, L. Su, et al. The role of shape selectivity in catalytic fast pyrolysis of lignin with zeolite catalysts. Applied Catalysis A: General, 2012, 447-448: 115-123.
[50]. A. Riaz, C. S. Kim, Y. Kim, et al. High-yield and high-calorific bio-oil production from concentrated sulfuric acid hydrolysis lignin in supercritical ethanol. Fuel, 2016, 172: 238-247.
[51]. L. Lin, S. Nakagame, Y. Yao, et al. Liquefaction mechanism of β-O-4 lignin model compound in the presence of phenol under acid catalysis: Part 2. Reaction behavior and pathways. Holzforschung, 2001, 55: 625-630.
[52]. M. Meshgini, K. V. Sarkanen. Synthesis and kinetics of acid-catalyzed hydrolysis of some alpha-aryl ether lignin model compounds. Holzforschung, 1989, 43:239-243.
[53]. U. Wongsiriwan, Y. Noda, C. S. Song, et al. Lignocellulosic biomass conversion by sequential combination of organic acid and base treatments. Energy Fuels, 2010, 24: 3232-3238.
[54]. B. J. Cox, S. Jia, Z. C. Zhang, et al. Catalytic degradation of lignin model compounds in acidic imidazolium based ionic liquids: Hanunett acidity and anion effects. Polymer Degradation and Stability, 2011, 96: 426-431.
[55]. Z. S. Yuan, S. N. Cheng, M. Leitch, et al. Hydrolytic degradation of alkaline lignin in hot-compressed water and ethanol. Bioresource Technology, 2010, 101:9308-9313.
[56]. J. M. Lavoie, W. Bare, M. Bilodeau. Depolymerization of steam-treated lignin for the production of green chemicals. Bioresource Technology, 2011， 102: 4917-4920.
[57]. N. Mahmood, Z. Yuan, J. Schmidt, et al. Production of polyols via direct hydrolysis of kraft lignin: effect of process parameters. Bioresource Technology, 2013, 139: 13-20.
[58]. J. E. Miller, L. Evans, A Littlewolf. Batch microreactor studies of lignin and lignin model compound depolymerization by bases in alcohol solvents. Fuel, 1999, 78: 1363−1366.
[59]. H. J. Parker, C. J. Chuck, T. Woodman, M. D. Jones. Degradation of β-O-4 model lignin species by vanadium Schiff-base catalysts: influence of catalyst structure and

reaction conditions activity and selectivity. Catalysis Today, 2016, 269, 40-47.
[60]. S. Jia, B. J. Cox, X. Guo, et al. Decomposition of a phenolic lignin model compound over organic N-bases in an ionic liquid. Holzforschung, 2010, 64: 577-580.
[61]. J. X. Long, Y. Xu, T. J. Wang, et al. Efficient base-catalyzed decomposition and in situ hydrogenolysis process for lignin depolymerization and char elimination. Applied Energy, 2015, 141:70-79.
[62]. J. X. Long, Q. Zhang, T. J. Wang, et al. An efficient and economical process for lignin depolymerization in biomass-derived solvent tetrahydrofuran. Bioresource Technology, 2014, 154: 10-17.
[63]. X. Erdocia, R. Prado, M. A. Corcuera, et al. Base catalyzed depolymerization of lignin: influence of organosolv lignin nature. Biomass and Bioenergy, 2014, 66: 379-386.
[64]. A. Toledano, L. Serrano, J. Labidi. Improving base catalyzed lignin depolymerization by avoiding lignin repolymerization. Fuel, 2014, 116: 617-624.
[65]. K. Barta, G. R. Warner, E. S. Beach, et al. Depolymerization of organosolv lignin to aromatic compounds over Cu-doped porous metal oxides. Green Chemistry, 2014, 16: 191-196.
[66]. J. Y. Kim, J. Park, H. H. wang, et al. Catalytic depolymerization of lignin macromolecule to alkylated phenols over various metal catalysts in supercritical tent-butanol. Journal of Analytical and Applied Prolysis, 2015, 113: 99-106.
[67]. A. G. Sergeev, J. F. Hartwig. Selective nickel-catalyzed hydrogenolysis of aryl ethers. Science, 2011，332:439-443.
[68]. N. Ji, X. Wang, C. Weidenthaler, et al. Iron (II) disulfides as precursors of highly selective catalysts for hydrodeoxygenation of dibenzyl ether into toluene. ChemCatChem, 2015, 7: 960-966.
[69]. X. L. Ma, Y. Tian, W. Y. Hao, et al. Production of phenols from catalytic conversion of lignin over a tungsten phosphide catalyst. Applied Catalysis, 2014, 481:64-70.
[70]. A. Popov, E. Kondratieva, J. P. Gilson, et al. IR study of the interaction of phenol with oxides and sulfided CoMo catalysts for bio-fuel hydrodeoxygenation. Catalysis Today, 2011, 172: 132-135.
[71]. C. Zhao, Y. Kou, A. A. Lemonidou, et al. Highly selective catalytic conversion of phenolic bio-oil to alkanes. Angewandte Chemie-international Edition, 2009, 48: 3987-3990.
[72]. S. M. Zhang, L. Su, L. Liu, et al. Degradation on hydrogenolysis of soda lignin using $CuO/SO_4^{2-}/ZrO_2$ as catalyst. Industrial Crops and Products, 2015, 77: 451-457.
[73]. C. Crestini, P. Pro, V. Neri, et al. Methyltrioxorhenium: a new catalyst for the activation of hydrogen peroxide to the oxidation of lignin and lignin model compounds. Bioorganic & Medicinal Chemistry Letters, 2005, 13: 2569-2578.
[74]. R. Ma, M. Guo, X. Zhang. Selective conversion of biorefinery lignin into dicarboxylic acids. ChemSusChem, 2014, 7: 412-415.

[75]. X. P. Ouyang, Y. D. Tan, X. Q. Qiu. Oxidative degradation of lignin for producing monophenolic compounds. Journal of Fuel Chemistry and Technology, 2014, 42: 677-682.

[76]. G. X. Wu, M. Heitz. Catalytic mechanism of Cu^{2+} and Fe^{3+} in alkaline O_2 oxidation of lignin. Journal of Wood Chemistry and Technology, 1995, 15: 189-202.

[77]. K. R. Seddon. Ionic liquids for clean technology. Journal of Chemical Technology and Biotechnology, 1997, 68: 351-356.

[78]. D. W. Kim, C. E. Song, D. Y. Chi. New method of fluorination using potassium fluoride in ionic liquid: significantly enhanced reactivity of fluoride and improved selectivity. Journal of the American Chemical Society, 2002, 124: 10278-10279.

[79]. H. Zhang, F. Xu, X. Zhou, et al. Bronsted acidic ionic liquid as an efficient and reusable catalyst system for esterification. Green Chemistry, 2007, 9: 1208-1211.

[80]. A. H. M. Fauzi, N. A. S. Amin. An overview of ionic liquids as solvents in biodiesel synthesis. Renewable and Sustainable Energy Reviews, 2012, 16: 5770-5786.

[81]. A. Casas, J. Palomar, M. V. Alonso, et al. Comparison of lignin and cellulose solubilities in ionic liquids by COSMO-RS analysis and experimental validation. Industrial Crops and Products, 2012, 37: 155-163.

[82]. S. H. Lee, T. V. Doherty, J. S. Linhardt. Ionic liquid-mediated selective extraction of lignin from wood leading to enhanced enzymatic cellulose hydrolysis. Biotechnology and Bioengineering, 2009, 102: 1368-1376.

[83]. C. Li, Q. Wang, Z. K. Zhao. Acid in ionic liquid: an efficient system for hydrolysis of lignocellulose. Green Chemistry, 2008, 10: 177-182.

[84]. R. P. Swatloski, S. K. Spear, J. D. Holbrey. Dissolution of cellulose with ionic liquids. Journal of the American Chemical Society, 2002, 124(18): 4974-4975.

[85]. Y. Pu, N. Jiang, A. J. Ragauskas. Ionic liquid as a green solvent for lignin. Journal of Wood Chemistry and Technology, 2007, 27(1): 23-33.

[86]. M. Zavrel, D. Bross, M. Funke, et al. High-throughput screening for ionic liquids dissolving (ligno-)cellulose. Bioresource Technology, 2009, 100(9): 2580-2587.

[87]. M. Abe, Y. Fukaya, H. Ohno. Extraction of polysaccharides from bran with phosphonate or phosphinate-derived ionic liquids under short mixing time and low temperature. Green Chemistry, 2010, 12(7): 1274-1280

[88]. A. A. Shamsuri, D. K. Abdullah. Isolation and characterization of lignin from rubber wood in ionic liquid medium[J]. Modern Applied Science, 2010, 4(11): 19-27

[89]. N. Muhammad, Z. Man, M. A. Bustam. Dissolution and delignification of bamboo biomass using amino acid-based ionic liquid. Applied Biochemistry and Biotechnology, 2011, 165(3-4): 998-1009

[90]. X. D. Hou, T. J. Smith, N. Li, et al. Novel renewable ionic liquids as highly effective solvents for pretreatment of rice straw biomass by selective removal of lignin. Biotechnology and Bioengineering, 2012, 109(10): 2484-2493

[91]. A. Brandt, J. P. Hallett, D. J. Leak, et al. The effect of the ionic liquid anion in the pretreatment of pine wood chips. Green Chemistry, 2010, 12(4): 672-679.
[92]. S. H. Lee, T. V. Doherty, R. J. Linhardt, et al. Ionic liquid-mediated selective extraction of lignin from wood leading to enhanced enzymatic cellulose hydrolysis. Biotechnology and Bioengineering, 2009, 102(5): 1368-1376.
[93]. I. Kilpeläinen, H. Xie, A. King, M. Granstrom, S. Heikkinen, D. S. Argyropoulos. Dissolution of wood in ionic liquids. Journal of Agricultural and Food Chemistry, 2007, 55(22), 9142-9148.
[94]. N. Muhanunad, Z. Man, M. A. Bustam, et al. Investigations of novel nitrile-based ionic liquids as pre-treatment solvent for extraction of lignin from bamboo biomass. Journal of Industrial and Engineering Chemistry, 2013, 19: 207-214.
[95]. M. Zavrel, D. Bross, M. Funke, et al. High-throughput screening for dissolving (ligno)-cellulose. Bioresource Technology, 2009, 100: 2580-2587.
[96]. B. G. Janesko. Modeling interactions between lignocellulose and ionic liquids using DFT-D. Physical Chemistry Chemical Physics, 2011, 13: 11393-11401.
[97]. D. A. Fort, R. C. Remsing, R. P. Swatloski, et al. Can ionic liquids dissolute wood? Processing and analysis of lignocellulosic materials with 1-H-butyl-3-methylimidazolium chloride. Green Chemistry, 2007, 9: 63-69.
[98]. S. Kubo, K. Hashida, T. Yamada, et al. A characteristic reaction of lignin in ionic liquids: glycelol type enol-ether as the primary decomposition product of β-O-4 model compound. Journal of Wood Chemistry and Technology, 2008, 28: 84-96.
[99]. S. K. Boovanahalli, D. W. Kim, D. Chi. Application of ionic liquid halide nucleophilicity for the cleavage of ethers: a green protocol for the regeneration of phenols from ethers. The Journal of Organic Chemistry, 2004, 69: 3340-3344.
[100]. J. B. Binder, M. J. Gray, J. F. White, et al. Reactions of lignin model compounds in ionic liquids. Biomass and Bioenergy, 2009, 33: 1122-1130.
[101]. K. Stark, N. Taccardi, A. Bosmann, et al. Oxidative depolymerization of lignin in ionic liquids. ChemSusChem, 2010, 3: 719-723.

Chapter 2

Extraction of Lignin from Red Pine by Ionic Liquid and Modification of Extracted Lignin Structure

Abstract

Pyridinium- and imidazolium-based ionic liquids with different anions were synthesized and used for the catalytic depolymerization of alkali lignin. All the ionic liquids used had a mild modification effect on the structure of the alkali lignin at 100 °C. In the ionic liquids used, the extracted alkali lignin by N-allyl pyridine chloride ([Apy]Cl) was easier to decompose under the same conditions, which made the catalytic depolymerization activity of alkali lignin higher than that of other ionic liquids at 200 °C. Therefore, [Apy]Cl was chosen as the promising ionic liquid to extract lignin from red pine under atmospheric pressure. Extraction of lignin ([Apy]Cl-R-lignin) from red pine was achieved, with recovery ratio of 98.7 wt.% at 90 °C for 6 h of dissolution in [Apy]Cl. The extracted [Apy]Cl-R-lignin and cellulose-rich solids were characterized and compared with the raw alkali lignin and cellulose. Additionally, compared to the fresh [Apy]Cl, regenerated [Apy]Cl had no change in structure and thermal stabilities, which demonstrated potential recyclability.

2.1 Introduction

With the increasing concern for the global environment and energy security coupled with the reduction of fossil fuel resources, the development of renewable resources to replace fossil fuels has attracted more and more attention [1]. Lignocellulose biomass as a renewable resource could be converted into liquid transport fuel, and it produces high value-added products. Many value-added products, such as bioethanol, have been commercialized from cellulose and hemicellulose, but there are relatively few studies focused on the utilization of lignin [2,3]. Lignin is a complex biopolymer that accounts for 25–35% of renewable carbon in lignocellulosic materials [4], and is also a potentially valuable source of aromatic compounds [5], which is an important component in bio-oil. The extended network of lignin is constructed by the monomers of coumaryl, coniferyl and sinapyl alcohols in a random order through intermolecular C–O and C–C bonds [6–9]. As a potentially valuable source of aromatic compounds, efficient means of extracting and depolymerizing are required for the utilization of lignin. However, the traditional extraction methods, such as the kraft, sulfite, soda and organosolv processes, have several disadvantages including high energy cost, potential pollutants under harsh conditions and significant modification of the lignin structure, which seriously impedes their application [10–12].

Among different lignin extraction methods, ionic liquids (ILs) as one of superior green solvents were employed in the lignin extraction with more advantages than traditional methods [13,14]. Different types of ILs have been studied for the extraction of lignin from biomass. Muhammad et al. [15] used 1-propyronitrile-3-(2-hydroxyethyl) imidazolium chloride ([C_2CN HEim]Cl), successfully extracting 53% of lignin at 120 °C for 24 h with acetone-water mixture and ethanol as the antisolvents, and the relatively low yield of lignin and the longer extraction time was possible due to the low extraction ability of the antisolvents. Achinivu et al. [16] reported that more than 70% of

the lignin was extracted from corn stock using pyrrolidinium acetate ([Pyrr]Ac) at 90 ℃ with ethanol and water under a long extraction time of about 24 h. Li et al. [17] obtained 44% lignin from corn stalks using 1-ethyl-3-methylimidazolium acetate ([Emim]Ac) at 125 °C for 1 h. Most of the extraction processes typically require long processing time with a relatively low yield of lignin extracted from the biomass. Additionally, even though many studies have applied ILs to lignin extraction, there are relatively few studies focus on using ILs as solvents and catalysts for lignin depolymerization, especially in flow-through reactor system. Different ILs have different solubility and depolymerization reactivity for lignin. Our previous study [18] indicated that N-allylpyridinium chloride ([Apy]Cl) could dissolve lignin effectively with partial lignin macromolecules converted into low-molecular-weight compounds with the cleavage of methyl aryl ethers and β-O-4 bonds, which further promoted the catalytic depolymerization of lignin. Meanwhile, the synergistic effect of the SO_4^{2-}/ZrO_2 catalyst and [Apy]Cl was proven for the efficient catalytic depolymerization of alkali lignin at 210 °C without external hydrogen or oxygen. Therefore, choosing an IL with a high reactivity in lignin depolymerization and with a high lignin extraction ability is very necessary for the utilization of lignin, especially for a continuous flow-reaction system.

In this study, due to red pine biomass being one of the dominant pine species in Japan and commercially valuable for paper pulp and fuel, to make full use of this biomass, it was applied to the extraction of lignin. In order to select an IL with high catalytic activity for alkali lignin depolymerization but also one that could efficiently extract lignin from red pine, a series of ILs with pyridinium- and imidazolium-based cations were synthesized and the catalytic activity for alkali lignin depolymerization was tested. The effect of the amounts of antisolvents (e.g., methanol, water and acetonitrile) on the extraction of lignin under ambient pressure and low temperature were investigated. Based on above results, the promising IL were determined and used for the extraction

from red pine. The extracted IL-lignin and cellulose-rich solids were characterized with Fourier transform infrared spectroscopy (FT-IR), thermogravimetric analysis (TGA) together with differential thermal analysis (DTG) and elemental analysis (CHN).

2.2 Experimental Section

2.2.1 Materials

The raw materials used in this experiment were alkali lignin, microcrystalline cellulose and xylan used as a model material for hemicellulose, and these were purchased from Sigma-Aldrich Chemical Company. The chemical composition of red pine was analyzed by the National Renewable Energy Laboratory (NREL) method [19]: cellulose, 56.2 wt.%; hemicellulose, 13.4 wt.%; lignin, 26.2 wt.%; lipid, 4.0 wt.% and ash 0.2 wt.%. Prior to the process, red pine was milled and sieved to obtain a wood meal with 250–106 μm, and it was air dried. Five kinds of ILs including 1-butyl-3-methylimidazolium chloride ([Bmim]Cl), 1-butyl-3-methylimidazolium bromide ([Bmim]Br), N-allylpyridinium chloride ([Apy]Cl), N-allylpyridinium bromide ([Apy]Br) and N-butylpyridinium bromide ([BPy]Br) were investigated. Among these, [Bmim]Cl (>98.0%) and [Bmim]Br (>98.0%) were acquired from Wako Pure Chemical Industries. [Apy]Cl, [Apy]Br and [Bpy]Br, with yields of 98.8 wt.%, 97.4 wt.% and 96.0 wt.%, were synthesized with the same method as the procedures listed in our previous literature [18,20]. The catalyst, SO_4^{2-}/ZrO_2, was prepared as reported in our previous research [18]. The rest of chemicals used in this study, including pyridine, allyl chloride, allyl bromide, butyl bromide, methanol and acetonitrile, were of analytical grade and used as received. Distilled water was used in all cases.

2.2.2 Synthesis of ionic liquid

According to our previous studies [20] [Apy]Cl was synthesized in a 60 ml glass pressure vessel. [Apy]Br and [Bpy]Br used the same synthesis method as [Apy]Cl by the following process: firstly, acetonitrile, pyridine and allyl bromide were placed into a glass pressure vessel with the mole ratio of 1:1:1 and the mixture was reacted in a

microwave reactor at 150 W for 3 min, which was repeated 3 times, and then air-cooled to room temperature. After that, the residual pyridinium salt was washed by ether and the unreacted reactants, residual solvent and water were removed by using vacuum distillation at 70 °C for 60 min. Then [Apy]Br was synthesized with a yield of 97.4 wt.%. The content of H_2O in [Apy]Br was obtained by thermogravimetric analysis, which was 0.3 wt.%. The content of the impurity components in [Apy]Br were measured by gas chromatography with a flame ionization detector (GC-FID, Shimadzu Co., Japan) with the column of Ultra alloy-5 (Agilent, 60 m × 0.25 mm i.d., 0.25 μm) by diluting 10 mg of [Apy]Br 100 times with H_2O, and the specific method was described below. The purity of [Apy]Br was about 99.1%. The same method was used to synthesize [Bpy]Br with butyl bromide instead of allyl bromide with yield of about 96.0 wt.%, and the purity was about 99.4% including 0.5 wt.% of H_2O. Similarly, the H2O content and purity of the synthesized [Apy]Cl were around 0.3 wt.% and 99.5%.

2.2.3 Catalytic Depolymerization of Alkali Lignin.

In order to select ILs with high activity for lignin depolymerization, the depolymerization of alkali lignin by using different ILs was studied. Prior to reaction, alkali lignin was dried at 110 °C for 2 h and ILs were re-dried at 70 °C under high vacuum for 2 h. A measure of 0.5 g of alkali lignin was dissolved in the different ILs and H_2O mixtures with the mass ratio of lignin: IL: H_2O = 1:10:1 at 100 °C in a glass tube reactor, which was defined as feedstocks. Then 1.1 g of the catalyst, SO_4^{2-}/ZrO_2, was added in the reactor and heated to 200 °C for 3 h. The dissolution and reaction temperatures were monitored and measured by an oil bath with magnetic stirring at 700 rpm.

In this study, lignin was firstly extracted from the alkali lignin and IL solution to study the effect of the ILs dissolution on lignin before reaction. After dissolution and

reaction, the mixture was cooled to room temperature with the potential antisolvents (H_2O and acetonitrile) added to precipitate solid residues, which was defined as IL-lignin. The IL-lignin was isolated by filtering through a glass sinter and heating to 70 °C for 30 min. Then the filtered IL-lignin was air-dried and further dried in an oven at 60 °C for 10 hours, and then weighed and measured. The supernatant was extracted by adding ether, and the amount of ether added was twice those of H_2O and acetonitrile to regenerate the ILs as an ether insoluble fraction, which was defined as the liquid products that were analyzed by gas chromatography with flame ionization detector (GC-FID, Shimadzu Co., Japan) and gas chromatography-mass spectrometer (GC-MS, Shimadzu Co., Japan) with the same column of Ultra alloy-5 (Agilent, 60 m × 0.25 mm i.d., 0.25 μm). GC-FID and GC-MS used same analysis methods as following: 1 μL of the liquid products was injected on the column with a split ratio of 1:80, and then used helium as carrier gas with a constant flow at 1.5 $mL \cdot min^{-1}$. The GC oven was programmed from 45 °C (1 min) to 100 °C at 10 $°C \cdot min^{-1}$ and held for 10 min, and then increased to 320 °C at 10 $°C \cdot min^{-1}$ and held for 5 min. The interface temperature was 200 °C. O-xylene was used as the internal standard (IS) for the confirmation of the peaks position and the mass-to-charge ratio [18]. The mole yield of carbon-based products for the whole reaction was calculated with respect to the IS. All the tests were repeated three times, and the data were reported as the mean values of three trials. The mole yield of the carbon-based products (*Y*c, C, mol%) was calculated by following equation (Equation (2-1)):

$$Y_c,\ (C,\ mol\%) = \frac{\text{Carbon moles in products}}{\text{Carbon moles in feedstock}} \times 100\% \qquad (2\text{-}1)$$

The regenerated ILs and liquid products were concentrated through vacuum distillation and the regenerated ILs were dried at 70 °C under high vacuum to remove the extraction solvents.

2.2.4 Extraction of Lignin from Simulated Mixture and Red Pine

In preliminary studies, 0.1 g of a simulated mixture, which consisted of alkali lignin, cellulose and xylan with the mass ratio of 1:1:1, was dissolved in 3.3 g of IL completely at 100 °C in a 100 ml glass reactor, and then cooled to room temperature. A two-step process of extracting lignin from the simulated mixture was proposed and appeared most promising, as shown in Scheme 2.1. Firstly, methanol was used as antisolvent1, and the methanol-insoluble fraction, which was defined as the cellulose-rich solids, was precipitated while the lignin remained in solution. The lignin was precipitated in a second step. H_2O and acetonitrile used as antisolvent2 were added in turn to extract the H_2O-soluble and H_2O-insoluble fractions, respectively, which were collected and defined as IL-M-lignin. The extracted cellulose-rich solids or IL-M-lignin was washed by methanol, H_2O and acetonitrile to make sure the IL was essentially removed, and then they were centrifuged at 3000 rpm for 4 min and vacuum dried at 70 °C for 3 h. The antisolvents were removed by distillation, followed by IL recovery with the addition of excess ether and concentrated by vacuum distillation at 70 °C. After that, the extracted cellulose-rich solids or IL-M-lignin were weighed and analyzed by FT-IR and TGA. The same extraction process was applied to the extraction of lignin (IL-R-lignin) from red pine. Furthermore, the effect of the mass ratio of antisolvent (methanol, H_2O and acetonitrile):IL from 1:1 to 1:20 and the different dissolution time from 3 h to 12 h for IL-lignin extraction were investigated. The yields of extracted IL-R-lignin and cellulose-rich solids were calculated according to Equation (2-2) and (2-3):

$$Yield_{\text{lignin}} = \frac{\text{Extracted lignin (mg)}}{\text{Original content of lignin in red pine (mg)}} \times 100\% \quad (2\text{-}2)$$

$$Yield_{\text{cellulose}} = \frac{\text{Extracted cellulose-rich solids (mg)}}{\text{Red pine (mg)}} \times 100\% \quad (2\text{-}3)$$

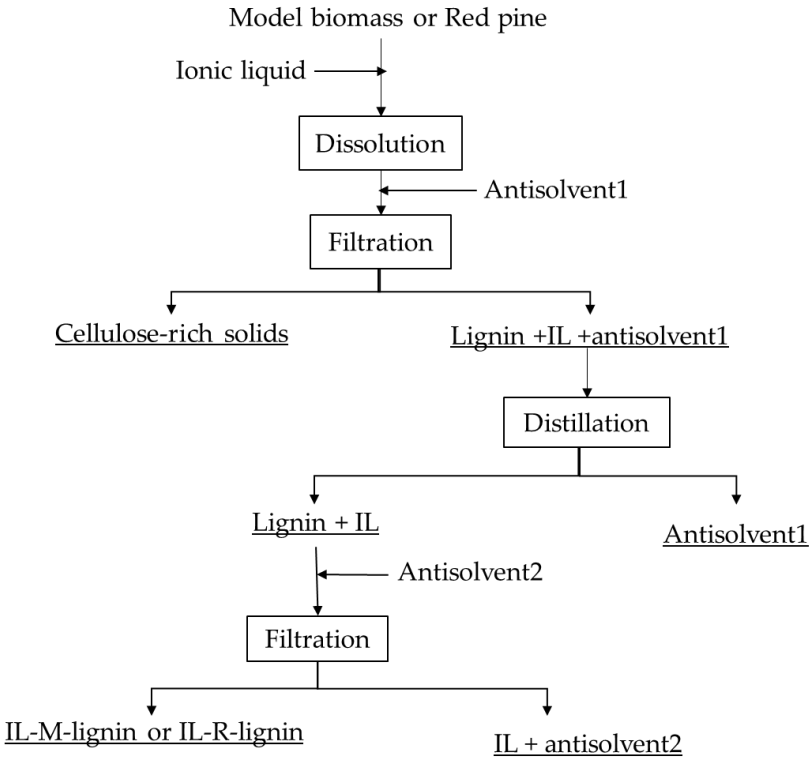

Scheme 2.1. Flow chart of extraction procedure.

2.2.5 Characterization of Extracted Lignin

The extracted lignin was characterized by FT-IR spectrophotometer compared with that of alkali lignin. Approximately 2.00 mg of lignin was mixed with 200 mg of KBr and mechanically pressed to form a transparent wafer. FT-IR spectra were performed by an IR Prestige-21 (Shimadzu Co., Japan) spectrometer from 4000 to 600 cm^{-1} with 64 scans at a resolution of 2 cm^{-1}.

A thermal gravimetric analyzer (DTG-60, Shimadzu Co., Japan) was used to measure the thermal decomposition temperature (T_d) of the IL-lignin. Approximately 10 mg of the samples was placed in an aluminum pan and heated at a rate of 10 °C min^{-1} with a temperature range of 100–800 °C at a rate of 50 ml/min in N_2.

Elemental analysis (CHN) of the extracted lignin and cellulose-rich solids, including

the amount of carbon, hydrogen and nitrogen in the samples, were analyzed by a CHN analyzer (JM10, J-science Lab Co., Japan). About 2 mg of each sample covered in a silver capsule was analyzed.

^{13}C-NMR analysis was recorded to study the structure of the synthesized IL and regenerated IL. ^{13}C-NMR spectra were obtained in D_2O using JNM-ECA-500 (JEOL Ltd., Japan) at 500 MHz. A measure of 10 mg of the sample of fresh or regenerated [Apy]Cl was diluted 10 times with D_2O and 600 µl of sample was injected into a quartz glass sample tube, which was then performed for 800 scans.

2.3 Results and discussion

2.3.1 Thermal Stability of ILs

TGA analysis was conducted to explore the thermal stabilities of the fresh ILs. The DTG curves of ILs are shown in Figure 2.1. The maximum thermal decomposition temperatures of [Apy]Cl, [Apy]Br, [Bpy]Br, [Bmim]Cl and [Bmim]Br were 232, 253, 262, 288 and 311 °C, respectively. The thermal stability of the ILs was [Bmim]Br > [Bmim]Cl > [Bpy]Br > [Apy]Br > [Apy]Cl.

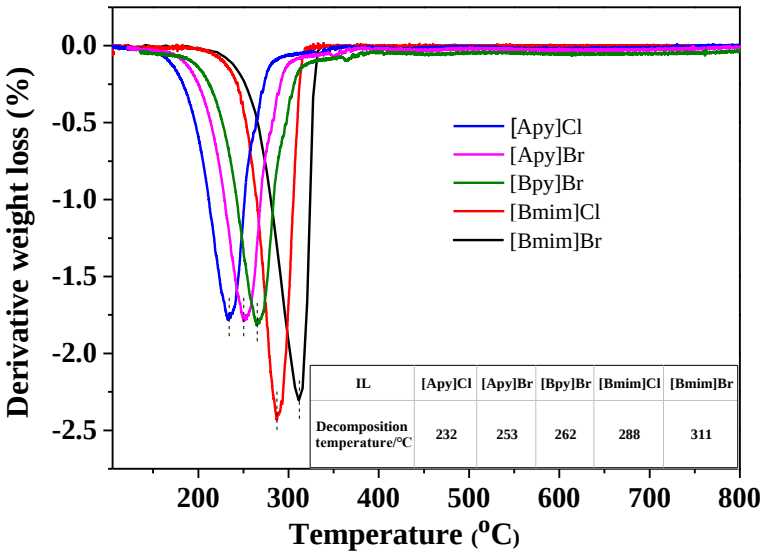

Figure 2.1. TGA and DTGA curves of the fresh ILs.

2.3.2 Effect of ILs Dissolution on Alkali Lignin

In order to study the effect of ILs dissolution on lignin, alkali lignin, as a model, was extracted and characterized from different ILs solution. The DTG curves of raw alkali lignin and extracted IL-lignin are shown in Figure 2.2. The maximum decomposition temperature of raw alkali lignin was 350 °C, due to different ILs presenting distinct solubility for alkali lignin with the disruption of intramolecular hydrogen or β-O-4 bonds. The ones that extracted IL-lignin by using [Apy]Cl, [Apy]Br, [Bpy]Br, [Bmim]Cl and [Bmim]Br appeared at 235, 250, 264, 286 and 288 °C, which indicated that the extracted IL-lignin became more ready to decompose than that of the raw alkali

lignin, especially for the extracted [Apy]Cl-lignin.

FT-IR analysis was performed for IL-lignin with raw alkali lignin used as the standard. FT-IR spectra of alkali lignin and IL-lignin are compared in Figure 2.3. Different types of peaks characteristic to aryl ring stretching, aromatic skeleton vibration and aromatic C–H deformation were observed according to the reference [21–23]. As shown in Figure 2.3, there was no significant difference between the raw alkali lignin and extracted IL-lignin.

All of IL-lignin and alkali lignin samples were dominated by a wide band at 3418 cm^{-1}, which is attributed to phenolic and aliphatic O–H groups. Bands around 1635 cm^{-1} are attributed to the C=C stretching vibration [24]. It was obviously found that after the dissolution of [Apy]Cl, [Apy]Br and [Bpy]Br, the absorbance intensity of the peak at 1635cm^{-1} increased compared to the raw alkali lignin, indicating these IL-lignin had a much higher content of double bonds [25]. Meanwhile, the absorbance intensity of the peak at 770 cm^{-1} was increased after ILs dissolution, which represented deformation vibrations of C–H bonds associated to aromatic rings, indicating that IL-lignin was more prone to aryl substitution reaction. Overall, all of the ILs used in dissolution had an insignificant modification effect on the structure of alkali lignin.

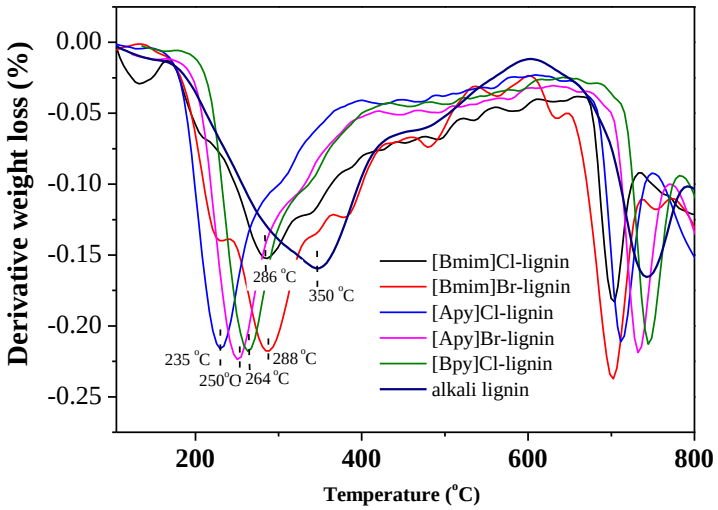

Figure 2.2. DTG thermograms of alkali lignin and extracted IL-lignin from dissolution.

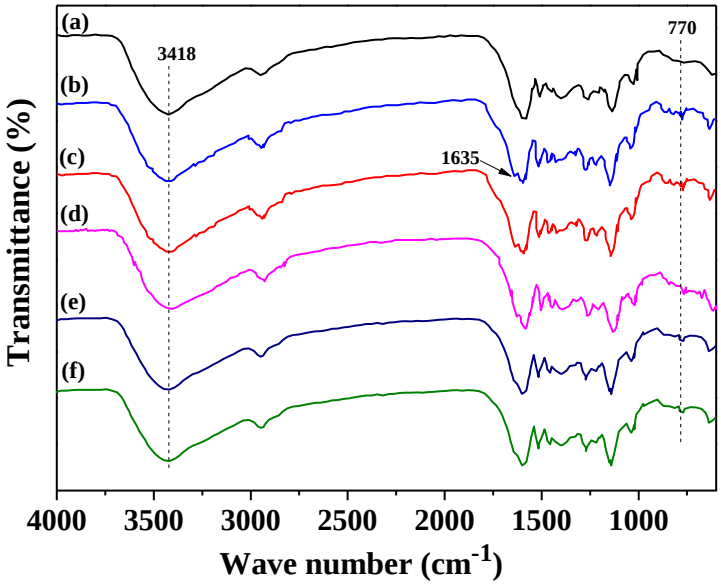

Figure 2.3. Comparison of FT-IR spectrum of the alkali lignin and IL-lignin; (a): alkali lignin; (b)–(f): [Apy]Cl-lignin, [Apy]Br-lignin, [Bpy]Br-lignin, [Bmim]Cl-lignin and [Bmim]Br-lignin (dissolution condition: 100 °C, 6 h).

2.3.3 Catalytic Depolymerization of Alkali Lignin in IL

Firstly, alkali lignin was dissolved into the ILs and H_2O mixture, and in the presence of the SO_4^{2-}/ZrO_2 catalyst, the catalytic depolymerization of alkali lignin was carried out in a glass tube reactor at 200 °C for 3 h. After depolymerization, the main liquid products obtained by using different ILs were quantified and identified by GC-FID and GC-MS. Figure 2.4 and Table 2.1 show the main liquid products and their details of structure from alkali lignin depolymerization using [Apy]Cl. Based on these results, the products obtained by using other ILs were analyzed and calculated. The yields of the main products obtained by different ILs are summarized in Table 2.2. The peaks for (i) and (ii) were the extract solvents and the residue of pyridine in the process of the synthesis of ILs, respectively. As listed in Table 2.2, phenolic compounds showed higher yield and *p*-methylguaicol was the main product. Notably, [Apy]Cl showed higher catalytic activity for lignin depolymerization than those of others ILs under mild condition. It was consistent with the results of the DTG analysis that [Apy]Cl-lignin was more ready to decompose after dissolution. Considering the high reactivity of [Apy]Cl in lignin catalytic depolymerization and its mild modification of alkali lignin

structure, the further study on the extraction of lignin from red pine was conducted by using [Apy]Cl.

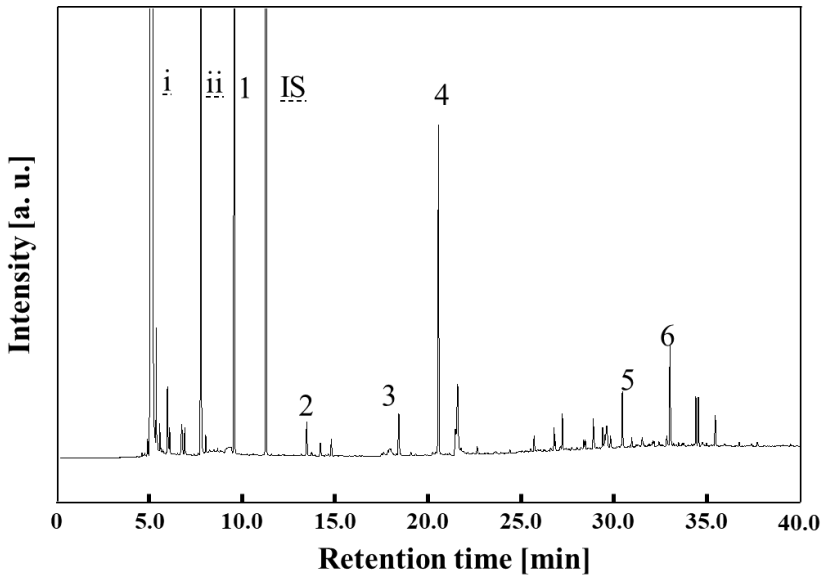

Figure 2.4. GC-FID spectra of liquid products over ZrO_2/SO_4^{2-} catalyst in [Apy]Cl.

Table 2.1. Identification of liquid products by means of GC-MS.

No.	Compounds	Structure
1	Furfuryl alcohol	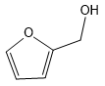
2	Benzaldehyde	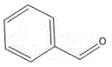
3	Guaiacol	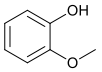
4	*P*-methylguaicol	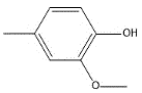
5	2,2'-Biphenol	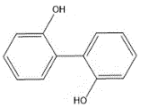
6	1-(4-Hydroxy-3,5-dimethoxyphenyl) propan-1-one	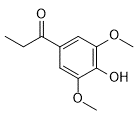

Table 2.2. Effect of ILs on alkali lignin depolymerization at 200 °C for 3 h over SO_4^{2-}/ZrO_2 catalyst.

Products	Yield/C, mol%				
	[Apy]Cl	**[Apy]Br**	**[Bpy]Br**	**[Bmim]Cl**	**[Bmim]Br**
Furfuryl alcohol	3.08	7.47	-	-	-
Benzaldehyde	1.45	0.35	-	-	-
Guaiacol	1.78	0.04	-	-	-
P-methylguaicol	8.9	3.22	-	-	-
2,2'-Biphenol	0.73	0.54	-	-	-
1-(4-Hydroxy-3,5-dimethoxyphenyl) propan-1-one	1.91	1.01	-	0.61	0.49
Unknown	12.33	8.61	-	4.42	4.13
***Y*c**	30.18	21.24	-	5.03	4.62

Unknown, uncertain components in the products; ***Y*c**, total mole yields of carbon-based products.

2.3.4 Effect of Mass Ratios of Antisolvent to IL

In preliminary studies, the raw cellulose could be dissolved into [Apy]Cl completely and almost all of the cellulose was extracted when the mass ratio of methanol:[Apy]Cl was 1:1. Under the same conditions, the extraction result of xylan showed that the xylan was almost completely decomposed and could not have the xylan-[Apy]Cl solid extracted from it. Considering the amount of antisolvent (methanol, H_2O and acetonitrile) was an important factor for extracting lignin from the simulated mixture and red pine, the effects of different mass ratios of antisolvent:IL from 1:1 to 20:1 were investigated. A measure of 0.1 g of simulated mixture was put into 3.3 g of [Apy]Cl, and then we used the two-step process (Scheme 2.1) to extract the lignin. As presented in Figure 2.5, under the condition that methanol was the antisolvent1 and that the mass ratio of methanol:[Apy]Cl was 1:1, the content of the precipitated lignin ([Apy]Cl-M-lignin) from the simulated mixture increased when the mass ratio of antisolvent:IL increased from 1:1 to 20:1. The recovery ratio of [Apy]Cl-M-lignin by adding H_2O and

acetonitrile was studied separately and it was proven to be the most efficient antisolvent with recovery ratios of 75.0 wt.% and 66.1 wt.% under the same mass ratio of 20:1. Due to the high recovery ratio of [Apy]Cl-M-lignin precipitated and the insignificant change in the content elements compared to alkali lignin (Table 2.3), H_2O and acetonitrile with the mass ratio of 20:1 were considered as promising antisolvents and used for the further extraction of lignin from red pine. Meanwhile, it was found that [Apy]Cl-M-lignin was also precipitated when methanol was used as antisolvent2 and the mass ratio of methanol:[Apy]Cl was more than 3:1. Additionally, 0.5 wt.% of [Apy]Cl-M-lignin and 99.1 wt.% of cellulose-rich solids were precipitated with a mass ratio of methanol:[Apy]Cl at 3:1. As shown in Table 2.3, elements of the extracted cellulose-rich solids were similar to the raw cellulose, even with almost the same thermogravimetry as that of raw cellulose (Figure 2.6), which indicated that during [Apy]Cl dissolution, most of the xylan in the simulated mixture was decomposed. Therefore, the extraction of cellulose-rich solids from red pine was conducted by using methanol with a mass ratio of methanol:[Apy]Cl at 3:1.

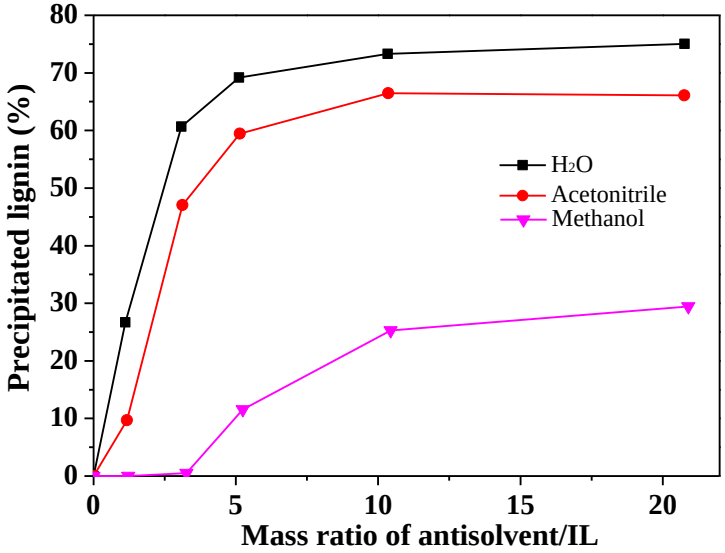

Figure 2.5. Effect of the mass ratio of antisolvent:IL on lignin extraction from simulated mixture.

Table 2.3. Elemental analysis.

Content (wt.%)	H	C	N
Cellulose [a]	6.47	42.89	0.15
Cellulose-rich solids [b]	6.78	43.41	0.17
Cellulose-rich solids [c]	6.83	46.77	0.20
Alkali lignin [a]	4.32	50.23	0.13
[Apy]Cl-M-Lignin [b]	4.01	50.00	0.47
[Apy]Cl-R-Lignin [c]	3.74	49.97	0.21

[a] Supplied by Sigma Aldrich; [b] From dissolution of simulated mixture using [Apy]Cl; [c] From dissolution of red pine using [Apy]Cl.

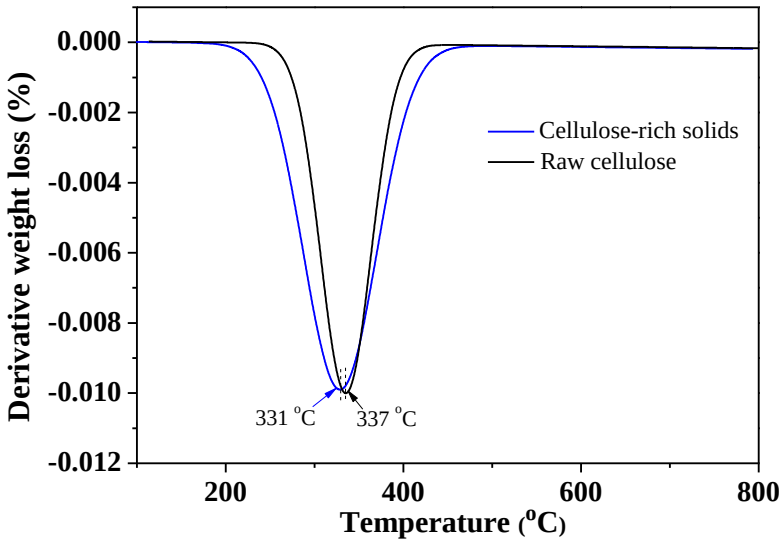

Figure 2.6. DTG thermograms of cellulose and extracted cellulose-rich solids from simulated mixture using [Apy]Cl**.**

2.3.5 Effect of Dissolution Time on Lignin Separation from Red Pine

A measure of 0.1 g of a ground sample of red pine (250–106 μm) was dissolved in 3.3 g of [Apy]Cl at 100 °C; then methanol, H_2O and acetonitrile were added and the mass ratio of [Apy]Cl to methanol, H_2O and acetonitrile were 1:3, 1:20 and 1:20 for extracted cellulose-rich solids and [Apy]Cl-R-lignin using the process showed in Scheme 1. Different dissolution times for red pine in [Apy]Cl from 3 to 12 h were investigated, as shown in Table 2.4. With the increase of dissolution time from 3 h to 6 h, the total recovery ratio of [Apy]Cl-R-lignin, based on the original content of lignin (26.2 wt. %) in red pine, was increased from 56.9 to 98.7 wt.%, and then decreased to

97.3 wt.% after 12 h of dissolution. In addition, the total recovery ratio of cellulose-rich solids was reduced from 104.7 to 76.4 wt.% with the dissolution time increased, possibly due to partial of hemicellulose, and cellulose was decomposed during [Apy]Cl dissolution.

Table 2.4. Effect of dissolution time on lignin recovery at 100 °C.

Time/h	Recovery Ratio (wt.% ± 1.5)	
	Lignin	Cellulose-Rich Solids
3	56.9	104.7
6	98.7	95.2
9	97.9	84.6
12	97.3	76.4

Table 2.3 shows the main elemental composition of alkali lignin, cellulose, the extracted [Apy]Cl-R-lignin and the cellulose-rich solids. The [Apy]Cl-R-lignin and cellulose-rich solids were extracted from red pine after [Apy]Cl dissolution at 100 °C for 6 h. Based on the results, there was an insignificant change in the content elements for the [Apy]Cl-R-lignin compared to alkali lignin. Therefore, the extracted lignin basically maintained its original functionality. The slight change of element content was due to the breakage of partial bonds during dissolution, which was consistent with the conclusion for the extracted alkali lignin seen above. For the extracted cellulose-rich solids, it possessed a slightly larger carbon content compared to commercial cellulose, which was due to part of the hemicellulose or decomposed macromolecules being precipitated during separation. The elemental analyses also showed a slight increase in the N amount for the extracted [Apy]Cl-R-lignin, which was from the cation of [Apy]Cl. This was possibly due to a small amount of residual [Apy]Cl due to the interaction between the ionic liquid and lignin molecules during the dissolution process.

2.3.6 Characterization of [Apy]Cl-R-Lignin from Red Pine

For alkali lignin and [Apy]Cl-R-lignin, under the premise of eliminating different production processes, a wide band at 3401 cm^{-1} represented the phenolic and aliphatic OH groups [26,27], followed by bands for carbonyl stretching (1710 cm^{-1}), C–O stretching of syringyl groups (1390 cm^{-1}), C=O deformation of guaiacyl groups (1216 cm^{-1}), C–O absorption of the methoxy group on the benzene ring (1129 cm^{-1}) and C–O(C) stretching of ether groups (1036 cm^{-1}) [28,29]. As shown in Figure 2.7, the absorbance intensity of the peak at 1710, 1216 and 1036 cm^{-1} increased compared to alkali lignin, indicating that [Apy]Cl-lignin had a much higher content of unsaturated bonds. Additionally, the absorbance intensity of the peak at 1390 and 1129 cm^{-1} decreased for [Apy]Cl-R-lignin, indicating that the demethylation reaction and breakage of the ether bond occurred during [Apy]Cl dissolution.

As shown in Figure 2.8, the intensity of peak at 1513 cm^{-1} was attributed to the aromatic skeletal vibrations in lignin increasing, indicating that partial lignin was precipitated with the methanol extraction. The band at 1155 cm^{-1} corresponded to C–O–C asymmetric stretching vibration in cellulose/hemicellulose [30], and the intensity of this bond decreased, indicating that partial cellulose or hemicellulose was decomposed in [Apy]Cl.

The spectra of the extracted [Apy]Cl-R-lignin and cellulose-rich solids from red pine are compared to those of raw alkali lignin and cellulose in Figure 2.7 and Figure 2.8. The close similarity of the spectra indicates that lignin was extracted from red pine with mild modification.

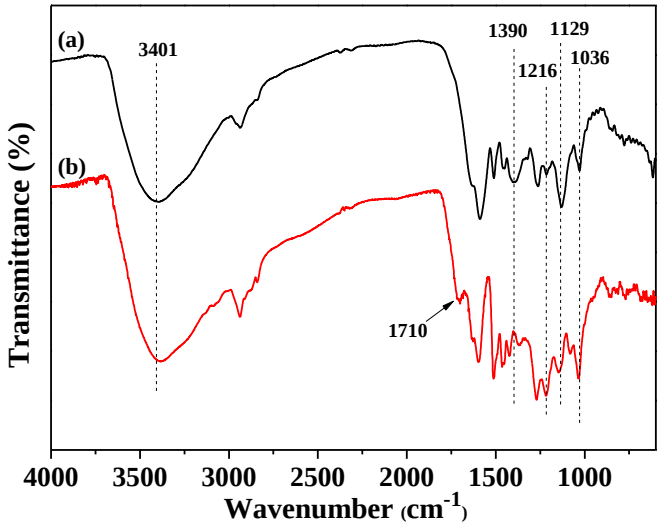

Figure 2.7. FT-IR spectrum of raw alkali lignin (a) and extracted [Apy]Cl-R-lignin (b) from red pine.

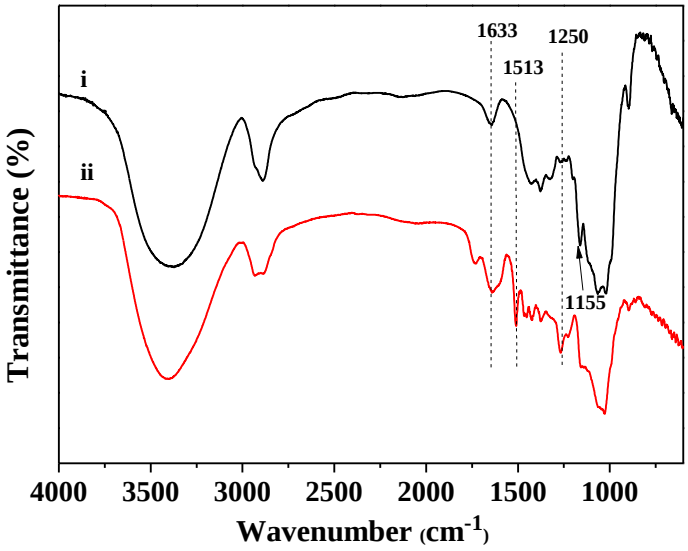

Figure 2.8. FT-IR spectrum of commercial cellulose (i) and cellulose-rich solids (ii) from red pine.

The TGA and DTGA curves of the raw alkali lignin and extracted [Apy]Cl-R-lignin from red pine are shown in Figure 2.9. The maximum decomposition temperature of raw alkali lignin was 350 °C, and the temperature for extracted lignin from red pine appeared at 231 °C, due to the partial decomposition of [Apy]Cl-R-lignin during the dissolution of [Apy] Cl, which was also consistent with our previous research results [19]. Meanwhile, this result indicates that the extracted [Apy]Cl-R-lignin was more ready to decompose.

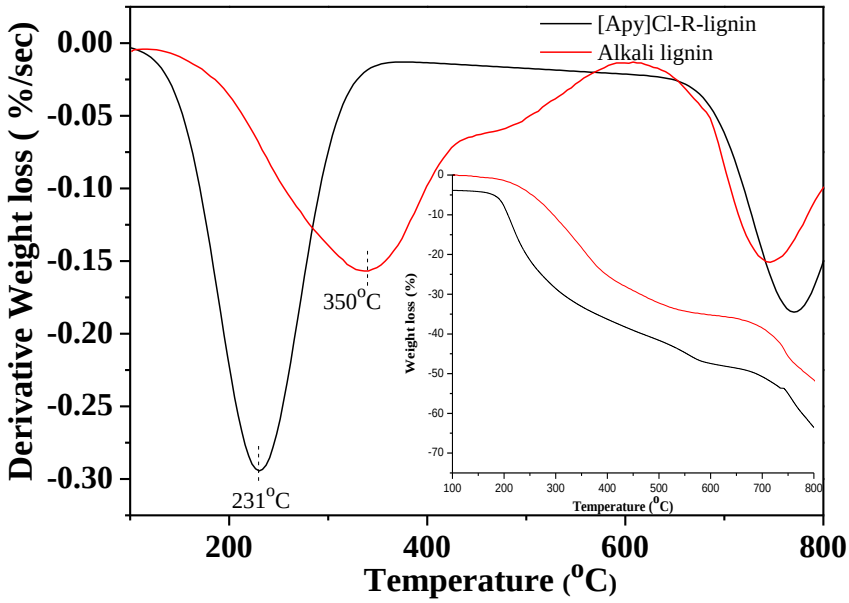

Figure 2.9. TGA and DTGA curves of raw lignin and extracted lignin from red pine.

2.3.7 Recovery of [Apy]Cl

The regenerated mass yield of the ionic liquid was 96.1 ± 0.5 wt.%. The ^{13}C-NMR spectra of the regenerated [Apy]Cl and fresh [Apy]Cl showed no change in structure (Figure 2.10). Also, TGA analysis results showed the maximum weight loss rates of both appeared to be around 232 °C (Figure 2.11), and the overall thermal decomposition behavior of the regenerated [Apy]Cl was found to be similarly to that of the fresh, which demonstrated potential recyclability.

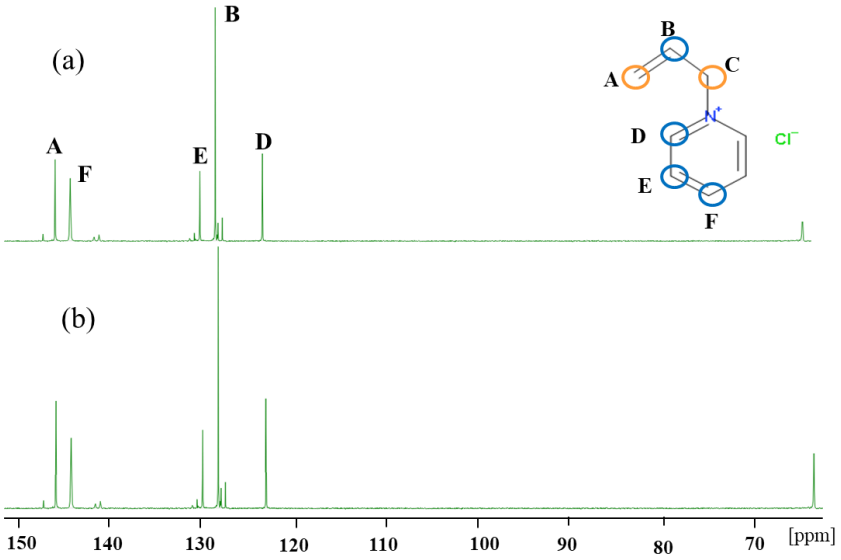

Figure 2.10. ^{13}C-NMR spectrums of fresh [APy]Cl (a) and [Apy]Cl-lignin (b) from red pine.

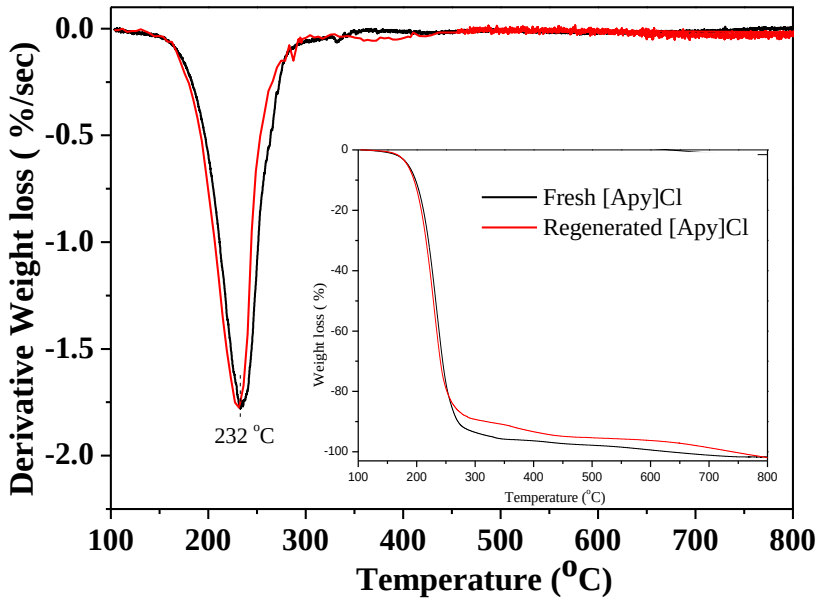

Figure 2.11. TGA and DTGA curves of [Apy]Cl and the regenerated [Apy]Cl.

2.4 Pathway of alkali lignin dissolution in [Apy]Cl

Based on above results and analysis, the mechanism of alkali lignin dissolution in [Apy]Cl was studied by using guaiacol and the synthesized lignin model compounds (2-(2-methoxyphenyl)oxy-acetophenone and 2-(2-methoxyphenyl)oxy-1-phenethanol , Table 2.3, Scheme 2.2 and Scheme 2.3), which were dissolved in [Apy]Cl completely.

Table 2.3. Structure of synthesized lignin model compounds.

Compounds	Chemical structure
Guaiacol	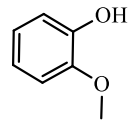
2-(2-methoxyphenyl)oxy-acetophenone	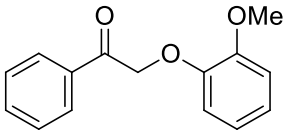
2-(2-methoxyphenyl)oxy-1-phenethanol	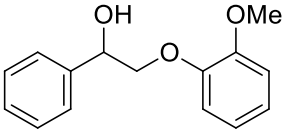

2-(2-methoxyphenyl)oxy-acetophenone (model a) was synthesized by the following methods: 2-bromo-1-phenylethanone and guaiacol with the mole ratio of 1:1 with moderate amount of acetone and potassium carbonate were added in a three-necked round bottom flask. Then reflux for 3 hours and filtered through a membrane filter to separate potassium carbonate. After that, the filtrate was concentrated by rotary evaporator and washed by ethanol to obtain the substrates of 2-(2-methoxyphenyl)oxy-acetophenone (yield, 70.3 %) as shown in Scheme 2.2.

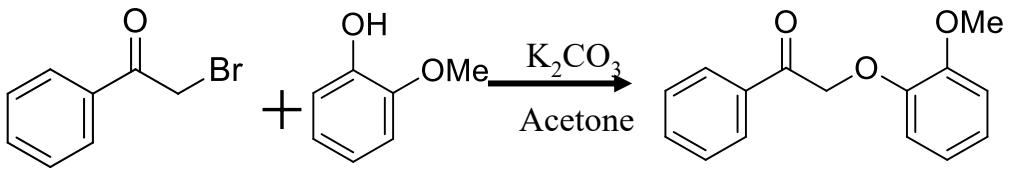

Scheme 2.2. Synthesis of 2-(2-methoxyphenyl)oxy-acetophenone.

2-(2-methoxyphenyl)oxy-acetophenone (model b) was synthesized by the following methods: the solvent including 28 mL of tetrahydrofuran and 7 mL of distilled water with 1.97 g (8.06 mmol) of 2-(2-methoxyphenyl)oxy-acetophenone were added to a three-necked round bottom flask, then 704 mg (18.6 mmol) of sodium borohydride was added as a reducing agent. After 4 hours of reaction at room temperature, 50 mL

saturated ammonium chloride solution was added to terminate the reaction. After further conversion and dilution of 50 mL distilled water, the product was extracted three times with 50 mL diethyl ether. In addition, the ether layer was washed twice with saturated sodium chloride solution, and then dried with anhydrous sodium sulfate. Finally, 2-(2-methoxyphenyl)oxy-1-phenethanol was obtained by concentrating in a rotary evaporator (yield, 63.5 %) as shown in Scheme 2.3.

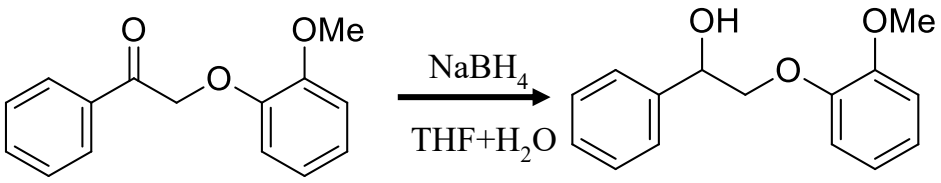

Scheme 2.3 Synthesis of 2-(2-methoxyphenyl)oxy-1-phenethanol.

After dissolution, acetonitrile was added to the liquid mixtures, including [Apy]Cl and products, with the mass ratio of acetonitrile/liquid mixtures was 20, the acetonitrile-insoluble fraction was defined as the solid residue. The acetonitrile-soluble fraction was extracted by ether and the amount of ether added was twice that of acetonitrile, and the ether-insoluble fraction was defined as the regenerated IL, whereas the ether-soluble fraction was defined as the liquid products. Then, the liquid products were further concentrated via vacuum distillation at 70 °C to remove the extraction solvents.

For each test, samples of liquid products were collected after concentration, weighed to obtain the mass and then analyzed by gas chromatography with flame ionization detector (GC-FID, Shimadzu Co.) and gas chromatography-mass spectrometer (GC-MS, Shimadzu Co.). The compounds were quantified by GC-FID with a column of Ultra alloy-5 (Agilent, 60 m×0.25 mm i.d., 0.25 μm) and identified by GC-MS using a J&W Scientific DB-1 column (Agilent, 60 m×0.25 mm i.d., 0.25 μm). To confirm the position and the mass-to-charge ratio of the peaks, internal standard (IS) was chose by

comparing to GC-FID spectra of the liquid products with/without o-xylene. The results showed that there was no o-xylene in the liquid products, o-xylene was used as IS for the further study with the mass fraction of 1 wt. %. After repeated three times of all the test, the average of three trials were used in this study.

The liquid products obtained from dissolution of those three lignin model compounds in [Apy]Cl were quantified and identified as shown in Figure 2.12, Table 2.4 and 2.5. According to the results of guaiacol conversion, 2.81 % of catechol was produced after [APy]Cl pretreatment, indicating the demethylation occurred and [Apy]Cl cloud be treated as a reagent to cleave of methyl aryl ethers in lignin. For the synthesized lignin model compounds (model a and b), the composition and distribution of the products indicated that [Apy]Cl could lead to the cleavage of β-O-4 bond and methyl aryl ethers. Based on above analysis, the produced catechol originated from two parts: one was from the demethylation of guaiacol in ionic liquids; the other part was from the depolymerization of the model under the effect of [Apy]Cl in the pretreatment process. A hypothetical mechanism of model a and b under [Apy]Cl pretreatment was proposed as shown in Scheme 2.4.

Based on above results, the proposed mechanism of alkali lignin dissolution in [Apy]Cl was suggested in Scheme 2.5, which including the cleavage of β-O-4 bond in [Apy]Cl pretreatment. Based on the distribution of the liquid products obtained from the model compounds, lignin was effectively depolymerized with the partial cleavage of β-O-4 into low molecular weight products with the increase of phenolic hydroxyl content after [Apy]Cl pretreatment. As illustrated in Scheme 2.5, [Apy]Cl contains strong coordinating anion (Cl^-) was used as a reaction media to stabilize the hydroxyl group on the intermedia compounds. Products with β-O-4 bond converted into an enol ether isomer by dehydration, then hydrolyzed to release guaiacol and carbonyl compounds. Meanwhile, under the demethylation of [Apy]Cl partial of guaiacol

converted into catechol.

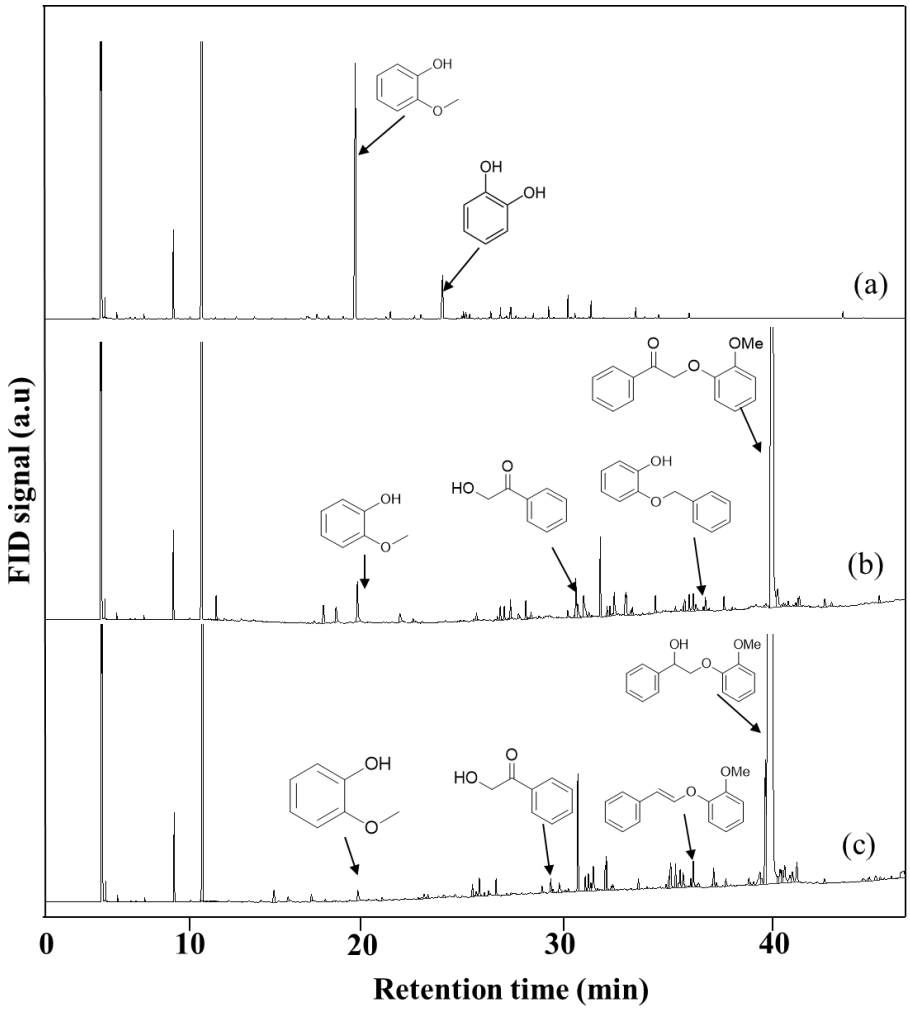

Figure 2.12. GC-FID spectra of liquid products from [Apy]Cl pretreatment, (a) guaiacol; (b) model a; (c) model b.

Table 2.4. Quantification of the identified liquid products from model a.

No.	Compounds	Structure	Yield, %
1	Guaiacol	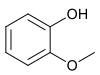	0.42
2	2-hydroxy-1-phenyl-ethanone	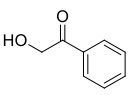	0.35
3	1-methoxy-2-phenethoxybenzene	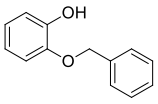	0.10
4	Model a		92.64
Others	Unknown		6.49

Table 2.5. Quantification of the identified liquid products from model b.

No.	Compounds	Structure	Yield, %
1	Guaiacol	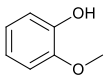	0.02
2	2-hydroxy-1-phenyl-ethanone	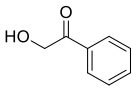	0.03
3	1-methoxy-2-(styryloxy)benzene	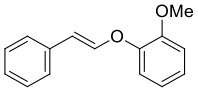	0.06
4	Model b		97.13
Others	Unknown		2.76

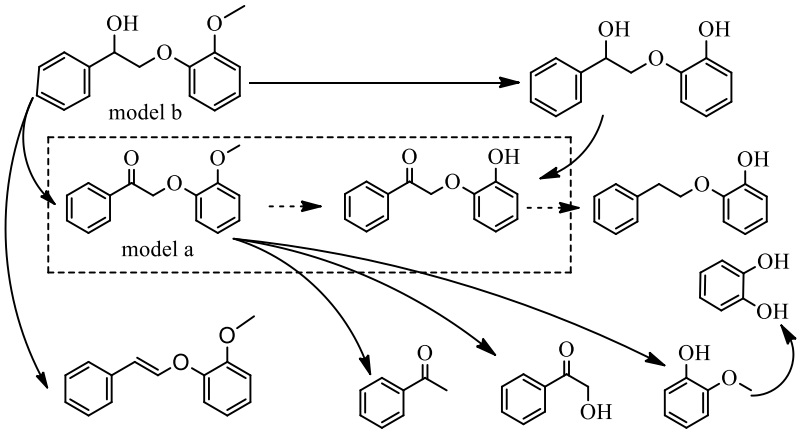

Scheme 2.4. Pathway of model a and b dissolution in [Apy]Cl.

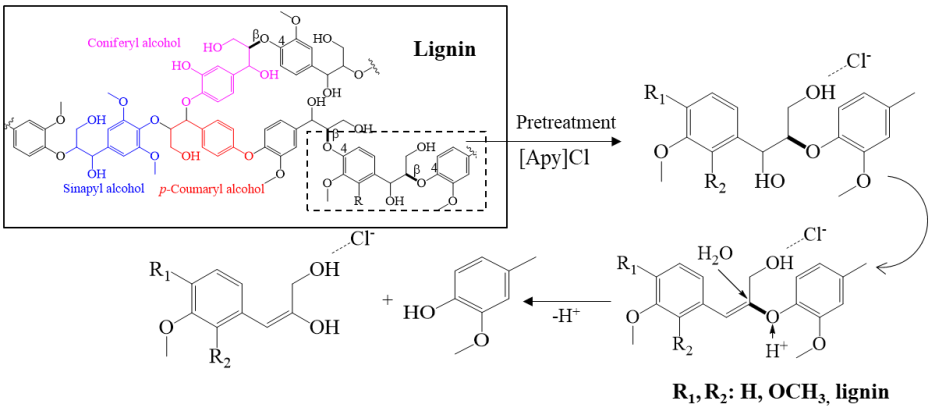

Scheme 2.5. Pathway of lignin dissolution in [Apy]Cl.

2.5 Conclusions

In order to compare the catalytic activity for lignin depolymerization and the mild modification effect on the structure of alkali lignin among the used ILs, [Apy]Cl was chosen as a promising ionic liquid. By investigating the effect of the amount of antisolvent on the recovery ratio of lignin, the mass ratios of methanol:[Apy]Cl, H2O:[Apy]Cl and acetonitrile:[Apy]Cl were 3:1, 20:1 and 20:1, respectively, and were used to extract cellulose-rich solids and [Apy]Cl-lignin from red pine. The extraction of lignin from red pine was successfully achieved at atmospheric pressure, with 98.7 wt.% yield after 6 h of dissolution. Meanwhile, the regenerated [Apy]Cl had no change in structure and thermal stabilities, which demonstrated potential recyclability. Furthermore, based on results in the depolymerization and demethylation of guaiacol and 1-(4-hydroxyphenyl)-2-(2-methoxyphenoxy) ethenone, the effect of ionic liquid pretreatment was elucidated and a hypothetical mechanism of lignin dissolution in ionic liquid was proposed.

References

[1]. Sannigrahi, P.; Pu, Y.; Ragauskas, A. Cellulosic biorefineries—Unleashing lignin opportunities. Curr. Opin. Environ. Sust. 2010, 2, 383–393.

[2]. Goh, C.S.; Tan, K.T.; Lee, K.T.; Bhatia, S. Bio-ethanol from lignocellulose: Status, perspectives and challenges in Malaysia. Bioresour. Technol. 2010, 101, 4834–4841.

[3]. De Wild, P.; Reith, H.; Heeres, E. Biomass pyrolysis for chemicals. Biofuels 2011, 2, 185–208.

[4]. Carrier, M.; Loppinet-Serani, A.; Denux, D.; Lasnier, J.M.; Ham-Pichavant, F.; Cansell, F.; Aymonier, C. Thermogravimetric analysis as a new method to determine the lignocellulosic composition of biomass. Biomass Bioenerg. 2011, 35, 298–307.

[5]. Tuck, C.O.; Pérez, E.; Horváth, I.T.; Sheldon, R.A.; Poliakoff, M. Valorization of biomass: Deriving more value from waste. Science 2012, 337, 695–699.

[6]. Holladay, J.E.; White, J.F.; Bozell, J.J.; Johnson, D. Top value-added chemicals from biomass-volume II: Results of screening for potential candidates from biorefinery lignin. Biomass Fuels 2007, 2, 263–275.

[7]. Zakzeski, J.; Bruijnincx, P.C.; Jongerius, A.L.; Weckhuysen, B.M. The catalytic valorization of lignin for the production of renewable chemicals. Chem. Rev. 2010, 110, 3552–3599.

[8]. Li, C.; Zhao, X.; Wang, A.; Huber, G.W.; Zhang, T. Catalytic transformation of lignin for the production of chemicals and fuels. Chem. Rev. 2015, 115, 11559–11624.

[9]. Rinaldi, R.; Jastrzebski, R.; Clough, M.T.; Ralph, J.; Kennema, M.; Bruijnincx, P.C.; Weckhuysen, B.M. Paving the way for lignin valorisation: Recent advances in bioengineering, biorefining and catalysis. Angew. Chem. Int. Ed. 2016, 55, 8164–8215.

[10]. Baptista, C.; Robert, D.; Duarte, A. Relationship between lignin structure anddelignification degree in Pinus pinaster kraft pulps. Bioresour. Technol. 2008, 99, 2349–2356.

[11]. Gellerstedt, G.; Henriksson, G. Lignins: Major sources, structure, andproperties. In Monomers Polymers and Composites fromRenewable Resources; Gandini, M.N.B., Ed.; Elsevier: Amsterdam, The Netherlands, 2008; pp. 201–224.

[12]. Vila, C.; Santos, V.; Parajo, J.C. Recovery of lignin and furfural from aceticacid-water-HCl pulping liquors. Bioresour. Technol. 2003, 90, 339–344.

[13]. Liu, C.; Wang, H.; Karim, A.M.; Sun, J.; Wang, Y. Catalytic fast pyrolysis of lignocellulosic biomass. Chem. Soc. Rev. 2014, 43, 7594−7623.

[14]. Singh, S.K.; Dhepe, P.L. Ionic liquids catalyzed lignin liquefaction: Mechanistic studies using TPO-MS, FT-IR, RAMAN and 1D, 2D-HSQC/NOSEY

NMR. Green Chem. 2016, 18, 4098–4108.
[15]. Muhammad, N.; Man, Z.; Bustam, M.A.; Mutalib, M.I.A.; Rafiq, S. Investigations of novel nitrile-based ionic liquids as pre-treatment solvent for extraction of lignin from bamboo biomass. J. Ind. Eng. Chem. 2013, 19, 207–214.
[16]. Achinivu, E.; Howard, R.; Li, G.; Gracz, H.; Henderson, W. Lignin extraction from biomass with protic ionic liquids. Green Chem. 2014, 16, 1114–1119.
[17]. Li, Q.; He, Y.; Xian, M.; Jun, G.; Xu, X.; Yang, J.; Li, L.Z. Improving enzymatic hydrolysis of wheat straw using ionic liquid 1-ethyl-3-methyl imidazolium diethyl phosphate pretreatment. Bioresour. Technol. 2009, 100, 3570–3575.
[18]. Wang, X.; Wang, N.; Nguyen, T.T.; Qian, E.W. Catalytic depolymerization of lignin in ionic liquid using a continuous flow fixed-bed reaction system. Ind. Eng. Chem. Res. 2018, 57, 16995–17002.
[19]. Sluiter, A.; Ruiz, R.; Scarlata, C.; Sluiter, J.; Templeton, D. Determination of extractives in biomass. Laboratory Analytical Procedure (LAP). 2005, 1617.
[20]. Qian, E.; Tominaga, H.; Chen, T.; Isoe, R. Synthesis of functional ionic liquids and their application for the direct saccharification of cellulose. J. Chem. Eng. Jpn. 2016, 49, 466–474.
[21]. Yu, H.; Hu, J.; Fan, J.; Chang, J. One-pot conversion of sugars and lignin in ionic liquid and recycling of ionic liquid. Ind. Eng. Chem. Res. 2012, 51, 3452–3457.
[22]. Prado, R.; Brandt, A.; Erdocia, X.; Hallet, J.; Welton, T.; Labidi, J. Lignin oxidation and depolymerization in ionic liquids. Green Chem. 2016, 18, 834–841.
[23]. Das, L.; Xu, S.; Shi, J. Catalytic Oxidation and Depolymerization of Lignin in Aqueous Ionic Liquid. Front. Energy Res. 2017, 5, 21.
[24]. Qian, Y.; Zuo, C.; Tan, J.; He, J. Structural analysis of bio-oils from sub-and supercritical water liquefaction of woody biomass. Energy 2007, 32, 196–202.
[25]. Long, J.; Zhang, Q.; Wang, T.; Zhang, X.; Xu, Y.; Ma, L. An efficient and economical process for lignin depolymerization in biomass-derived solvent tetrahydrofuran. Bioresour. Technol. 2014, 154, 10–17.
[26]. Tejado, A.; Pena, C.; Labidi, J.; Echeverria, J.M.; Mondragon, I. Physico-chemical characterization of lignins from different sources for use in phenol–formaldehyde resin synthesis. Bioresour. Technol. 2007, 98, 1655–1663.
[27]. Xiao, B.; Sun, X.F.; Sun, R.C. Chemical, structural, and thermal characterizations of alkali-soluble lignins and hemicelluloses, and cellulose from maize stems, rye straw, and rice straw. Polym. Degrad. Stab. 2001, 74, 307–319.
[28]. Lou, R.; Wu, S.B.; Lv, G.J. Effect of conditions on fast pyrolysis of bamboo lignin. J. Anal. Appl. Pyrol. 2010, 89, 191–196.
[29]. Abdelaziz, O.Y.; Hulteberg, C.P. Physicochemical characterisation of technical lignins for their potential valorisation. Waste Biomass Valori. 2017, 8, 859–869.

[30]. Liu, C.; Sun, R.; Zhang, A.; Ren, J. Preparation of sugarcane bagasse cellulosic phthalate using an ionic liquid as reaction medium. Carbohydr. Polym. 2007, 68, 17–25.

Chapter 3

Catalytic Depolymerization of Alkali Lignin in [Apy]Cl Synergizing Solid Acid catalyst using a continuous flow fixed-bed reaction system

Abstract

The catalytic depolymerization of alkali lignin dissolved in a mixed solvent of ionic liquid (N-allylpyridinium chloride, [Apy]Cl) and water, with ZrO_2/SO_4^{2-} or Pt-ZrO_2/SO_4^{2-} catalyst, were performed in a continuous flow fixed-bed reaction system at low temperature (from 150 °C to 210 °C). The yields (carbon-based) of total products and phenolic compounds catalyzed by ZrO_2/SO_4^{2-}, which increased with increasing temperature, were 30.6 % and 13.4 % at 210 °C, respectively. Furthermore, the addition of platinum to the ZrO_2/SO_4^{2-} catalyst enhanced the depolymerization of alkali lignin. In the case of Pt-ZrO_2/SO_4^{2-}, the yields (carbon-based) of total products and phenolic compounds reached 44.9 % and 18.7 %, respectively, at 210 °C. Additionally, [Apy]Cl readily dissolved lignin and served as a medium for lignin depolymerization, which improved the reactivity of lignin for the use in the continuous flow system at low temperature.

3.1 Introduction

Lignin is a complex compound composed of phenylpropane structural units, which contains abundant aromatic polymers in lignocellulosic biomass, and the utilization of lignin has been studied for decades. The three main types of phenylpropane structural units in lignin are *p*-coumaryl alcohol, sinapyl alcohol and coniferyl alcohol. Due to unique chemical structure of lignin, makes it become a kind of alternative resources for the high-value chemicals through chemical, physical, or biological technologies [1]. The aromatic units in lignin are linked by C–O–C and C–C bonds in random order [2]. Among various types of C–O–C bonds, β–O–4 bond is the most abundant one, accounting for approximately 50–65 % of all bonds in lignin; in addition, it contains a small number of β–β, β–5 and 4–O–5 bonds [3,4].

Among various reported lignin utilization techniques, depolymerization is a promising one for converting lignin into value-added aromatic compounds. Methods for the depolymerization process of lignin vary according to different approaches, and mainly include acid- and/or base-catalyzed [5-8], thermochemical treatment-assisted, e.g., pyrolysis [9] and gasification [10,11], metal-catalyzed [12-15], biocatalysis-assisted [16-18] and Ionic liquids-assisted [19-21] lignin depolymerizations. Up to now, many researchers had studied the lignin depolymerizations by use of different catalysts associated with organic solvents [22-24], however, most of which operated at either higher temperature (≥ 250 °C) or pressure (> 2.5 MPa) with hydrogen or oxygen in batch reactors. To a certain extent, organic solvents used in the process will pollute the environment, on the other hand, the application of gas not only increases energy consumption, but also increases the requirements for the devices.

Nowadays, ionic liquids (instead of organic solvents)-assisted depolymerization process of lignin has been getting more and more attention, due to ionic liquids (ILs) are green and functional solvents with different kinds of anions and cations [25]. ILs in

the process are used as reaction media to dissolve lignin can promote the lignin depolymerization, moreover, the catalytic effects of the catalyst on the target bond are improved [1]. Therefore, the reaction conditions of lignin depolymerization using ILs are generally milder.

Due to the complexity of lignin structure, many researchers have studied lignin model compounds to explore optimum reaction conditions for lignin depolymerization. Kubo et al.[26] and Binder et al. [27] employed model compounds to study lignin depolymerization in several dialkylimidazolium ILs without or with catalysts in the presence of hydrogen in a batch reactor blew 200 °C, which suggested that ILs could not cleave the β–O–4 linkage in the absence of catalysts. Stärk et al. [19] studied the depolymerization of organosolv beech lignin by 1-ethyl-3-methylimidazolium trifluoromethansulfonate under the catalysis of $Mn(NO_3)_2$ at 100 °C and 8.4 MPa of air in a batch reactor, 2,6-dimethoxy-1,4-benzoquinone, rather than phenolic compounds, was the main product with the yield of 11.5%.

In order to select suitable ILs, Casas et al. [28] and Kilpeläinen et al. [29] studied on solubility of lignin in various ILs and suggested that ILs with the anions having smaller size, and higher coordination capacity such as chloride allowed the IL molecule to form hydrogen bonds with lignin and favorited dissolution of lignin. In addition, when a cation contains an unsaturated double bond or a benzene ring structure which can form strong π-π interactions with aromatic rings in lignin also tend to promote dissolution of lignin.

Therefore, taking into account the drawbacks of these reports, it is indispensable to develop a continuous flow system for efficient catalytic depolymerization of actual lignin into value-added aromatic products at low temperature (from 150 to 210 °C) without hydrogen or oxygen pressure. Based on the research of Zhang et al. [22] and Kimura [30], β–O–4 linkages were mainly cleaved with $ZrO_2/SO_4^{2-}$and Pt-promoted

SO_4^{2-}/ZrO_2 (Pt-SO_4^{2-}/ZrO_2) can be obtained steady activity during reaction, because of the stability of the strong acid sites in sulfated zirconium were improved with the addition of platnium. As far as we know, there is no related research on lignin depolymerization using ionic liquid as solvent in a continuous flow fix-bed reaction system has been reported.

In the present study, N-allylpyridinium chloride ([Apy]Cl) added less water where the water was also considered as a reactant was used as the solvent for lignin as well as a medium for lignin catalytic depolymerization, and a continuous flow fixed-bed reaction system was developed to study the catalytic depolymerization of alkali lignin at a low temperature (150, 170, 190 and 210 °C), with ZrO_2/SO_4^{2-} and Pt-ZrO_2/SO_4^{2-} as the catalysts. The effects of different reaction temperatures and catalysts were investigated. Furthermore, the relationship between the chemical structure of the alkali lignin and residues and the thermal stability of the IL and regenerated IL were investigated. Also, the effect of the IL pretreatment of lignin was estimated.

3.2 Experimental section

3.2.1 Materials

Alkali lignin was purchased from Sigma-Aldrich Chemical Company, and the ultimate analysis results are: C, 50.23 %; H, 4.32 %; N, 0.13 %; and O, 45.32 % by weight. Zirconia powder was supplied by Daiichi Kigenso Kagaku Kogyo. Pyridine, allyl chloride and o-xylene were purchased from Wako Pure Chemical Industries with purity of 99.5 %, 98.0 %, 98.0 %, respectively. $H_2PtCl_6 \cdot 6H_2O$ was purchased from Sigma-Aldrich Chemical Company with purity of 98.5 %. Ether, acetonitrile, and the rest of the chemicals were used as received. Distilled water was used in all cases.

3.2.2 Synthesis of ionic liquid

Based on our previous studies [31] N-allylpyridinium chloride ([Apy]Cl) was synthesized with a yield of 98.8 %. One-dimensional ^{1}H-nuclear magnetic resonance (NMR) spectra was measured using an ECA500 Delta V5 (JEOL Co.), which operated with the frequency of 500 MHz and at room temperature. DMSO-d_6 was used as the solvent for the ^{1}H-NMR analysis of [Apy]Cl. The thermo stability of [Apy]Cl was analyzed by thermogravimetric analysis (TGA). The results of the analysis are: 4.8 (2H, d), 5.1(1H, d), 5.3 (1H, d), 6.0 (1H, m), 8.0 (2H, t), 8.4 (1H, t), 8.7 (2H, d); and maximum thermal decomposition temperature (T_d) was 232 °C. The main structures of the IL used in the present study are shown in Scheme 3.1.

IL	Cation	Anion
[Apy]Cl	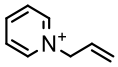	Cl^-

Scheme 3.1. The main structures of the IL used in the present study.

3.2.3 Preparation of catalyst

The solid acid catalysts, ZrO_2/SO_4^{2-} and Pt-ZrO_2/SO_4^{2-}, prepared based on our previous studies [32]. Prior to impregnation, Zirconia pellet and the prepared ZrO_2/SO_4^{2-} (as support) were ground into 425-850 μm particles. Then Pt-ZrO_2/SO_4^{2-} with 1 wt. % platinum was prepared by the impregnation with $H_2PtC1_6•6H_2O$. After the impregnation, the samples were dried and followed by calcination in air. Prior to the reaction, all of the catalysts were ground into 425-850 μm particles and Pt-ZrO_2/SO_4^{2-} was reduced by H_2 in situ at 400 °C for 3 h.

3.2.4 Catalytic depolymerization reaction

Firstly, to verify the feasibility of experiments under mild conditions, the depolymerization of alkali lignin in [Apy]Cl was explored in the presence of SZ catalyst in pressure resistant glass reactor as shown in Figure 3.1. 0.2 g of alkali lignin dissolved in 2.0 g of [Apy]Cl were added into the reactor and held in 90 ℃ using oil bath, which was stirred at 300 rpm for 3 h with a magnetic stirrer. After the dissolution, 0.2 g of SZ catalyst and 0.2 g of distilled water were added to the reaction system, and the reaction system was reacted at 210 ℃ for 1h, 2h and 3 h, respectively.

After the lignin depolymerization, samples of the liquid mixtures were collected and weighed each hour. Acetonitrile was added to the liquid mixtures with the mass ratio of acetonitrile/liquid mixtures was 20, the acetonitrile-insoluble fraction was defined as the solid residue, which contained unreacted lignin then centrifuged to separate. The acetonitrile-soluble fraction was extracted by ether and the amount of ether added was twice that of acetonitrile, and the ether-insoluble fraction was defined as the regenerated IL, whereas the ether-soluble fraction was defined as the liquid products. Then, the liquid products were further concentrated via vacuum distillation at 70 °C to remove the extraction solvents.

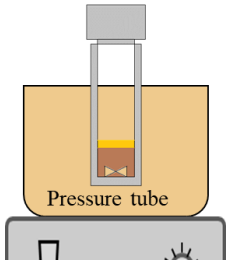

Figure 3.1 The batch reactor for lignin depolymerization.

Based on our previous researches, a continuous-flow fix-bed reaction system was developed, including pretreatment unit, reaction unit and separation unit, as shown in Figure 3.2. Lignin was dissolved completely in the [APy]Cl and H_2O mixed solvent with the mass ratio of lignin: [APy]Cl: H_2O = 0.2:10:1 at 90 °C for 3 h in the pretreatment unit which defined as feedstock. Then a certain amount of feedstock (from vessel 2) was pumped into the pipeline. Through pumping pump oil (from vessel 1) to push the feedstock into the fixed-bed reactor in reaction unit under the weight hourly space velocity (WHSV) of 3.8 h^{-1}. The length and inner diameter of the reactor were 160 mm and 8 mm, respectively. And the fixed-bed reactor with 0.452 g catalyst (ZrO_2/SO_4^{2-} or Pt-ZrO_2/SO_4^{2-}) was heated to the reaction temperatures and maintained for 0.5 h before the feedstock fed into the system.

During the lignin depolymerization, samples of the liquid mixtures were collected and weighed each hour and the separation methods were same as those for batch reactor.

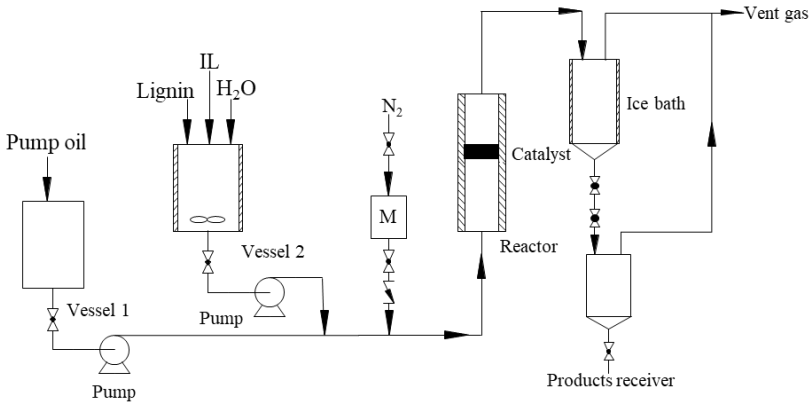

Figure 3.2. Flow diagram of a flow fixed-bed reactor for lignin depolymerization.

3.2.5 Analysis of liquid product and solid residue

For each test either in batch or flow reactor, samples of liquid products were collected after concentration, weighed to obtain the mass and then analyzed by gas chromatography with flame ionization detector (GC-FID, Shimadzu Co.) and gas chromatography-mass spectrometer (GC-MS, Shimadzu Co.). The compounds were quantified by GC-FID with a column of Ultra alloy-5 (Agilent, 60 m×0.25 mm i.d., 0.25 μm) and identified by GC-MS using a J&W Scientific DB-1 column (Agilent, 60 m×0.25 mm i.d., 0.25 μm). To confirm the position and the mass-to-charge ratio of the peaks, internal standard (IS) was chose by comparing to GC-FID spectra of the liquid products with/without o-xylene. The results showed that there was no o-xylene in the liquid products, o-xylene was used as IS for the further study with the mass fraction of 1 wt. %. The liquid products identified by GC-MS were divided into phenolic and nonphenolic compounds. Product yield was obtained in terms of molar carbon yield, and the total mole yield of carbon-based products and phenolic compounds are divided by the moles of carbon in the feedstock which fed in the reactor with respect to the IS. After repeated three times of all the test, the average of three trials were used in this study. The total mole yield of carbon-based products (Y_c, C, mol %) and phenolic compounds (Y_p, C, mol%) were calculated by equation (3-1) and (3-2):

$$\mathrm{Y_c,\ (C,\ mol\%)} = \frac{\text{Carbon moles in liquid products}}{\text{Carbon moles fed in}} \times 100\% \quad (3\text{-}1)$$

$$\mathrm{Y_p,\ (C,\ mol\%)} = \frac{\text{Carbon moles in phenolic compounds}}{\text{Carbon moles fed in}} \times 100 \quad (3\text{-}2)$$

The solid residues after pretreatment and reaction were analyzed by use of Fourier transform infrared analysis (FT-IR) with an IR Prestige-21 (Shimadzu Co.) spectrometer from 4000 to 600 cm^{-1}, scanning 64 times with a resolution of 2 cm^{-1}. The solid residue was mixed with KBr with mass ratio of 1:100, then mechanically pressed

to form a pellet.

X-ray diffraction (XRD) patterns of the raw and regenerated lignin from the pretreatment unit were recorded using RINT2100 VPC/N with Cu-Kα radiation (40 kV, 30 mA) at 2θ angles from 5 to 85 °.

The thermal behavior of the samples was measured by a thermal gravimetric analyzer (DTG-60, Shimadzu Co.) by heating 10 mg of the samples, which were placed in an aluminum pan, at a rate of 10 °C/ min from100 to 800 °C under N_2 gas atmosphere.

3.3 Results and discussion

3.3.1 Analysis of liquid product and solid residue

The TGA and DTGA curves of raw lignin and regenerated lignin after pretreatment with [Apy]Cl are shown in Figure 3.3. The maximum decomposition temperature of raw lignin was 350 °C, and the one of regenerated lignin from the pretreatment unit appeared at 227 °C, indicating that after pretreatment lignin became more readily to be decomposed.

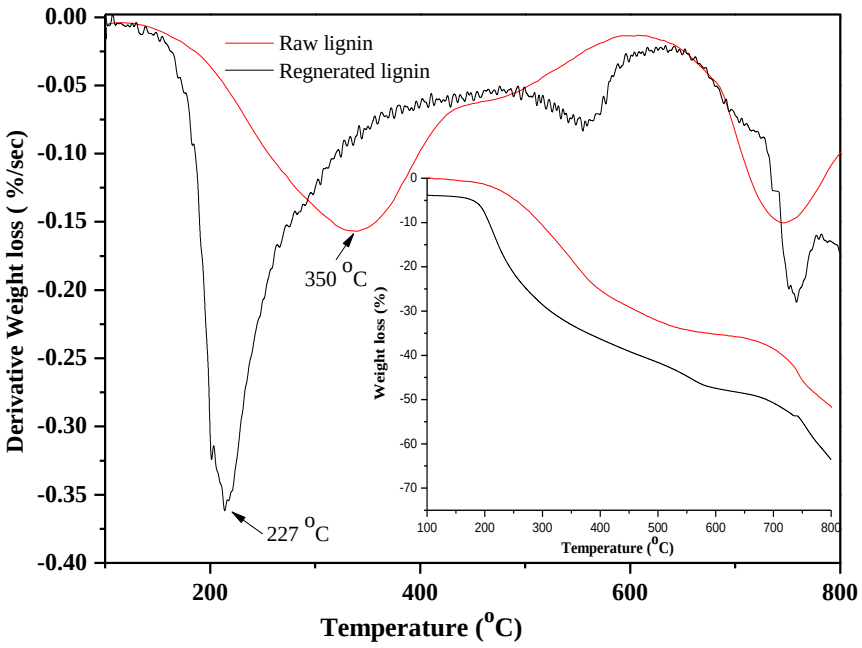

Figure 3.3. TGA and DTGA curves of raw lignin and regenerated lignin from the pretreatment unit at 90 °C for 3 h.

Meanwhile, the change in the crystal phase of lignin before and after pretreatment with [Apy]Cl were analyzed by XRD. The results of XRD showed in Figure 3.4. Alkali lignin without [Apy]Cl pretreatment showed a broad peak and had a few characteristic peaks [33] of Na_2SO_4 at 19.08°, 28.00°, 33.97°, 38.55° and 46.37°. And at 31.97° was NaCl characteristic peak, which was consistent with the production process of the sample. In contrast to this, after pretreatment, almost all the characteristic peaks

disappeared and the formation of amorphous materials was observed. It means that the application of IL as the solvent by dissolving the lignin macromolecules into relatively small molecular weight products, which improve the accessibility of targeted bonds for catalysts in reaction and make the reaction conditions typically less harsh.

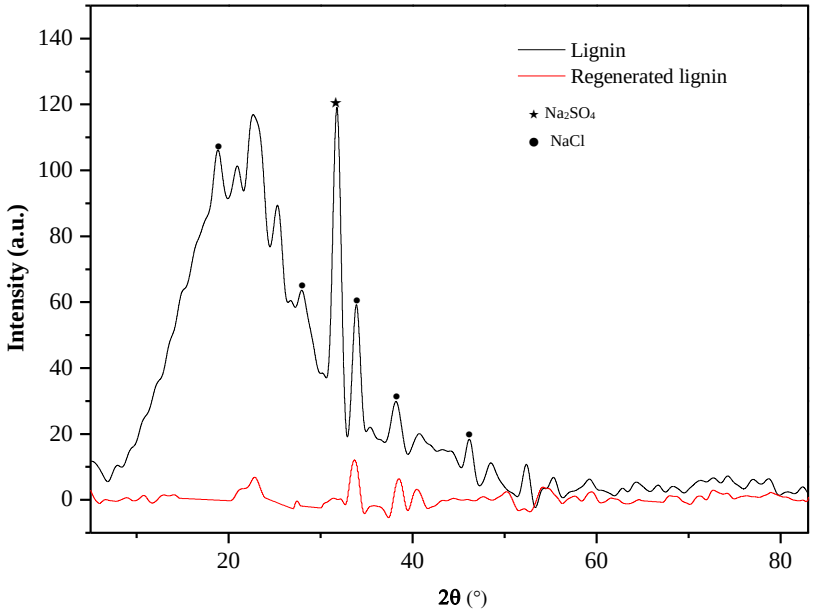

Figure 3.4. XRD patterns of raw and regenerated lignin from pretreatment unit.

3.3.2 Catalytic depolymerization of lignin in batch reactor

After depolymerization, the liquid products obtained from batch reactor were separated and identified by GC-FID and GC-MS. The details of structure and yields of major products are summarized in Table 3.1 and Table 3.2. Figure 3.5 shows the results of liquid products analyzed by GC-FID. The peaks i and ii represent the extract solvents and pyridine residue from the process of synthesis of IL, respectively.

As Table 3.2 showed, the main compounds observed in identified compounds at 210 °C were the phenolic compounds. The total yields of the phenolic compounds increased as the reaction time increased. At the same time, it is feasible to decompose lignin under mild conditions using ILs combine with catalysts, which lays the foundation for the study of the flow fix-bed reaction system.

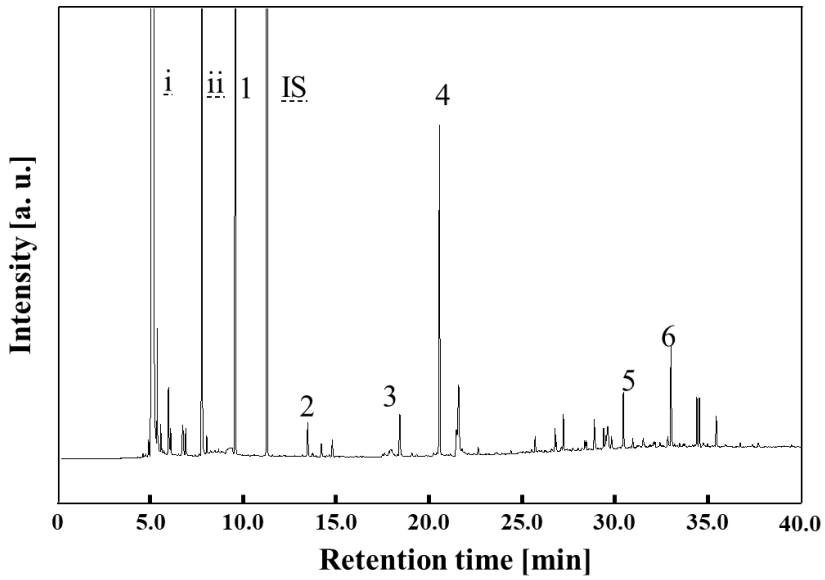

Figure 3.5. GC-FID spectra of liquid products from batch reactor at 210 ℃ for 3 h.

Table 3.1. Identification of liquid products by means of GC-MS.

No.	Compounds	Structure
1	Furfuryl alcohol	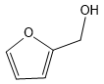
2	Benzaldehyde	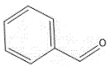
3	4-Vinylphenol	
4	*P*-methylguaicol	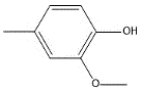
5	2,2'-Biphenol	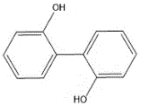
6	1-(4-Hydroxy-3,5-dimethoxyphenyl) propan-1-one	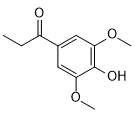

Table 3.2. Quantification of the identified liquid products by means of GC-FID at 210 ℃.

No.	Compounds	Yield/C, mol %		
		ZrO_2/SO_4^{2-}		
		1 h	2 h	3 h
1	Furfuryl alcohol	3.73	6.48	10.59
2	Benzaldehyde	0.58	0.48	0.28
3	4-Vinylphenol	-	0.05	0.01
4	*P*-methylguaicol	0.22	0.59	2.64
5	2,2'-Biphenol	-	0.15	1.16
6	1-(4-Hydroxy-3,5-dimethoxyphenyl) propan-1-one	-	0.17	0.80
	$\boldsymbol{Y_c}$	16.9	19.4	29.6

Y_c, total yields of carbon-based products.

3.3.3 Catalytic depolymerization of lignin in flow reactor

The catalytic depolymerization of alkali lignin dissolved in a mixed solvent of [Apy]Cl and water, in the presence of ZrO_2/SO_4^{2-} or Pt-ZrO_2/SO_4^{2-} catalyst, was carried out in a continuous-flow fixed-bed reaction system at low temperature. After depolymerization, the liquid products obtained from pretreatment unit and reaction unit were separated and identified by GC-FID and GC-MS. The details of structure and yields of major products are summarized in Table 3.3 and Table 3.4. Figure 3.6 shows the results of liquid products analyzed by GC-FID: (a) is the results of liquid products from extraction of the feedstock in the pretreatment unit; (b) ~ (e) are catalyzed by ZrO_2/SO_4^{2-} at 150, 170, 190 and 210 °C under WHSV of 3.8 h^{-1}, respectively; (f) is catalyzed by Pt-ZrO_2/SO_4^{2-} at 210 °C under WHSV of 3.8 h^{-1}. The peaks i and ii represent the extract solvents and pyridine residue from the process of synthesis of IL, respectively. As Table 3.4 showed, the main compounds observed in identified compounds at 210 °C were the phenolic compounds. The total yields of the phenolic compounds increased as the reaction temperature increased; Pt-ZrO_2/SO_4^{2-} showed

higher yields than those of ZrO_2/SO_4^{2-} at 210 °C, and 1-(4-hydroxy-3,5-dimethoxyphenyl) propan-1-one (1.21 %) was obtained. Among the phenolic compounds, the main products were 4-vinylphenol, 4-hydroxyphenylacetic acid and 5-dihydroxy-1,2,3,4-tetrahydronaphthalene, and the yields of these increased with the increase of temperature. As shown in Table 3.4, 4-vinylphenol was the main phenolic compound with a high yield. Moreover, the yields of nonphenolic compounds also increased with increasing reaction temperature. Meanwhile, *p*-methylguaicol was the main product with a low yield in the pretreatment unit, indicating that the lignin structures were partially depolymerized.

3.3.4 Effect of reaction temperatures on the yields of liquid products

As shown in Figure 3.6 and Table 3.4, over the entire reaction temperature range, the yields of carbon-based products and phenolic compounds increased as the temperature increased. The yields of the carbon-based products and phenolic compounds catalyzed by ZrO_2/SO_4^{2-} appeared to be minimized (14.9 % and 2.96 %, respectively) at 150 °C and increased to 30.6 % and 13.4 % at 210 °C, respectively. Under the catalysis of Pt-ZrO_2/SO_4^{2-}, the yields of the carbon-based products and phenolic compounds increased to 44.9 % and 18.7 % at 210 °C, respectively as shown in Figure 3.7. This significant increase might be due to the depolymerization of the degraded lignin intermediates as the temperature increased.

The distribution of phenolic compounds with temperature increased was shown in Figure 3.7 and Table 3.4. According to Table 3.4, the yield of the phenolic compounds of *p*-methylguaicol (No. 5) and 1-(4-hydroxy-3,5-dimethoxyphenyl propan-1-one (No. 12)) were increased from 0.00 % to 0.446 % and from 0.00% to 1.21 %, respectively, in the presence of Pt-ZrO_2/SO_4^{2-} with temperature increased to 210 °C. The yields of most phenolic compounds (2,6-xylenol (No. 3), 4-vinylphenol (No. 4), 1,5-dihydroxy-

1,2,3,4-tetrahydronaphthalene (No. 9), butylated hydroxytoluene (No. 11) and 4-hydroxyphenylacetic acid (No. 7)) was also increased. However, the yield of 6-methylsalicylic acid ethyl ester (No. 6) increased at first before decreasing, with the highest yield of 0.874 % observed at 210 °C. This effect probably resulted from 6-methylsalicylic acid ethyl ester being depolymerized as the reaction temperature increased. Further, the yield of 2, 2'-biphenol (No. 10) was decreased at 190 °C, then it increased to 1.04 % at 210 °C in the presence of Pt-ZrO_2/SO_4^{2-}, which indicated repolymerization occurred at 210 °C.

In short, the reaction temperature was an important factor in lignin depolymerization [34-36] and it had a significant effect on the yield and composition of liquid products. The above results indicated 4-vinylphenol was the main product.

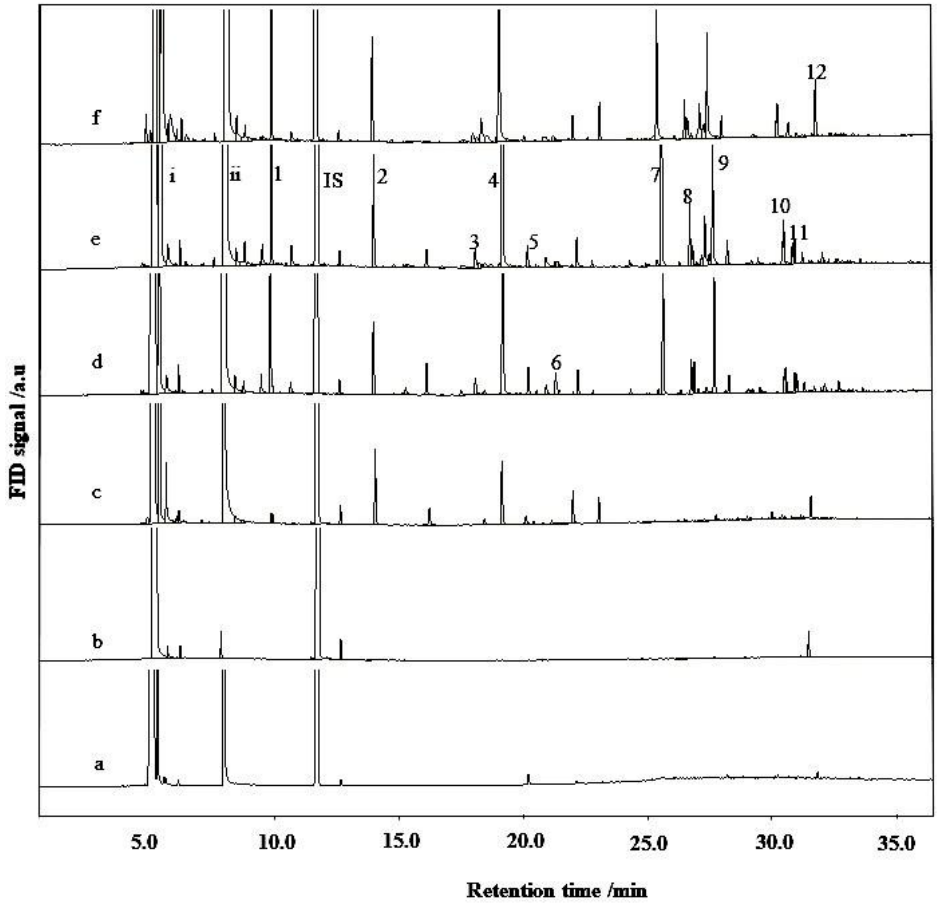

Figure 3.5. GC-FID spectra of liquid products from pretreatment and reaction units.

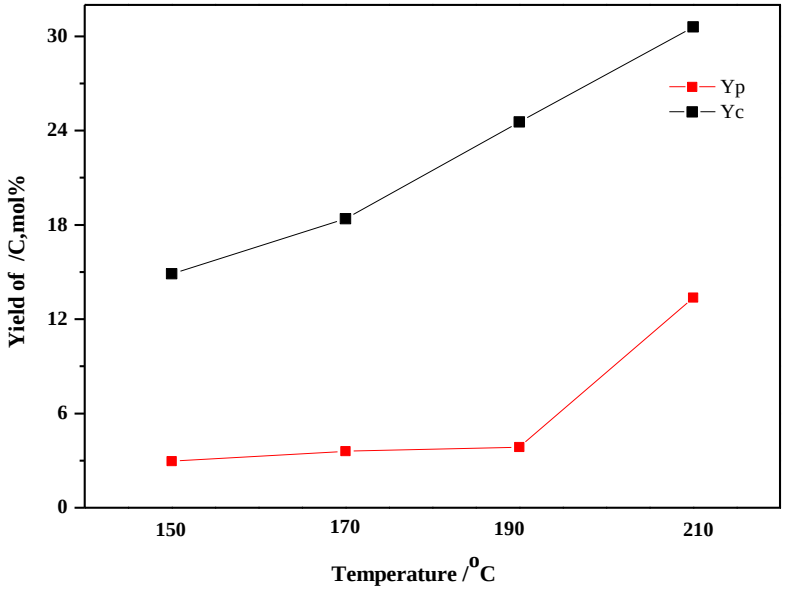

Figure 3.6. Effects of different reaction temperatures on the yields of carbon-based products and phenolic compounds (C, mol%; based on lignin) catalyzed by ZrO_2/SO_4^{2-}.

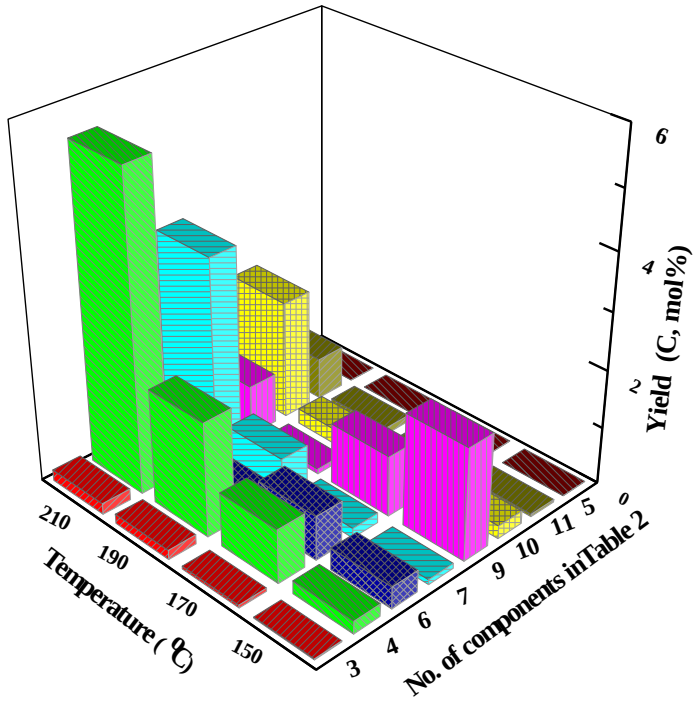

Figure 3.7. Effects of different reaction temperatures on the yields of phenolic compounds (C, mol%; based on lignin) catalyzed by ZrO_2/SO_4^{2-}.

3.3.5 Effect of metal-supported catalysts on the yields of liquid products

According to the above results, to investigate the effect of metal loading of the

catalyst on the yields of liquid products, the lignin depolymerization reactions were conducted at 210 °C. The 1 wt. % Pt-ZrO_2/SO_4^{2-} catalyst was used for comparison. The effects of the catalysts on the yields of carbon-based products and phenolic compounds, based on lignin, are shown in Table 3.4 and Figure 3.5. It was observed that 1 wt. % Pt-ZrO_2/SO_4^{2-} catalytic depolymerization produced higher yields of all compounds than those of ZrO_2/SO_4^{2-}, and the yields of the carbon-based products and phenolic compounds were increased from 30.6 % to 44.9 % and 13.4 % to 18.7 %, respectively. Meanwhile, the yields of 1,5-dihydroxy-1,2,3,4-tetrahydronaphthalene (No. 9) and 1-(4-hydroxy-3,5-dimethoxyphenyl propan-1-one (No. 12)) in the presence of Pt-ZrO_2/SO_4^{2-} were higher than those of catalyzed by ZrO_2/SO_4^{2-}, indicated that combined with solid acid catalyst, hydrogen ions from partial H_2O and acidic IL could be migrated and adsorbed at Pt sites, which promoted lignin depolymerization.

Table 3.3. Identification of liquid products by means of GC-MS.

No.	Compounds	Structure
1	Furfuryl alcohol	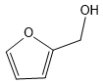
2	Benzaldehyde	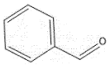
3	2,6-Xylenol	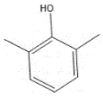
4	4-Vinylphenol	
5	*P*-methylguaicol	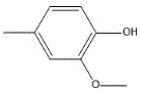
6	6-Methylsalicylic acid ethyl ester	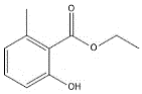
7	4-Hydroxyphenylacetic acid	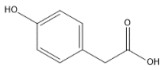
8	2,6-Dimethylstyrene	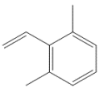
9	1,5-Dihydroxy-1,2,3,4-tetrahydro naphthalene	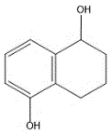
10	2,2'-Biphenol	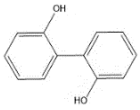
11	Butylated hydroxytoluene	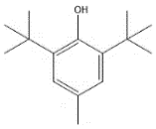
12	1-(4-Hydroxy-3,5-dimethoxyphenyl) propan-1-one	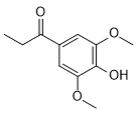

Table 3.4. Quantification of the identified liquid products by means of GC-FID.

No.	Compounds	Yield/C, mol %				
		ZrO_2/SO_4^{2-}				Pt-ZrO_2/SO_4^{2-}
		150 °C	170 °C	190 °C	210 °C	210 °C
	Non-phenolic compounds (np)					
1	Furfuryl alcohol	0.233	0.332	2.200	3.440	4.500
2	Benzaldehyde	0.140	0.925	0.570	1.400	2.440
8	2,6-Dimethylstyrene	0.175	0.424	0.560	1.030	1.060
	Total yield (Y_{np})	0.548	1.680	3.330	5.870	8.000
	Phenolic compounds					
3	2,6-Xylenol	0.019	0.051	0.161	0.193	1.060
4	4-Vinylphenol	0.225	0.946	2.00	5.490	9.430
5	*P*-methylguaicol	0.000	0.197	0.258	0.383	0.446
6	6-Methylsalicylic acid ethyl ester	0.386	0.778	0.330	0.874	0.658
7	4-Hydroxyphenylacetic acid	0.088	0.167	0.634	3.480	3.590
9	1,5-Dihydroxy-1,2,3,4-tetrahydro naphthalene	1.970	1.060	0.086	2.080	2.690
10	2,2'-Biphenol	0.224	0.283	0.265	0.728	1.040
11	Butylated hydroxytoluene	0.049	0.116	0.118	0.143	0.159
12	1-(4-Hydroxy-3,5-dimethoxyphenyl) propan-1-one	0.000	0.000	0.000	0.000	1.210
	Y_p	2.96	3.60	3.85	13.4	18.7
	Y_c	14.9	18.4	24.6	30.6	44.9

Y_c, total yields of carbon-based products; Y_p, yields of phenolic compounds; Y_{np}, yields of nonphenolic compounds.

3.3.6 Pathway of lignin depolymerization

Based on the above results and previous reports [43, 45], the distribution of the liquid products indicated that lignin was effectively depolymerized into low molecular weight products after [Apy]Cl pretreatment, which were proved in Chapter 2, two reaction pathways were suggested in Scheme 3.2. Both of pathways for catalytic depolymerization of lignin begins with the relatively low molecular weight products with β-O-4 ether bond after lignin pretreatment. As illustrated in Scheme 3.2, [Apy]Cl

contains strong coordinating anion (Cl^-) was used as a reaction media to stabilize thehydroxyl group on the intermedia compounds. In pathway A, under catalysis of ZrO_2/SO_4^{2-}, small molecular weight products with β-O-4 ether bond transformed into an enol ether isomer by releasing H_2O, then hydrolyzed to release guaiacol and carbonyl compounds. In pathway B, by the catalytic dehydrogenation of Pt ketone was generated, and then dehydrated to form α, β-unsaturated ketone. Then the hydrogenation and reduction cleavage reactions were performed with chemisorbed hydrogen catalyzed by Pt, from which aryl propylene was produced.

Additionally, in the whole process, the active intermediates can be protected and/or stabilized or side reactions were inhibited with [Apy]Cl used as the solvent and reaction media [44], which promoted lignin depolymerization to produce desired value-added products.

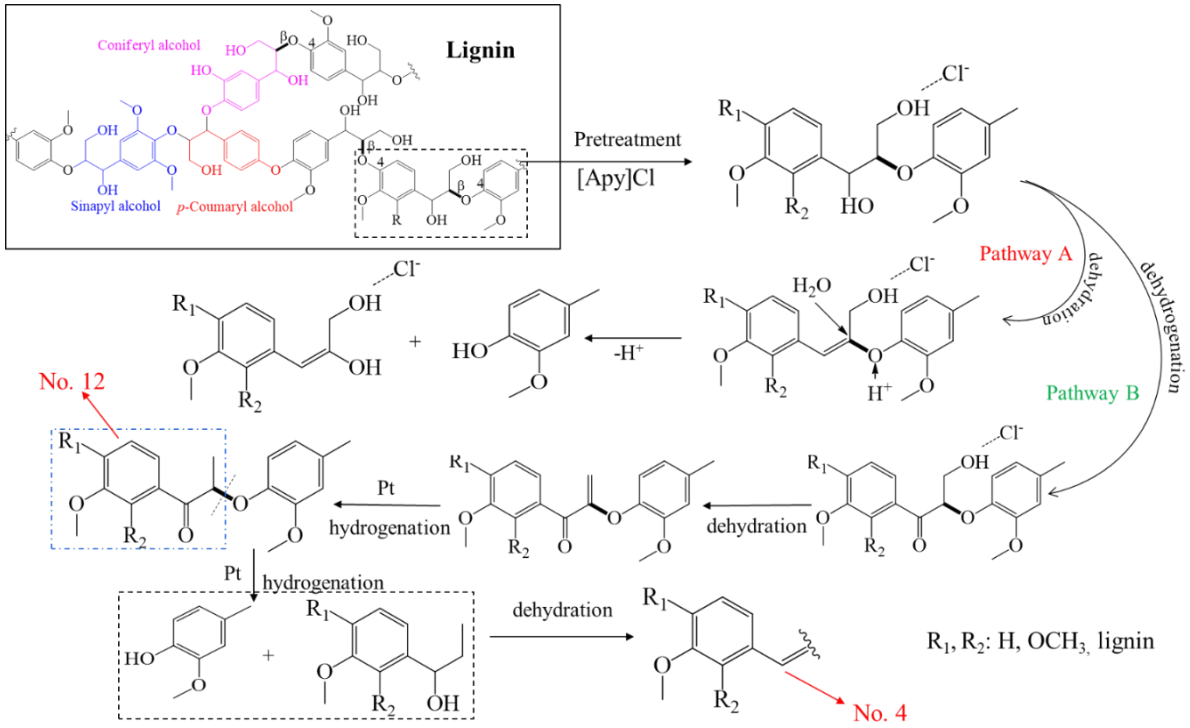

Scheme 3.2. Proposed pathway of lignin depolymerization under catalysis of ZrO_2/SO_4^{2-} and Pt-ZrO_2/SO_4^{2-}.

3.3.6 Changes in the structure of lignin after depolymerization

FT-IR analysis was performed for the solid residues obtained from lignin depolymerization in the reaction unit and pretreatment unit using commercially available alkali lignin as the standard. Various peaks were observed according to the previous studies [37-39].

All samples in Figure 3.8 showed a wide absorption band at 3400 cm^{-1}, which corresponded to the vibration of the O–H stretch in aromatic and aliphatic O–H groups. Peaks at approximately 2962, 2938 and 2873 cm^{-1} were assigned to C–H vibrations of the $–CH_2$ and $–CH_3$ groups [42], and the peak that appeared at 1707 cm^{-1} was assigned to carbonyl stretching vibration [35]. The band at 1635 cm^{-1} represented the structure of the C=C stretching vibration [40]. Compared to the raw lignin (a), with temperature increased from 150 to 210 °C the absorbance intensity of peak (b ~ e) at 1635cm^{-1} had no obvious change. However, the absorbance intensity of peak (f) at 1635cm^{-1} increased, indicating the content of double bonds was higher[41] than others. The intensity of peak at 1594 cm^{-1}, showed a decrease when compared to that of raw alkali lignin, indicating that a substitution reaction occurred on the aromatic ring and that a condensation reaction mainly occurs on the aromatic ring [38]. The absorption peak at 1131 cm^{-1} was attributed to the C–O absorption of the methoxy group on the benzene ring [42], and its absorption intensity was weakened or even disappeared as the temperature increased. This finding indicated that the demethoxylation reaction and breakage of the ether bond, such as beta β–O–4, occurred during lignin depolymerization.

In addition, the FT-IR spectra of the residues (b ~ e) regenerated from 150-210 °C catalyzed by ZrO_2/SO_4^{2-} showed that the absorbances of peaks at 2962, 2873, and 1447 cm^{-1} increased, which were attributed to C–H stretching vibrations of $–CH_2$ and $–CH_3$ groups, indicating alkyl groups existed in residues. The absorbance at 1568 cm^{-1} was

increased indicated the formation of the highly organized aromatic residues. Additionally, the absorbance approximately 1097 cm^{-1} decreased implied the breakage of ether bonds. As comparison, the residue (f) regenerated from 210 °C catalyzed by Pt-ZrO_2/SO_4^{2-} showed increased intensities for 1207 cm^{-1} band, which was associated with guaicyl ring breathing with C-O stretches [40].

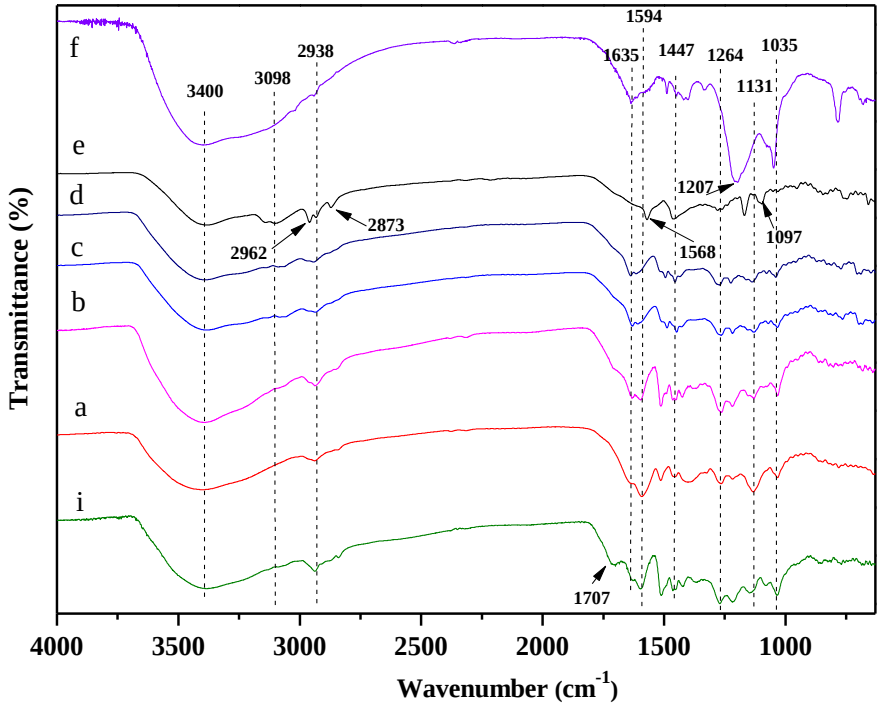

Figure 3.8. Comparison of FT-IR spectrum of commercial alkali lignin and residues: (i) is the residues regenerated from the solution in the pretreatment unit; (a) is commercial alkali lignin; (b) ~ (e) are residues regenerated from 150, 170, 190, and 210 °C catalyzed by ZrO_2/SO_4^{2-}, respectively; (f) is residue regenerated from 210 °C catalyzed by Pt-ZrO_2/SO_4^{2-}.

3.3.7 Thermal stability of [Apy]Cl

The thermal stabilities of the regenerated ILs and compare to fresh IL were explored by TGA. The TGA and DTGA curves of [Apy]Cl and the regenerated [Apy]Cl are shown in Figure 3.9. The maximum weight loss rates appeared at 232 °C for fresh [Apy]Cl, and the maximum weight loss rates of regenerated [Apy]Cl from the pretreatment unit appeared at 232 °C and from the reaction unit at 150, 170, 190, and

210 °C appeared at 228, 232, 225 and 235 °C, respectively. Changes in the decomposition temperature were probably due to the presence of low-melting inorganic mixtures and the ash derived from alkali lignin in regenerated [Apy]Cl after lignin depolymerization. However, the overall thermal decomposition behavior of all the regenerated [Apy]Cl was found to be similar to that of the fresh compound, which demonstrates reasonable recyclability.

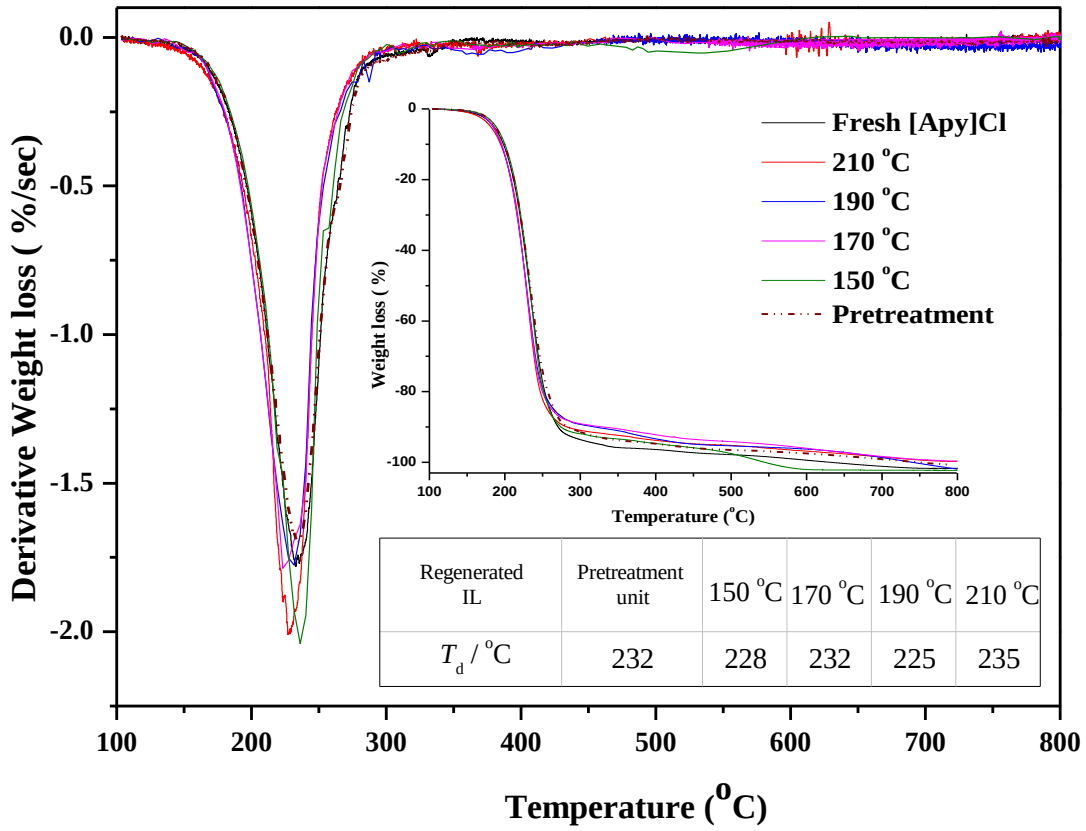

Regenerated IL	Pretreatment unit	150 °C	170 °C	190 °C	210 °C
T_d / °C	232	228	232	225	235

Figure 3.9. TGA and DTGA curves of [Apy]Cl and the regenerated [Apy]Cl from the pretreatment unit and reaction unit catalyzed by ZrO_2/SO_4^{2-} at 150, 170, 190, 210 °C.

3.4 Conclusions

In this work, after pretreatment with [Apy]Cl at 80 °C lignin macromolecules degraded into relatively small molecular weight products, which became more readily decomposed and the accessibility of targeted bonds for catalysts were improved for the catalytic depolymerization. In the presence of ZrO_2/SO_4^{2-}, the alkali lignin dissolved in [Apy]Cl and water decomposed even at 170 °C. 4-vinylphenol was the primary phenolic compounds during lignin depolymerization. The yields of carbon-based products and phenolic compounds catalyzed by Pt-ZrO_2/SO_4^{2-} were 44.9 % and 18.7 %, respectively, and were higher than those of ZrO_2/SO_4^{2-} (30.6 % and 13.4 %) at 210 °C. With the in-depth analysis of the liquid products two reaction pathways were suggested with part of the H_2O and acid IL in the system utilized as a source of hydrogen during lignin depolymerization by Pt-ZrO_2/SO_4^{2-}. Meanwhile, thermal stability results showed that [Apy]Cl was basically unchanged, demonstrating reasonable recyclability.

References

[1]. Zhang Z, Song J, Han B. Catalytic transformation of lignocellulose into chemicals and fuel products in ionic liquids. *Chem. Rev.* **2016**, *117(10)*, 6834-6880.

[2]. Chakar F. S., Ragauskas A. J. Review of current and future softwood kraft lignin process chemistry. *Ind. Crop. Prod*. **2004**, *20(2)*, 131-141.

[3]. Ralph, J., Lundquist, K., Brunow, G., Lu, F., Kim, H., Schatz, P. F. Boerjan, W. Lignins: Natural polymers from oxidative coupling of 4-hydroxyphenylpropanoids. *Phytochem Rev.* **2004**, *3(1-2)*, 29-60.

[4]. Chaudhary R., Dhepe P. L. Solid base catalyzed depolymerization of lignin into low molecular weight products. *Green Chem.* **2017**, *19(3)*, 778-788.

[5]. Rahimi, A., Ulbrich, A., Coon, J. J., Stahl, S. S. Formic-acid induced depolymerization of oxidized lignin to aromatics. *Nature*. **2014**, *515*, 249−252.

[6]. Singh S. K., Dhepe P. L. Ionic liquids catalyzed lignin liquefaction: mechanistic studies using TPO-MS, FT-IR, RAMAN and 1D. 2D-HSQC/NOSEY NMR. *Green Chem*. **2016**, *18*, 4098− 4108.

[7]. Rodriguez, A., Salvachúa, D., Katahira, R., Black, B. A., Cleveland, N. S., Reed, M., Beckham, G. T. Base-catalyzed depolymerization of solid lignin-rich streams enables microbial conversion. *ACS Sustain. Chem. Eng.* **2017**, *5(9)*, 8171-8180.

[8]. Abdelaziz, O. Y., Li, K., Tunå, P., Hulteberg, C. P. Continuous catalytic depolymerisation and conversion of industrial kraft lignin into low-molecular-weight aromatics. *Biomass Convers. Bior.* **2018**, *8(2)*, 455-470.

[9]. Cao, L., Iris, K. M., Liu, Y., Ruan, X., Tsang, D. C., Hunt, A. J., Zhang, S. Lignin valorization for the production of renewable chemicals: State-of-the-art review and future prospects. *Bioresource technol.* **2018**.

[10]. Saidi, M., Samimi, F., Karimipourfard, D., Nimmanwudipong, T., Gates, B. C., Rahimpour, M. R. Upgrading of lignin-derived bio-oils by catalytic hydrodeoxygenation. *Energy Environ. Sci*. **2014**, *7*, 103−129.

[11]. Yan, N., Zhao, C., Dyson, P. J., Wang, C., Liu, L. T., Kou, Y. Selective degradation of wood lignin over noble-metal catalysts in a two-step process. *ChemSusChem*. **2008**, *1(7)*, 626-629.

[12]. Xu, W., Miller, S. J., Agrawal, P. K., Jones, C. W. Depolymerization and hydrodeoxygenation of switchgrass lignin with formic acid. *ChemSusChem*. **2012**, *5(4)*, 667-675.

[13]. Song, Q., Wang, F., Cai, J., Wang, Y., Zhang, J., Yu, W., Xu, J. Lignin depolymerization (LDP) in alcohol over nickel-based catalysts via a fragmentation–hydrogenolysis process. *Energy Environ. Sci.* **2013**, *6(3)*, 994-1007.

[14]. Van den Bosch, S., Schutyser, W., Vanholme, R., Driessen, T., Koelewijn, S. F.,

Renders, T., Lagrain, B.. Reductive lignocellulose fractionation into soluble lignin-derived phenolic monomers and dimers and processable carbohydrate pulps. *Energy Environ. Sci.* **2015**, *8(6)*, 1748-1763.

[15]. Hita, I., Deuss, P. J., Bonura, G., Frusteri, F., Heeres, H. J. Biobased chemicals from the catalytic depolymerization of Kraft lignin using supported noble metal-based catalysts. *Fuel Process. Technol.* **2018**, *179*, 143-153.

[16]. Bugg, T. D. H., Ahmad, M., Hardiman, E. M., & Rahmanpour, R. Pathways for degradation of lignin in bacteria and fungi. *Nat. Prod. Rep*. **2011**, *28(12)*, 1883-1896.

[17]. Picart, P., Liu, H., Grande, P. M., Anders, N., Zhu, L., Klankermayer, J., Schallmey, A. Multi-step biocatalytic depolymerization of lignin. *Appl. Microbiol. Biot.* **2017**, *101(15)*, 6277-6287.

[18]. Abdelaziz, O. Y., Brink, D. P., Prothmann, J., Ravi, K., Sun, M., Garcia-Hidalgo, J., Gorwa-Grauslund, M. F. Biological valorization of low molecular weight lignin. *Biotechnol. adv*, **2016**, *34(8)*, 1318-1346.

[19]. Stärk, K., Taccardi, N., Bösmann, A., Wasserscheid, P. Oxidative depolymerization of lignin in ionic liquids. *ChemSusChem*. **2010**, *3(6)*, 719-723.

[20]. Liu, C.; Wang, H.; Karim, A. M.; Sun, J.; Wang, Y. Catalytic fast pyrolysis of lignocellulosic biomass *Chem. Soc. Rev*. **2014**, *43*, 7594−7623.

[21]. Chatel, G., Rogers, R. D. Oxidation of lignin using ionic liquids An innovative strategy to produce renewable chemicals. *ACS Sustain. Chem. Eng*. **2013**, *2(3)*, 322-339.

[22]. Zhang, S., Su, L., Liu, L., Fang, G. Degradation on hydrogenolysis of soda lignin using $CuO/SO_4^{2-}/ZrO_2$ as catalyst. *Ind. Crop. Prod*. **2015**, *77*, 451-457.

[23]. Zhao, Y., Xu, Q., Pan, T., Zuo, Y., Fu, Y., Guo, Q. X. Depolymerization of lignin by catalytic oxidation with aqueous polyoxometalates. *Appl. Catal. A-Gen*. **2013**, *467*, 504-508.

[24]. Long, J., Xu, Y., Wang, T., Yuan, Z., Shu, R., Zhang, Q., Ma, L. Efficient base-catalyzed decomposition and in situ hydrogenolysis process for lignin depolymerization and char elimination. *Appl. Energ*. **2015**, *141*, 70-79.

[25]. T. Dutta, J. Shi, J. Sun, X. Zhang, G. Cheng, B. Simmons and S. Singh, in Ionic Liquids in the Biorefinery Concept: Challenges and Perspectives, RSC, **2015**, p. 65.

[26]. Kubo, S., Hashida, K., Yamada, T., Hishiyama, S., Magara, K., Kishino, M., Hosoya1, S. A Characteristic Reaction of Lignin in Ionic Liquids; Glycelol Type Enol-Ether as the Primary Decomposition Product of β-O-4 Model Compound. *J. Wood Chem. Technol*. **2008**, *28(2)*, 84-96.

[27]. Binder, J. B., Gray, M. J., White, J. F., Zhang, Z. C., Holladay, J. E. Reactions of lignin model compounds in ionic liquids. *Biomass Bioenerg*. **2009**, *33(9)*, 1122-

1130.
[28]. Casas, A., Oliet, M., Alonso, M. V., Rodriguez, F. Dissolution of Pinus radiata and Eucalyptus globulus woods in ionic liquids under microwave radiation: lignin regeneration and characterization. *Sep. Purif. Technol.* **2012**, *97*, 115-122.
[29]. Kilpeläinen, I., Xie, H., King, A., Granstrom, M., Heikkinen, S., Argyropoulos, D. S. Dissolution of wood in ionic liquids. *J. Agr. Food Chem*. **2007**, *55(22)*, 9142-9148.
[30]. Kimura T. Development of $Pt/SO_4^{2-}/ZrO_2$ catalyst for isomerization of light naphtha. *Cataly. Today*, **2003**, *81(1)*, 57-63.
[31]. Qian, E. W., Tominaga, H., Chen, T. L., Isoe, R. Synthesis of functional ionic liquids and their application for the direct saccharification of cellulose. *J. Chem. Eng. Jpn*. **2016**, *49(5)*, 466-474.
[32]. Shirai H., Ikeda S., Qian E. W. One-pot production of 5-hydroxymethylfurfural from cellulose using solid acid catalysts. *Fuel Process Technol*. **2017**, *159*, 280-286.
[33]. Dos Santos P. S. B., Erdocia X., Gatto D. A., Labidi, J. Characterisation of Kraft lignin separated by gradient acid precipitation. *Ind. Crop. Prod*. **2014**, *55*, 149-154.
[34]. Cheng, S., D'cruz, I., Wang, M., Leitch, M., & Xu, C. Highly efficient liquefaction of woody biomass in hot-compressed alcohol− water co-solvents. *Energy Fuels*. **2010**, *24(9)*, 4659-4667.
[35]. Lou, R., Wu, S. B., Lv, G. J. Effect of conditions on fast pyrolysis of bamboo lignin. *J. Anal. Appl. Pyrol*. **2010**, *89*, 191–196.
[36]. Tejado, A., Pena, C., Labidi, J., Echeverria, J. M., Mondragon, I. Physico-chemical characterization of lignins from different sources for use in phenol–formaldehyde resin synthesis. *Bioresour. Technol*. **2007**, *98(8)*, 1655-1663.
[37]. Yu, H., Hu, J., Fan, J., Chang, J. One-pot conversion of sugars and lignin in ionic liquid and recycling of ionic liquid. *Ind. Eng. Chem. Res*. **2012**, *51(8)*, 3452-3457.
[38]. Prado, R., Brandt, A., Erdocia, X., Hallet, J., Welton, T., Labidi, J. Lignin oxidation and depolymerization in ionic liquids. *Green Chem*. **2016**, *18(3)*, 834-841.
[39]. Das L., Xu S., Shi J. Catalytic Oxidation and Depolymerization of Lignin in Aqueous Ionic Liquid. *Front. Energy Res*. **2017**, *5*, 21.
[40]. Qian Y., Zuo C., Tan J., He J.. Structural analysis of bio-oils from sub-and supercritical water liquefaction of woody biomass. *Energy*. **2007**, *32*, 196–202.
[41]. Long J., Zhang Q, Wang T., Zhang X., Xu Y., Ma L. An efficient and economical process for lignin depolymerization in biomass-derived solvent tetrahydrofuran. *Bioresour. Technol.* **2014**, *154*, 10–7.

[42]. Abdelaziz, O. Y., Hulteberg, C. P. Physicochemical characterisation of technical lignins for their potential valorisation. *Waste Biomass Valori.* **2017**, *8(3)*, 859-869.

[43]. El Hage R, Brosse N, Sannigrahi P, Ragauskas A. Effects of process severity on the chemical structure of Miscanthus ethanol organosolv lignin. *Polym. Degrad. Stab.* **2010**, *95*,997-1003.

[44]. Li, C., Zhao, X., Wang, A., Huber, G. W., Zhang, T. Catalytic transformation of lignin for the production of chemicals and fuels. *Chem. Rev*. **2015**, *115(21)*, 11559-11624.

[45]. Galkin M. V., Samec J. S. Selective route to 2-propenyl aryls directly from wood by a tandem organosolv and palladium-catalysed transfer hydrogenolysis. *Chemsuschem*. **2015**, *7(8)*, 2154-2158.

Chapter 4

Catalytic depolymerization of alkali lignin in ionic liquid on Pt-supported La_2O_3-SO_4^{2-}/ZrO_2 catalysts

Abstract

A series of PtLa$\chi/ZrO_2/SO_4^{2-}$ with different addition amount of La_2O_3 (χ: atomic ratio of La to Pt, 1, 3 and 6) catalysts were prepared, and used to catalytic depolymerization of alkali lignin with ionic liquid in a continuous flow fix-bed reaction system. Compared to the catalyst of SO_4^{2-}/ZrO_2, the introduction of Pt and La_2O_3 significantly enhanced the catalytic activity in alkali lignin depolymerization. Based on the characterization results of the catalysts obtained from BET measurement, FT-IR spectra of CO or pyridine adsorption, XPS, TEM, with the instruction of La_2O_3, the number of Lewis acid sites increased and resulted in the strong interaction between Pt and support which improved the dispersion of Pt particles. PtLa3/SO_4^{2-}/ZrO_2 catalyst showed the highest yield of phenolic compounds (28.7 Carbon. mol%) at 210 ℃. Furthermore, based on results in the depolymerization and demethylation of two model compounds of lignin, the synergistic effect of ionic liquid and catalysts was also elucidated and a hypothetical reaction pathway of lignin depolymerization was proposed.

4.1 Introduction

Lignin is a heterogeneous phenolic biopolymer with *p*-coumaryl, sinapyl and coniferyl alcohol as monolignols [1, 2]. Owing to its complex structure and properties make lignin-derived monomers as useful precursors for high value-added chemicals, however, previous researches mainly focused on either cellulose- or hemicellulose-based material as feedstocks to obtain value-added chemicals [3-5], remaining lignin underutilization. Therefore, it is imperative for developing lignin-processing methods to convert lignin into high value-added chemicals.

Recently, a series of catalytic depolymerization processes have been developed to convert lignin into low-molecular-weight compounds with different methods. Although traditional processes could depolymerize lignin effectively, most of them were very energy intensive, such as the presence of higher temperature (> 250 °C) or pressures (> 2.5 MPa) with external hydrogen or oxygen [7, 8], and the organic solvents used would be hazardous to the environment [9, 10]. Considering the drawbacks in the traditional processes, ionic liquids (ILs) with exploitable tunable properties were employed in the lignin depolymerization as one of superior green solvents and catalysts [11,12]. As superior green solvents, ILs could dissolve lignin effectively with partial lignin macromolecule converted into low-molecular-weight compounds, which further promoted the catalytic depolymerization of lignin [6]. Moreover, ILs were also the promising reagents for the cleavage of methyl aryl ethers and β-O-4 bonds of lignin model monomers in the presence or absence of catalysts even at room temperature [13-16]. In our previous study [6], the synergistic effect of SO_4^{2-}/ZrO_2 and N-allylpyridinium chloride ([Apy]Cl) was proved for the efficient catalytic depolymerization of alkali lignin at 210 °C without external hydrogen or oxygen. From preliminary experimental, Pt-containing SO_4^{2-}/ZrO_2 demonstrated a better activity than that of SO_4^{2-}/ZrO_2 might due to the presence of partial platinum oxide improved active sites by interacting with

adjacent sulfate particles [17] or the coordination of platinum oxide for S=O enhanced the acid strength of the catalyst [18], which improved the catalytic activity in lignin depolymerization. Additionally, the metal nitrate ($Mn(NO_3)_2$) combination with IL of 1-ethyl-3-methylimidazolium trifluoromethane sulfonate ($[EMIM]CF_3SO_3$) were also proved to mediate depolymerization of lignin with 11.5 wt. % of 6-dimethoxy-1,4-benzoquinone produced under high pressure of 8.4MPa (air) at 100 °C for 24 h [19]. Therefore, considering the presence of the synergistic effect of ILs and catalysts, it is possible to catalytic depolymerization of lignin under less harsh reaction conditions.

Although most of the metal site in catalysts works as the active site and some researchers also reported that the increase of the noble metal content would improve the activity of catalysts, the higher cost seriously impediment to their application. Therefore, the addition of modifiers, such as rare-earth metal oxides, were used as effective methods to favor the activity [20, 21]. The remarkable properties of La_2O_3, such as special electronic structure and acidic properties, make it enable to decrease the size of the Pt domain and stabilize Pt dispersion after the modification of the catalyst [22, 23]. These properties indicated that Pt supported on La_2O_3-SO_4^{2-}/ZrO_2 (as the support) would be a rather considerable catalyst for lignin depolymerization.

In the present study, N-allylpyridinium chloride ([Apy]Cl) and catalyst of Pt-La_2O_3-SO_4^{2-}/ZrO_2 (PtLaχ/SO_4^{2-}/ZrO_2 catalysts, χ was the atomic ratio of La to Pt of 1, 3 and 6) was prepared, characterized and tested for lignin depolymerization at 210 °C in a flow fix-bed reactor system. Among all the catalysts studied, the platinum content was constant at 1.0 wt. %. The effect of different catalysts on the distribution of liquid products and the properties of catalysts were investigated. Moreover, the synergistic effect of ionic liquid and catalysts and a hypothetical reaction pathway of lignin depolymerization was elucidated based on the results of guaiacol and guaiacylglycerol-β-guaiacyl ether in pretreatment and reaction unit.

4.2 Experimental

4.2.1 Materials

The raw material of alkali lignin was purchased from Sigma-Aldrich Chemical Company. Pyridine (99.5 %, Wako Pure Chemical Industries, Ltd.), allyl chloride (98.0 %, Wako Pure Chemical Industries, Ltd.), $H_2PtCl_6 \cdot 6H_2O$ (98.5 %, Sigma-Aldrich), $La(NO_3)_3 \cdot 6H_2O$ (98.0 %, Sigma-Aldrich), O-xylene (98.0 %, Wako Pure Chemical Industries, Ltd.), guaiacol (> 98.0 %, Sigma-Aldrich), guaiacylglycerol-β-guaiacyl ether (Sigma-Aldrich), ether, acetonitrile, and the rest of the chemicals used were of analytical grade and used as received without further purification. Distilled water was used in all cases. [Apy]Cl was synthesized based on our previous studies [24], the structure and decomposition temperature were characterized by one-dimensional ^{1}H and ^{13}C nuclear magnetic resonance (NMR) spectra (JNM-ECA500 Delta V5, JEOL Co.) and thermogravimetric analysis (TGA): δ_H (D_2O)= 4.8 (2H, d), 5.1(1H, d), 5.3 (1H, d), 6.0 (1H, m), 8.0 (2H, t), 8.4 (1H, t), 8.7 (2H, d); δ_C = 63.0, 123.0,128.0, 130.0, 144.0, 146.0; and the maximum thermal decomposition temperature (T_d) was 232 °C.

4.2.2 Preparation of catalyst

SO_4^{2-}/ZrO_2 (SZ) and Pt-SO_4^{2-}/ZrO_2 (Pt/SZ) catalysts were prepared based on our previous studies [6]. La_2O_3-SO_4^{2-}/ZrO_2 (La_2O_3/SZ) catalysts with different contents of La_2O_3 were prepared by using incipient wetness impregnation method. Prior to impregnation, SZ was ground and sieved to yield 425–850 μm particles, then impregnated with an aqueous solution of $La(NO_3)_3 \bullet 6H_2O$ with desire La content, followed ultrasonication for 15min. After ultrasonication, the solid dried at 120 °C for 2 h and calcined at 600 °C for 3 h, which was denoted as La_2O_3/SZ catalyst. Afterward, La_2O_3/SZ was used as the support to prepare the catalysts of PtLaχ/SZ (χ = 1, 3, 6),

where χ referred to the atomic ratio of La to Pt, with an aqueous solution of H_2PtC1_6•$6H_2O$. The preparation methods of PtLaχ/SZ were the same as that of La_2O_3/SZ, except that PtLaχ/SZ catalysts were calcined at 450 °C for 5 h. The nominal platinum loading was held constant at 1.0 wt. %. For comparison, the La_2O_3/SZ catalyst with 1.0 wt. % La was also investigated.

4.2.3 Catalyst characterization

BET surface area, pore volume and pore diameter of the prepared support and catalysts were measured by N_2-physisorption at 77 K using a Belsorp-mini II analyzer (Bel Japan Inc.). Before testing, all the catalysts were degassed in vacuum at 673K for 1 h.

X-ray fluorescence (XRF) analysis of the catalysts was conducted with an XRF spectrometer (JSX-3100RII, JEOL Corp.) for quantitative analysis of metallic elements.

X-ray diffraction (XRD) patterns of the reduced catalysts was recorded with an XRD instrument (RINT2100 VPC/N, Rigaku Corp.) using Cu-Kα radiation (40 kV, 30 mA) at 2θ angles from 5 to 85 ° with step-sizes of 1° and counting times of 2 s.

Ammonia temperature-programmed desorption (NH_3-TPD) analysis of the catalysts was performed using a chemisorption-physisorption analyzer (ChemBET PULSAR TPR/TPD; Quantachrome Instruments) with a thermal conductivity detector (TCD). 200 mg of catalyst was loaded and reduced at 400 °C for 3 h by a pure H_2 at a rate of 15 cm^3/min, then cooled to 30 °C in He stream. The ammonia adsorption was conducted in a flow of 10 vol. % NH_3/He flow (15 cm^3/min) for 40 min. The physically adsorbed ammonia was removed at 100 °C for 2 h under helium flow, and the TPD was measured by linearly increasing the cell temperature from 100 to 800 °C at a heating rate of 10 °C /min. The amount of desorbed ammonia was calculated by pulse calibration.

Hydrogen temperature-programmed reduction (H_2-TPR) of the catalysts was carried

out in the same instrument as NH_3-TPD. 100 mg of catalyst was pretreated with He at 500 °C for 1 h, then analyzed from room temperature to 900 °C with heating rate of 5 °C/min. The consumption of H_2 was monitored online by a TCD detector.

FT-IR spectra of CO adsorption were performed using an IRPrestige-21 instrument (Shimadzu) with a measurement cell with CaF_2 windows and investigated with 64 scans at 4 cm^{-1} resolution. The catalyst was ground and pressed into a wafer with a diameter of 10 mm and inserted into the measurement cell, which was connected to a vacuum apparatus. The measurement cell with catalyst wafer was heated to 400 °C (20 °C /min) and reduced for 3 h by H_2 (30 mL/min), then evacuated until the pressure less than 10^{-5} Torr for 2 h. The CO adsorption was investigated at 40 °C for 0.5 h, followed 20 min of evacuation.

The FT-IR spectra of pyridine adsorption was investigated on the same instrument as CO adsorption. Before adsorption, the catalyst was reduced at 400 °C for 3 h then degassed for 2 h. Pyridine adsorption was performed under the pyridine pressure of 4 Torr for 30 min at 100 °C. Prior to recording the IR spectra, the sample was degassed for 20 min at each temperature.

X-ray photoemission spectra (XPS) were obtained using an ESCA-3200 (Shimadzu) spectrometer equipped with monochromatic Mg Ka radiation (240 W, 8 kV, E = 1253.6 eV). The binding energy (BE) value of adventitious carbon (C 1s, 284.6 eV) was used as the reference. The catalyst sample prepared in a dry box under argon flow with a degassing pretreatment prior to perform.

TEM measurement of catalyst was performed on a JEM-1400 (JEOL) electron microscope operating at 200 kV. The catalyst was reduced ex-situ in H_2 flow at 400 °C for 3 h and dispersed in ethanol, then a drop of the suspension was deposited on a carbon-coated copper microgrid as test sample.

4.2.4 Catalytic test

The catalytic depolymerization of alkali lignin and was performed on the same process as reported in our previous study [6]: firstly, lignin was dissolved in a mixture solvent of [Apy]Cl and water as lignin-solution; then 0.452 g of SZ, Pt/SZ, PtLaχ/SZ and La_2O_3/SZ catalysts loaded in the reactor, among of which the Pt-supported catalysts were reduced at 400 °C under a 30 mL/min H_2 flow for 3 h at atmospheric pressure before reactions. After that, the lignin-solution was continuously pumped into the fixed-bed reactor (i.d. 8 mm, length 160 mm) and reacted at 210 °C under the weight hourly space velocity (WHSV) of 3.8 h^{-1}. During the depolymerization process, the liquid mixtures were collected per hour as a sample, then added acetonitrile and ether to separate solid residue and regenerate IL from the sample. After that, the liquid products of lignin depolymerization were collected and concentrated via vacuum distillation at 50 °C to remove the extraction solvents.

After concentration, the liquid products analyzed by gas chromatography with flame ionization detector (GC-FID, Shimadzu Co.) with a column of Ultra alloy-5 (Agilent, 60 m×0.25 mm i.d., 0.25 μm) and gas chromatography-mass spectrometer (GC-MS, Shimadzu Co.) with a J&W Scientific DB-1 column (Agilent, 60 m×0.25 mm i.d., 0.25 μm). O-xylene was used as internal standard (IS) to confirm the position and the mass-to-charge ratio of the peaks during GC-FID analysis [6]. The liquid products identified by GC-MS were divided into phenolic and nonphenolic compounds. Product yield was obtained in terms of carbon molar yield, and the total mole yield of carbon-based products and phenolic compounds are divided by the moles of carbon in the feedstock which fed in the reactor with respect to the IS. After three repetitions of all the tests, the average of three trials was used in this study. The total mole yield of carbon-based products (*Yc*, C, mol %) and phenolic compounds (*Yp*, C, mol%) were calculated by equation (4-1) and (4-2):

$$Y_c, (C, mol\%) = \frac{\text{Carbon moles in liquid products}}{\text{Carbon moles fed in}} \times 100\% \quad (4\text{-}1)$$

$$Y_p, (C, mol\%) = \frac{\text{Carbon moles in phenolic compounds}}{\text{Carbon moles fed in}} \times 100\% \quad (4\text{-}2)$$

Furthermore, guaiacol and guaiacylglycerol-β-guaiacyl ether (GG) were used as the model compounds of lignin to elucidate the reaction pathways of lignin depolymerization and the possibility role of [Apy]Cl in the whole process in the absence/presence of SZ and Pt/SZ catalysts corresponding to the pretreatment and reaction unit in pressure resistant glass reactor.

4.3 Results and discussion

4.3.1 Characterization of the properties of the catalysts

Textural properties and chemical compositions of the prepared catalysts were summarized in Table 4.1. No significant changes observed in pore diameter except for the slight decrease in BET surface area and the pore volume of the catalysts with the introduction of platinum and lanthanum, due to the blocking or filling of SZ micropores by the species of Pt and La_2O_3. Meanwhile, the chemical analyses results demonstrated the contents of platinum and lanthanum were approximately the same as nominal values.

Table 4.1. Physical and chemical characteristics of the catalysts.

Catalyst	BET			XRF	
	*V*m ($cm^3 \cdot g^{-1}$)[a]	*A*s ($m^2 \cdot g^{-1}$)[b]	*d* (nm)[c]	Pt (wt%)	La (wt%)
SZ	0.159	45.9	14.5	-	-
Pt/SZ	0.153	43.1	15.5	1.01	-
La_2O_3/SZ	0.168	40.7	16.5	-	1.05
PtLa1/SZ	0.163	42.5	15.0	1.03	0.74
PtLa3/SZ	0.144	38.4	15.4	0.98	2.43
PtLa6/SZ	0.130	34.3	15.1	1.05	4.35

a, Pore volume; b, surface area; c, pore diameter of the catalysts derived from nitrogen adsorption−desorption isotherms measured at 77 K.

The XRD patterns of catalysts were presented in Figure 4.1. Prior to analysis, the Pt-supported catalysts were reduced at 400 ℃ for 3h. Almost no changes in the XRD patterns among all of the catalysts were observed comparing with that of SZ, which suggested that the Pt and La_2O_3 were mainly deposited on the surfaces of the support (SZ, La_2O_3/SZ) without altering the structure. Also, no Pt peaks were detected by XRD, suggesting that Pt particles were dispersed well and less than 5 nm [25].

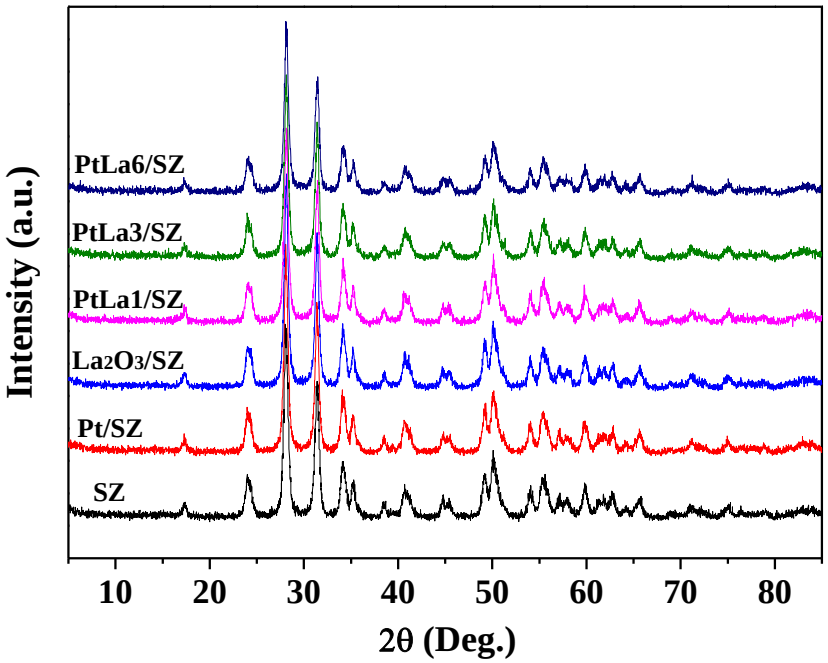

Figure 4.1. XRD patterns of the reduced catalysts. Reduction temperature: 400 °C.

The acidity of SZ and PtLaχ/SZ catalysts analyzed by NH_3-TPD as shown in Figure 4.2. All of the catalysts exhibited similar distributions of weak acid sites at a range of 200-270 °C, however, the medium and strong acid sites located at around 350 °C were almost disappeared after Pt and La_2O_3 addition compared with that of SZ. Taking the NH_3 desorption profile for SZ into account, the peaks of weak acid sites were mainly originated from the SZ support and the intensity were increased with the La_2O_3 content increased in PtLaχ/SZ catalysts, which significantly affected the distribution of the acid site. Additionally, the number of the acid site was calculated by a calibration curve as listed in Table 4.2. With the La_2O_3 content increased, the total acidity exhibited an increasing tendency. To identify the type of acidity, FT-IR spectra of pyridine adsorption of all the catalysts were shown in Figure 4.3. And the ratio of Lewis to Brønsted acid sites (L/B) at different evacuation temperatures was listed in Table 4.2. The main bands at around 1455 and 1542 cm^{-1} were assigned to Lewis and Brønsted acid [26], which contained in all of the catalysts. The addition of Pt and La_2O_3 onto SZ support caused an increase of the L/B ratio from 1.6 to 2.9 and 2.7 after evacuation at 100 °C,

respectively. Notably, Lewis acid sites as well as the L/B ratio significantly increased with adding lanthanum, due to the induced effect of S=O the electronic capacity of the corresponding Zr^{4+} increased resulting in a strong shift of Zr-O electrons and an increase of Lewis acid sites [20, 21]; meanwhile, partial of PtO or PtO_2 existed on the surface of catalysts also enhanced the Lewis acid strength through the coordination of PtO for S=O [18]. However, there was no significant change in the L/B ratio for the sample evacuated at 200 °C and 300 °C, suggesting the new Lewis acid sites exhibited weak acidity. In conclusion, the acid sites on PtLaχ/SZ catalysts were partially from the SZ support and the other from the introduction of platinum and lanthanum which enhanced the acidity of Lewis acid.

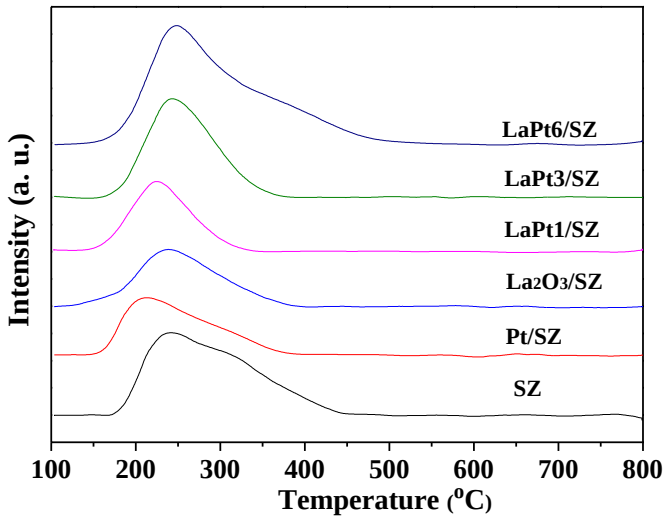

Figure 4.2. NH_3-TPD profiles of the support and reduced catalysts.

Table 4.2. Acidity of the support and reduced catalysts.

Catalyst	Total acidity (μmol NH_3/g)	Ratio of Lewis to Brønsted acid sites		
		100 ℃	200 ℃	300 ℃
SZ	387	1.6	1.1	0.7
Pt/SZ	322	2.9	7.9	3.5
PtLa1/SZ	473	13.8	7.7	3.4
PtLa3/SZ	544	17.3	6.0	3.2
PtLa6/SZ	570	22.1	8.3	3.5

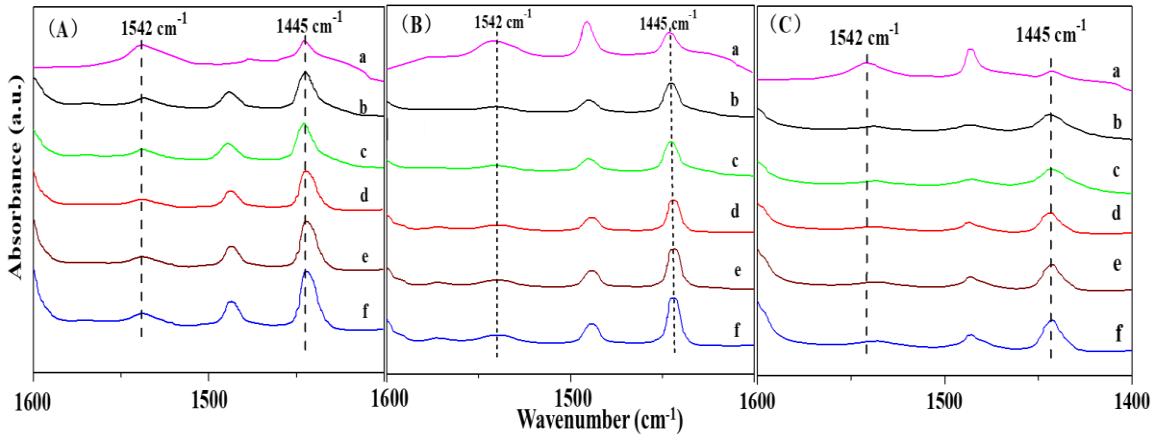

Figure 4.3. FT-IR spectra of pyridine adsorption on the (a)SZ, (b) Pt/SZ, (c) PtLa1/SZ, (d) PtLa3/SZ and (e) PtLa6/SZ catalysts after evacuation at (A) 100 °C, (B) 200 °C and (C) 300 °C.

The electronic properties of metal-supported particles were qualitatively evaluated by means of IR spectra of CO adsorption and the results were shown in Figure 4.4. Prior to the FT-IR spectra of CO adsorption at 40 °C, Pt/SZ and PtLaχ/SZ catalysts were reduced in-situ in H_2 at 400 °C for 3h. The main band at around 2090 cm^{-1} was assigned to CO adsorption on Pt^0 [27]. Compared to the Pt/SZ catalyst, with the increase of La_2O_3 content, the band of CO adsorption on Pt^0 in PtLaχ/SZ catalysts shifted to higher wavenumber, which associated with the Pt-support interaction (i.e., Pt-O-La bond) [23].

XPS spectra peaks corresponding to Pt 4f, La 3d, and O 1s of the reduced catalysts were shown in Figure 4.5 and 4.6 and the binding energy (BE) were summarized in Table 4.3. Binding energy (BE) values of Pt 4f signals at the peaks with BEs of 71.37 and 74.85 eV were assigned to the $4f_{7/2}$ and $4f_{5/2}$ peaks of Pt^0, respectively [28]. The higher BEs position of the two peaks (72.83 and 76.08; 77.90 and 79.43 eV) were assigned to the $4f_{7/2}$ and $4f_{5/2}$ peaks of Pt^{2+} (i.e. PtO and $Pt(OH)_2$) and Pt^{4+} (PtO_2) [28], respectively. With the increase of La_2O_3 content, the peaks of Pt^0 in PtLa1/SZ, PtLa3/SZ and PtLa6/SZ catalysts had slightly higher BE values by 0.13, 0.17 and 0.20 eV for $4f_{7/2}$

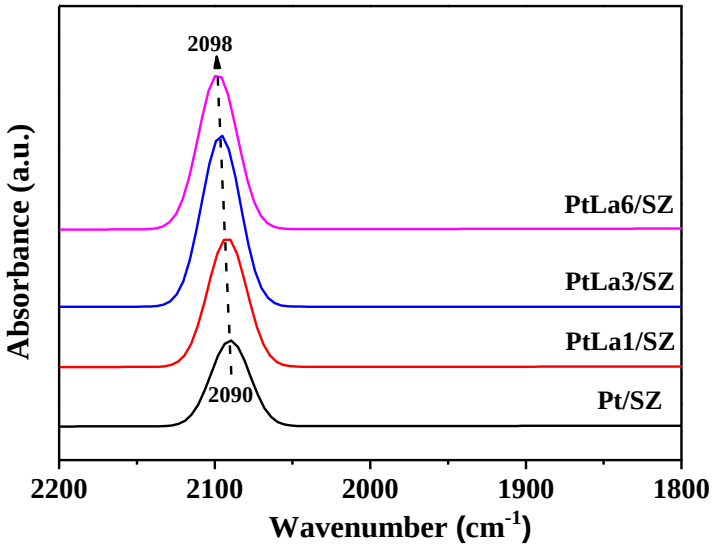

Figure 4.4. FT-IR spectrum of CO adsorption at 40 °C on the Pt/SZ and PtLaχ/SZ.

and 0.24, 0,28 and 0.31 eV for $4f_{5/2}$ peaks, respectively, than those of Pt/SZ catalyst, due to the strong interaction between Pt and La_2O_3/SZ [23]. Binding energy values of La $3d_{5/2}$ signals at the peaks with BEs of 837.8 and 834.1 eV were assigned peaks of La_2O_3 and $La(OH)_3$, respectively [29]. No significant differences were observed in the La $3d_{5/2}$, especially for PtLa1/SZ and PtLa3/SZ catalysts. However, in PtLa6/SZ catalyst peak of $La(OH)_3$ disappeared and the BE value of La_2O_3 shifted to a lower value (837.5 eV). The O 1s spectrum of Pt/SZ, which were divided into three peaks with BE values of 531.63, 532.45 and 533.45 eV assigned to the surface lattice oxygen species (O1), the surface adsorbed oxygen species (O2) and the electrophilic O-species (O^{2-} or O^{-}) (O3), respectively [29]. The presence of various oxygen species could be resulted in the formation of PtOx (i.e. PtO_2, PtO) species on the surface of the catalysts [30]. Compared to the O 1s in Pt/SZ, with the increase of La_2O_3 content, the BE value of O1 was gradually reduced, resulting in the generation of oxygen vacancies and promoting the formation of Lewis acid site. On the other hand, the BE values of O2 increased with higher La_2O_3 contents, which caused the partial $La(OH)_3$ oxidized to La_2O_3 and the disappearance of $La(OH)_3$ in PtLa6/SZ catalyst. Moreover, the increase of La/Pt content

shifted the BE values of O3 from 533.45 eV to 533.98 eV, which also meant the strong interaction between Pt and La_2O_3/SZ.

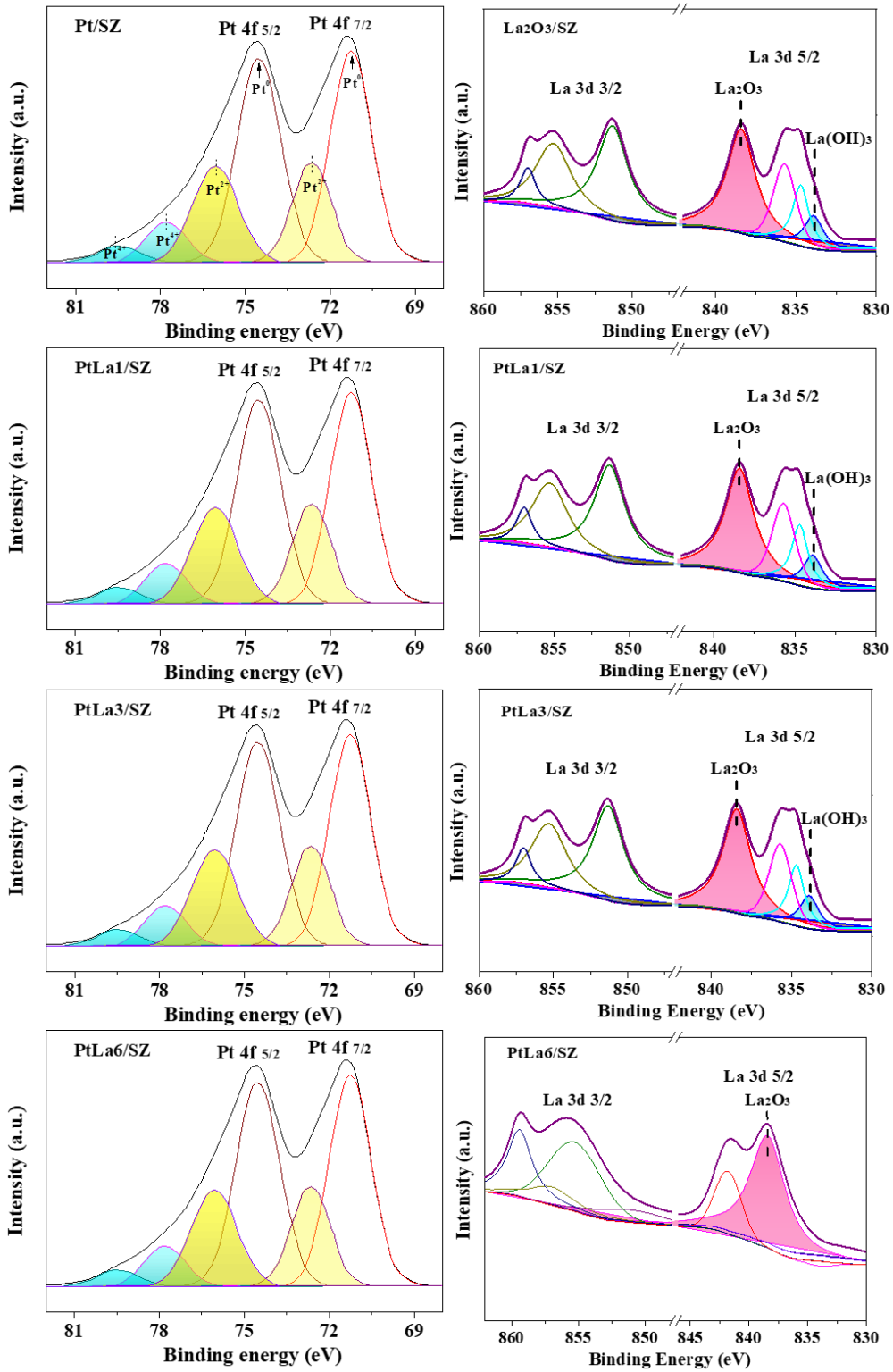

Figure 4.5. XPS spectra of Pt 4f and La 3d for the reduced La_2O_3/SZ, Pt/SZ and PtLaχ/SZ catalysts.

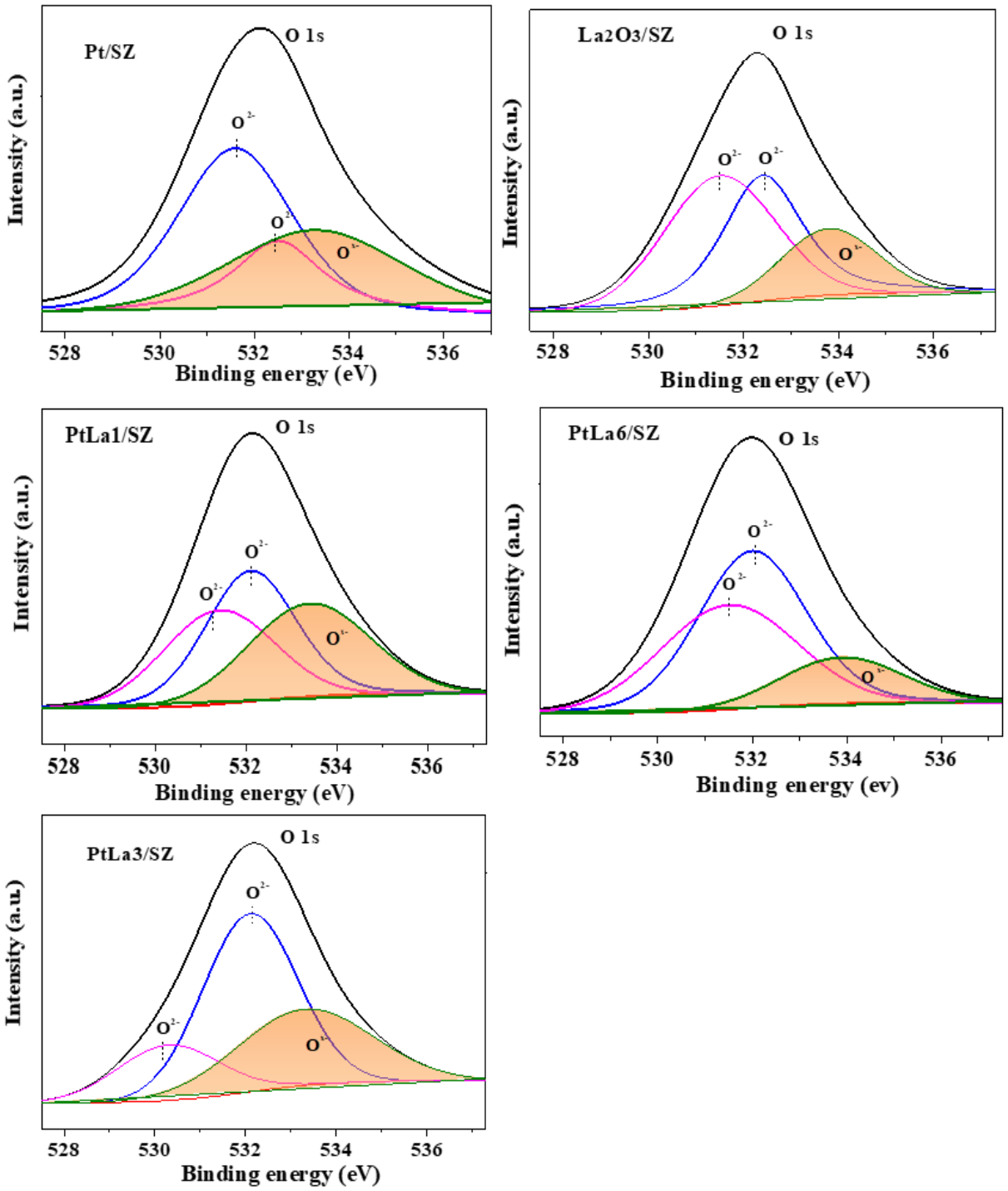

Figure 4.6. XPS spectra of O 1s for the reduced La_2O_3/SZ, Pt/SZ and PtLaχ/SZ catalysts.

Figure 4.7 showed TEM images and the statistic distributions of the Pt particle size of the Pt/SZ, La_2O_3/SZ, PtLa1/SZ, PtLa3/SZ and PtLa6/SZ catalysts after reduction at 400 °C for 3 h. The PtLa1/SZ, PtLa3/SZ and PtLa6/SZ catalysts exhibit smaller average

Table 4.3. Summary of XPS analyses on the reduced catalysts.

Catalyst	Pt 4f		La $3d_{5/2}$		O 1s		
	$4f_{7/2}$	$4f_{5/2}$	La_2O_3	$La(OH)_3$	O1	O2	O3
Pt/SZ	71.37	74.85	-	-	531.63	532.45	533.45
La_2O_3/SZ	-	-	837.81	834.12	531.63	532.45	533.77
PtLa1/SZ	71.5	75.09	837.82	834.11	531.42	532.07	533.43
PtLa3/SZ	71.54	75.13	837.82	834.10	530.29	532.11	533.45
PtLa6/SZ	71.57	75.16	837.58	-	530.48	532.15	533.98

Pt particle sizes (0.90, 0.84, 0,94 nm) than that of the Pt/SZ catalyst (1.26 nm), indicating the addition of La_2O_3 promoted Pt particles dispersion. Interestingly, the TEM images of Pt/SZ, PtLa1/SZ, PtLa3/SZ and PtLa6/SZ catalysts showed a core-shell structure with the core of Pt particles on the surface of all the Pt-supported catalysts. On the basis results of XPS and FT-IR of CO adsorption, Pt was mainly in metallic phase appeared to interact with SZ and/or La_2O_3/SZ with part of Pt oxidized state outside which formed self-assembled the Pt-O shell. And this result was consistent with previous research [31], in which X-ray absorption near edge structure (XANES) and extended X-ray absorption fine structure (EXAFS) were used to prove Pt-O shell presented in a reduced Pt/SZ catalyst. And the Pt particles distribution results of XPS were less than 2 nm also confirmed the conclusion of XRD analysis.

To investigate the reducibility of catalysts of Pt/SZ and PtLaχ/SZ, H_2-TPR was performed and the results were shown in Figure 4.8. Three main peaks were exhibited, small peak at 190-300 °C was attributed to the reduction of Pt oxide species in low interaction with the support (SZ, La_2O_3/SZ); the peak at 600–650 °C was assigned to the reduction of surface sulfate groups as compared with that of SZ; the peak at > 700 °C was assigned to the reduction of partial metal oxides with strong interaction with SZ and/or La_2O_3/SZ [26]. The introduction of Pt and La_2O_3 affected the reducibility of the catalysts [32], as the reduction peak of Pt in Pt/SZ was 238.9 °C which was shifted to

high temperature of 251.8 and 278.1 °C in the case of PtLa1/SZ and PtLa6/SZ catalysts, respectively. On the other hand, in the case of the PtLa3/SZ the reduction peak of Pt shifted to low temperatures about 191.0 °C. These changes might be associated to the promoting effect of La_2O_3 dispersed on the SZ giving finely Pt species interacting with La_2O_3. From H_2-TPR results, the low content of La_2O_3 was conducive to the formation of strong interaction of Pt with the supports and the reducibility of catalysts was PtLa3/SZ > Pt/SZ > PtLa1/SZ > PtLa6/SZ.

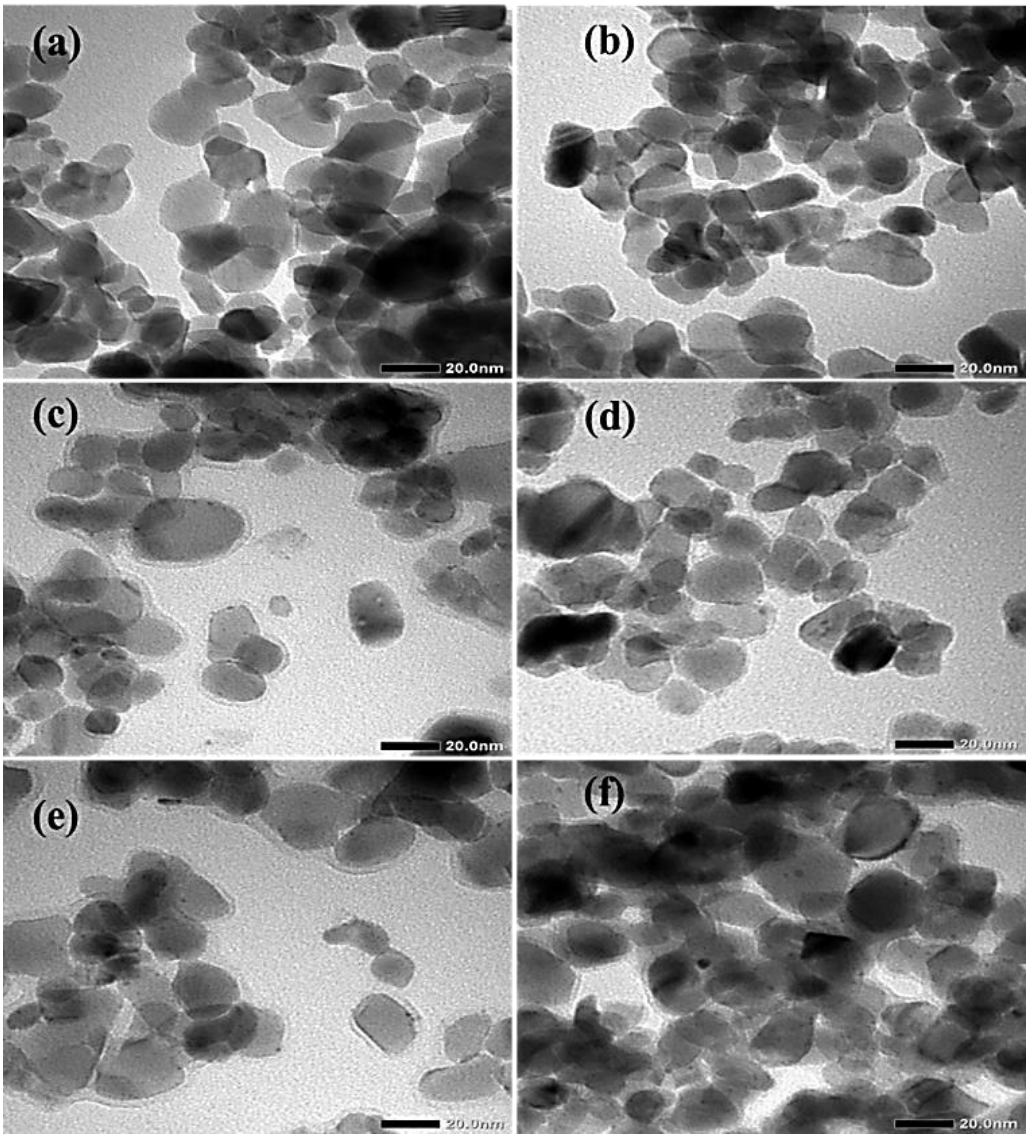

Figure 4.7. TEM images and Pt particle size distribution of the (a)SZ, (b) La_2O_3/SZ, (c)Pt/SZ, (d) PtLa1/SZ, (e) PtLa3/SZ and (f) PtLa6/SZ catalysts. The metal catalysts were reduced at 400 °C for 3 h.

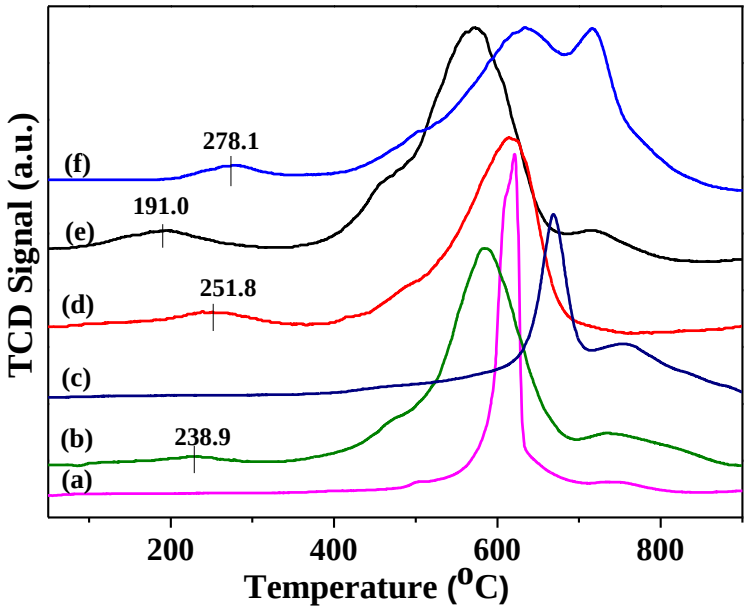

Figure 4.8. H_2-TPR profiles of the reduced (a) SZ, (b) Pt/SZ, (c) PtLa1/SZ, (d) PtLa3/SZ and (e) PtLa6/SZ catalysts.

From the characterization results of Pt/SZ and PtLaχ/SZ catalysts, it was inferred that the Pt-O shell with micropores structure exists on the surface. The possible mechanism of addition of Pt and La into sulfated zirconia and the possible structure of the Pt/SZ and PtLaχ/SZ catalysts were shown in Scheme 4.1. Before the introduction of Pt and La, the Brønsted sites of SZ catalysts were mainly derived from sulfate species and Lewis sites from unsaturated Zr atoms on the surface. With the introduction of Pt and La, some Brønsted sites were covered by Pt and La resulted in a decrement of Brønsted acidity. For Pt/SZ catalyst, Pt on the surface of Pt/SZ catalyst was mainly in metallic phase with part of Pt oxidized state (i.e., Pt^{4+}, Pt^{2+}) outside with larger Pt particles, which formed Pt-O shell with a high interaction with SZ. And the withdrawal of electrons from the framework hydroxyl group with the presented Pt oxidize also resulted the number of Brønsted acid sites and total acidity decreased. For La_2O_3/SZ catalysts, the introduction of La caused the condensation of Zr-OH with La^{3+} occurred with the new Brønsted acid sites formed, combined with the electronic capacity of the corresponding Zr^{4+} increased resulting in a strong shift of Zr-O electrons and an increase

of Lewis acid sites [21]. For PtLaχ/SZ catalysts, with Pt addition into the surface of La_2O_3/SZ, the number of new formed Brønsted acid sites decreased with the formation of Pt-O-La linkage, meanwhile, due to the strong interaction the dispersion of Pt particles on the surface of PtLaχ/SZ catalysts was improved with smaller Pt particles. In conclusion, the introduction of Pt and La_2O_3 caused highly covalent character of sulfate species on the catalyst surface and high interaction between Pt and La_2O_3, which led to an increase of the number of Lewis acid site and a more highly dispersion of Pt particles on the surface of PtLaχ/SZ catalysts.

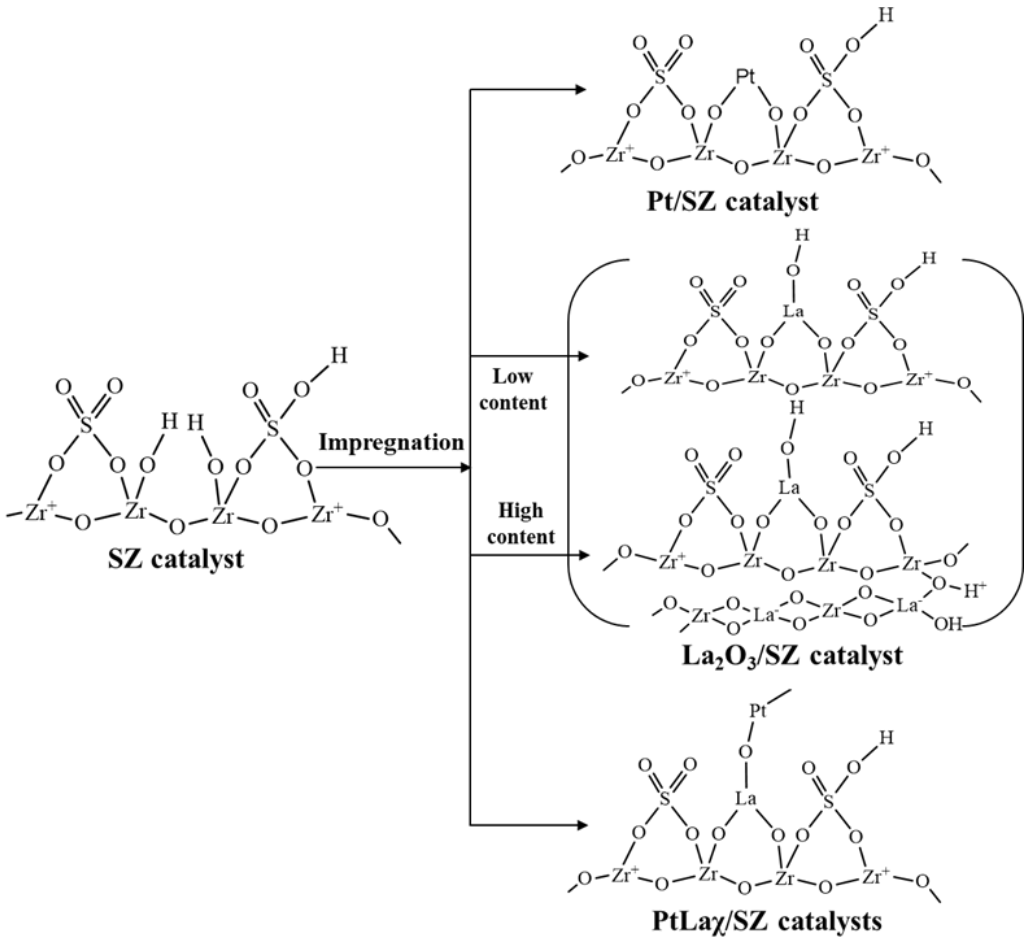

Scheme 4.1. Possible mechanism of addition of Pt and La into sulfated zirconia and structure of the Pt/SZ and PtLaχ/SZ catalysts.

4.4 Depolymerization of alkali lignin in [Apy]Cl

4.4.1 Products in lignin depolymerization

Similar to our previous report [6], a lot of the non-phenolic and phenolic compounds were produced during the depolymerization of alkali lignin as shown in Table 4.5. Figure 4.9 showed the GC-FID chart of liquid products in lignin depolymerization in the presence of studied catalysts at 210 °C under WHSV of 3.8 h^{-1}. The yields of various products were listed in Table 4.4. The total yields of the phenolic compounds increased with Pt and La_2O_3 addition, and the new product of 1-(4-hydroxy-3,5-dimethoxyphenyl) propan-1-one (No. 12) obtained. With the increasing La_2O_3 contents, PtLa3/SZ showed the highest yield of No.12 (1.25 C, mol %). Among the phenolic compounds, the main products were 4-vinylphenol, 4-hydroxyphenylacetic acid and 5-dihydroxy-1,2,3,4-tetrahydronaphthalene, and the yields of these increased with the increase of La_2O_3 contents. As shown in Table 4.4, 4-vinylphenol was the main phenolic compound with a higher yield.

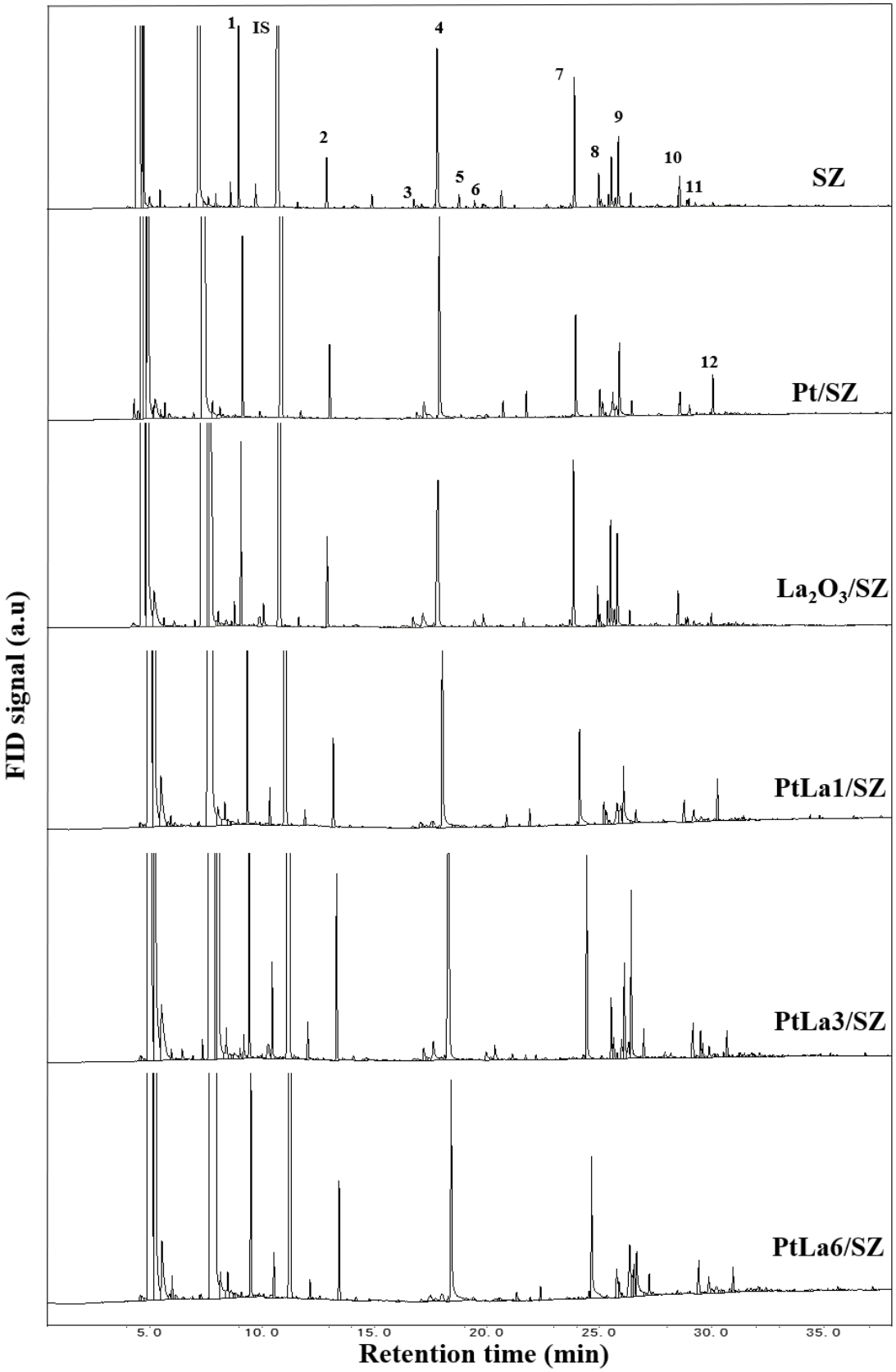

Figure 4.9. GC-FID spectra of liquid products in case of different catalysts at 210 °C under WHSV of 3.8 h^{-1}.

Table 4.4. Quantification of the identified liquid products by means of GC-FID.

No.	Yield/C, mol %					
	SZ	Pt/SZ	La_2O_3/SZ	PtLa1/SZ	PtLa3/SZ	PtLa6/SZ
1	3.44	4.50	4.07	7.50	6.46	5.96
2	1.40	2.44	2.64	2.39	4.50	3.37
8	1.03	1.06	1.26	1.24	1.58	1.18
$\boldsymbol{Y_{np}}$	5.87	8.00	7.98	11.10	12.50	10.50
3	0.193	1.06	1.21	1.08	1.12	0.59
4	5.49	9.43	9.91	8.09	13.67	9.28
5	0.38	0.45	0.415	0.42	0.42	0.17
6	0.87	0.66	0.361	0.24	0.20	0.33
7	3.48	3.59	4.87	3.72	5.02	5.32
9	2.08	2.69	3.10	3.58	1.58	2.73
10	0.73	1.04	2.77	2.30	2.45	2.26
11	0.15	1.21	1.25	1.17	4.05	1.31
12	0.00	0.16	0.26	0.65	1.25	0.68
$\boldsymbol{Y_p}$	13.4	18.7	24.1	21.2	28.7	22.7
Total	19.3	26.7	32.1	32.3	41.2	33.2
$\boldsymbol{Yc}$	30.6	44.9	47.8	58.4	63.9	52.1

Y_c, total yields of carbon-based products; Y_p, yields of phenolic compounds; Y_{np}, yields of nonphenolic compounds.

Table 4.5. Identification of liquid products by means of GC-MS.

No.	Compounds	Structure
1	Furfuryl alcohol	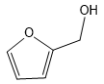
2	Benzaldehyde	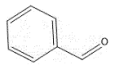
3	2,6-Xylenol	
4	4-Vinylphenol	
5	Iso-creosol	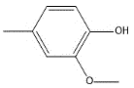
6	6-Methylsalicylic acid ethyl ester	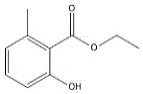
7	4-Hydroxyphenylacetic acid	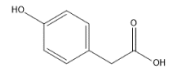
8	2,6-Dimethylstyrene	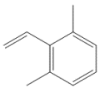
9	1,5-Dihydroxy-1,2,3,4-tetrahydro naphthalene	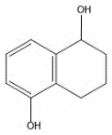
10	2,2'-Biphenol	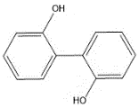
11	Butylated hydroxytoluene	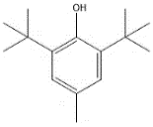
12	1-(4-Hydroxy-3,5-dimethoxyphenyl) propan-1-one	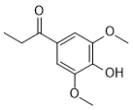

4.4.2 Effect of La_2O_3 content on the activity of PtLaχ/SZ catalysts.

The yields of carbon-based products (Y_c), phenolic compounds (Y_p) and nonphenolic compounds (Y_{np}) increased with Pt and La_2O_3 added, especially to the increase of La_2O_3 contents. It was noteworthy that the La_2O_3/SZ catalyst also showed a higher activity than that of SZ in the depolymerization, might be due to the induced effect of S=O, the electronic capacity of the corresponding Zr^{4+} increased, resulting in a strong shift of Zr-O electrons and an increase of Lewis acid sites [20]. This also indicated that the content of Lewis acid played an important role in lignin depolymerization. The yields of the carbon-based products and phenolic compounds catalyzed by SZ appeared to be minimized (30.6 and 13.4 C, mol %, respectively). In the case of PtLa3/SZ catalyst, the yields of the carbon-based products and phenolic compounds increased to 63.9 and 28.7 C, mol %, respectively. As shown in Figure 4.10 and 4.11, the highest yields of carbon-based products (Y_c), phenolic compounds (Y_p), nonphenolic compounds (Y_{np}) and the main product of 4-Vinylphenol were exhibited in the presence of PtLa3/SZ catalyst, which were 63.9, 28.7, 12.5 and 13.67 C, mol %, respectively, were higher than those of in PtLa6/SZ catalyst due to size distribution of Pt particles increased with higher La_2O_3 contents as XPS and TEM results revealed. Nevertheless, the low content of La_2O_3 promoted the reaction to produce the phenolic compounds in the overall reaction and the active Pt sites became accessible to lignin depolymerization with increased the atomic ratio of La to Pt to 3. The PtLa3/SZ catalysts had the larger pore diameter and higher dispersion of Pt particles resulted in the highest activity for lignin depolymerization.

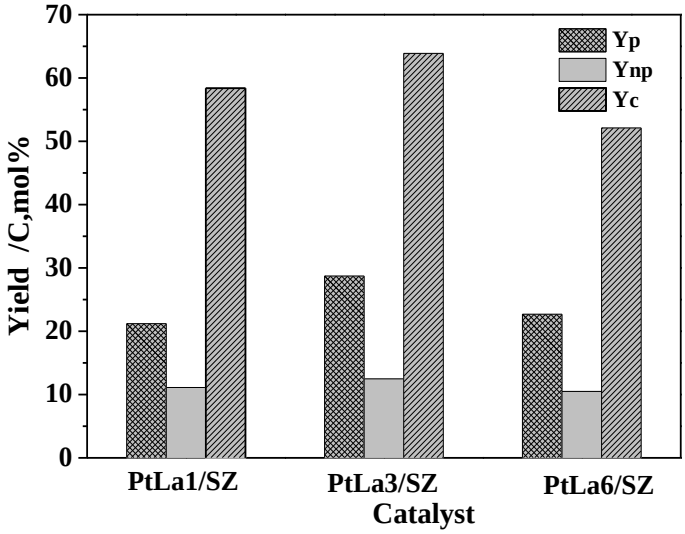

Figure 4.10. Effects of La_2O_3 content on the yields of carbon-based products (Yc) and phenolic compounds (Yp) (C, mol%; based on lignin).

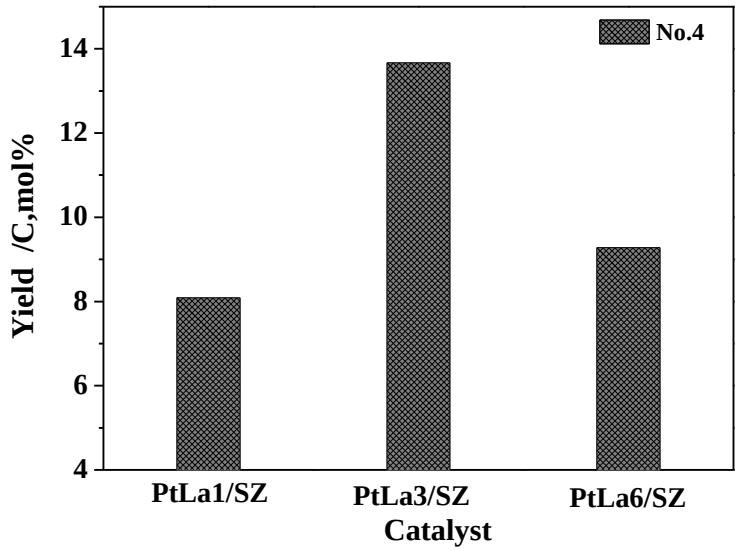

Figure 4.11. Effects of d La_2O_3 content on the yields of 4-Vinylphenol.

4.5 Reaction pathways of lignin depolymerization

In the present study, reaction pathways of lignin depolymerization and the possible role of [Apy]Cl in the whole process were studied by using the model compounds of lignin, guaiacylglycerol-β-guaiacyl ether (GG) in the absence/presence of SZ and Pt/SZ catalysts in pressure resistant glass reactor under the same condition of lignin depolymerization in the pretreatment and reaction unit.

After pretreatment and reaction processes, the liquid products obtained from those two substrates were quantified and identified by GC-FID and GC-MS were listed in Figure 4.12 and 4.13. Table 4.6. showed the relative content of liquid products from the depolymerization of guaiacylglycerol-β-guaiacyl ether (GG) at 210 ℃. For guaiacol, 2.81 % of catechol was produced during pretreatment, indicating [Apy]Cl was a promising reagent to cleave of methyl aryl ethers which was same as the previous reported [14]. For the depolymerization of GG in pretreatment unit, as shown in Table 4.6, there were two ways to degrade GG: 1) β-O-4 bond cleavage (pathway a); 2) Cγ-elimination reaction (pathway b), that is, Cγ was removed in the form of (Z)-2-methoxy-4-(2-(2-methoxyphenoxy)vinyl)phenol. The formation of guaiacol (19.2 %), coniferyl aldehyde (2.5 %) and coniferyl alcohol (0.8 %), indicating that the main depolymerization pathway of GG was mainly β-O-4 bond cleavage (pathway b), while the low relative content of 4-vinylguaiacol, indicating that the pathway b (i.e., Cγ-elimination reaction) was a secondary cleavage pathway. Through compared the results obtained from pretreatment and reaction unit, the addition of the catalyst promoted the depolymerization of lignin, in particular the cleavage of the β-O-4 bond in the form of guaiacol. Meanwhile, Pt/SZ showed higher catalytic activity than that of SZ which was consistent with lignin depolymerization results.

Based on above analysis, the produced catechol originated from two parts: one was from the demethylation of guaiacol in ionic liquids; the other part was from the

depolymerization of GG under the synergistic effect of [Apy]Cl and the catalysts in the overall process. These results indicated [Apy]Cl was not only a promising reagent, but intermediate medium with catalytic properties for lignin depolymerization. Simultaneously, the synergistic effect of ionic liquids and catalysts promoted the depolymerization of lignin under mild conditions. The hypothetical reaction pathway of the depolymerization of GG under synergistic effect of ionic liquids and the catalysts was proposed as shown in Scheme 4.2.

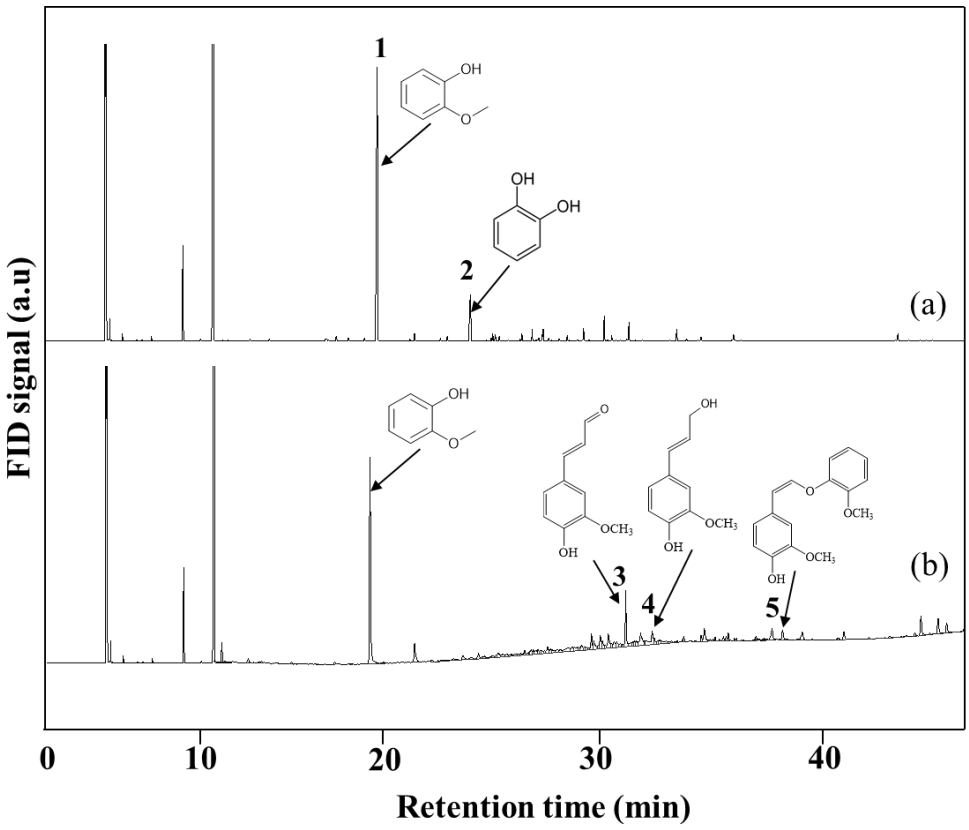

Figure 4.12. GC-FID chart of liquid products from pretreatment unit (90 ℃, 3h), a: guaiacol; b: guaiacylglycerol-β-guaiacyl ether (GG).

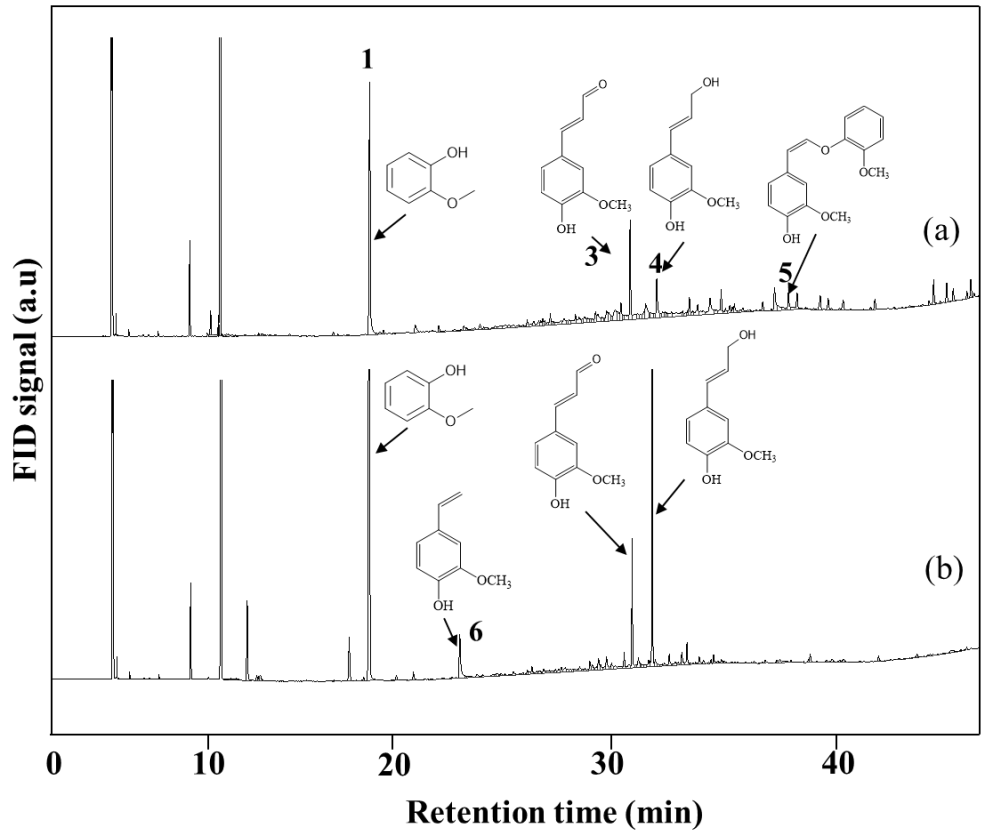

Figure 4.13. GC-FID chart of liquid products from guaiacylglycerol-β-guaiacyl ether (GG) in reaction unit with different catalysts (210 ℃; 1h; a: SZ catalyst; b: Pt/SZ catalyst).

Table 4.6. The relative content of liquid products in depolymerization of guaiacylglycerol-β-guaiacyl ether (%).

Product	Pretreatment	Reaction	
		SZ	Pt/SZ
Guaiacol	19.2	23.6	41.3
4-Vinylguaiacol	trace	trace	3.2
Coniferyl aldehyde	2.5	5.3	4.9
Coniferyl alcohol	0.8	1.9	12.4
(Z)-2-methoxy-4-(2-(2-methoxyphenoxy)vinyl)phenol	0.5	0.1	trace

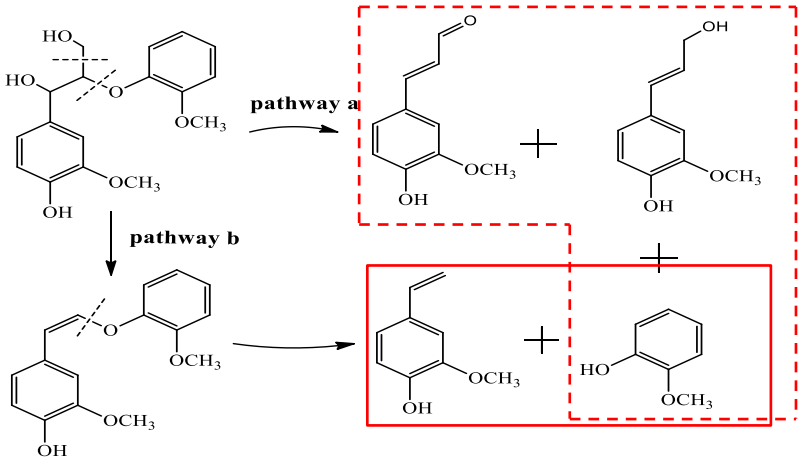

Scheme 4.2. Depolymerization pathways of guaiacylglycerol-β-guaiacyl ether in the system of [Apy]Cl and catalysts.

Based on above results, the proposed reaction pathways of lignin depolymerization under the synergistic effect of ionic liquids and catalysts were suggested in Scheme 4.3, which including the cleavage of β-O-4 bond in [Apy]Cl pretreatment, but also the catalytic depolymerization of lignin with catalyst in reaction unit. Based on previous reports [33, 34] and the distribution of the liquid products obtained from the model depolymerization and demethylation, lignin was effectively depolymerized with the partial cleavage of β-O-4 into low molecular weight products with the increase of phenolic hydroxyl content after [Apy]Cl pretreatment. As illustrated in Scheme 4.3, [Apy]Cl contains strong coordinating anion (Cl^-) was used as a reaction media to stabilize the hydroxyl group on the intermedia compounds. Under the catalysis of catalysts, products with β-O-4 bond converted into an enol ether isomer by dehydration, then hydrolyzed to release guaiacol and carbonyl compounds. Meanwhile, under the demethylation of [Apy]Cl partial of guaiacol converted into catechol. By the catalytic dehydrogenation of Pt, ketone was generated and dehydrated to form α, β-unsaturated ketone. Then the hydrogenation and reduction cleavage reactions were performed with chemisorbed hydrogen, which from partial H_2O and acidic IL that migrated and adsorbed at Pt sites, from which the main product of aryl propylene (No. 4) in phenolic

compounds was produced.

From the characterization results of Pt/SZ and PtLaχ/SZ catalysts, it was inferred that the Pt-O shell with micropores structure exists on the surface. Based on the results of characterization and catalytic test, we proposed a representation of the catalyst structure as shown in Scheme 4.3. For Pt/SZ catalyst, Pt was mainly in metallic phase with part of Pt oxidized state (i.e., Pt^{4+}, Pt^{2+}) outside with larger Pt particles, which formed Pt-O shell with a high interaction with SZ. The withdrawal of electrons from the framework hydroxyl group with the presented Pt oxidize mainly resulted the number of Brønsted acid sites and total acidity decreased. For PtLaχ/SZ catalysts, the introduction of La_2O_3 caused the condensation of Zr-OH with La^{3+} occurred with the new Brønsted acid sites formed, combined with the electronic capacity of the corresponding Zr^{4+} increased resulting in a strong shift of Zr-O electrons and an increase of Lewis acid sites [21]. With Pt addition, the number of new formed Brønsted acid sites decreased with the formation of Pt-O-La linkage, which improved the dispersion of Pt particles on the surface of PtLaχ/SZ catalysts. In conclusion, the introduction of La_2O_3 on the prepared PtLaχ/SZ catalysts showed a more highly dispersion of Pt particles with the number of Lewis acid site increased. The PtLa3/SZ catalysts had the larger pore diameter and higher dispersion of Pt particles resulted in the highest activity for lignin depolymerization.

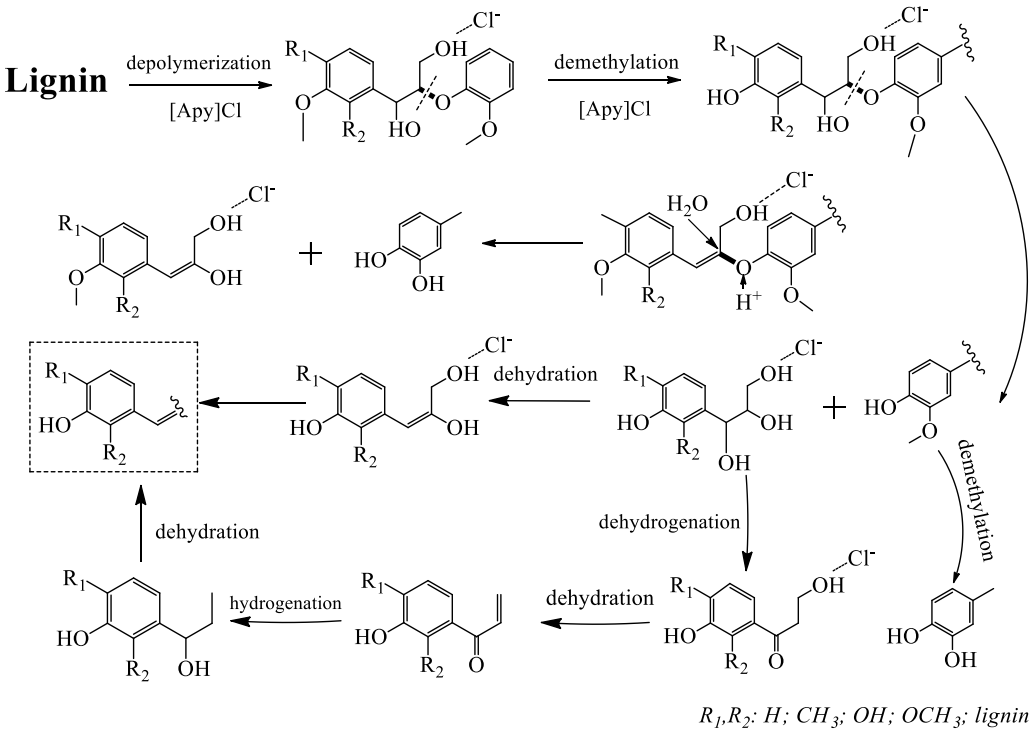

Scheme 4.3. Possible pathway of lignin depolymerization with synergistic effect of ionic liquids and catalysts.

4.5 Conclusions

Comparing to solid acid catalyst SZ, the introduction of Pt and La_2O_3 significantly enhanced the catalytic activity in depolymerization of alkali lignin. Based on the results obtained from FT-IR spectra of pyridine or CO adsorption and XPS, it was found that with La_2O_3 addition, the number of Lewis acid sites increased and resulted in the strong interaction between Pt and support through Pt-O-La bond. The interaction improved Pt particles dispersion as TEM analyzed. PtLa3/SZ catalyst showed the highest yield of phenolic compounds with yield of 28.7 C, mol % at 210 ℃. Furthermore, based on results in the depolymerization and demethylation of guaiacol and 1-(4-hydroxyphenyl)-2-(2-methoxyphenoxy) ethenone, the synergistic effect of ionic liquid and catalysts was elucidated and a hypothetical mechanism of lignin depolymerization was proposed.

References

[1] P. McKendry, Energy production from biomass (part 1): overview of biomass, Bioresour. Technol. 83 (2002) 37-46.

[2] P. Mäki-Arvela, B. Holmbom, T. Salmi, D. Y. Murzin, Recent progress in synthesis of fine and specialty chemicals from wood and other biomass by heterogeneous catalytic processes, Catal. Rev. 49 (2007) 197-340.

[3] P. Kaparaju, M. Serrano, A. B. Thomsen, P. Kongjan, I. Angelidaki, Bioethanol, biohydrogen and biogas production from wheat straw in a biorefinery concept, Bioresour. Technol. 100 (2009) 2562-2568.

[4] A. Banerjee, G. R. Dick, T. Yoshino, M. W. Kanan, Carbon dioxide utilization via carbonate-promoted C–H carboxylation, Nature 531 (2016) 215-219.

[5] G. R. Dick, A. D. Frankhouser, A. Banerjee, M. W. Kanan, A scalable carboxylation route to furan-2,5-dicarboxylic acid, Green Chem. 19 (2017) 2966-2972.

[6] X. Wang, N. Wang, T. T. Nguyen, E. W. Qian, Catalytic depolymerization of lignin in ionic liquid using a continuous flow fixed-bed reaction system, Ind. Eng. Chem. Res. 57(49) (2018) 16995-17002.

[7] L. Cao, K. M. Iris, Y. Liu, X. Ruan, D. C. Tsang, A. J. Hunt, S. Zhang, Lignin valorization for the production of renewable chemicals: State-of-the-art review and future prospects, Bioresource technol. 2018.

[8] W. Xu, S. J. Miller, P. K. Agrawal, C. W. Jones, Depolymerization and hydrodeoxygenation of switchgrass lignin with formic acid, ChemSusChem 5(4) (2012) 667-675.

[9] A. Rahimi, A. Ulbrich, J. J. Coon, S. S. Stahl, Formic-acid induced depolymerization of oxidized lignin to aromatics, Nature 515 (2014) 249-252.

[10] O. Y. Abdelaziz, K. Li, P. Tunå, C. P. Hulteberg, Continuous catalytic depolymerisation and conversion of industrial kraft lignin into low-molecular-weight aromatics, Biomass Convers. Bior. 8(2) (2018) 455-470.

[11] C. Liu, H. Wang, A. M. Karim, J. Sun, Y. Wang, Catalytic fast pyrolysis of lignocellulosic biomass, Chem. Soc. Rev. 43 (2014) 7594−7623.

[12] S. K. Singh, P. L. Dhepe, Ionic liquids catalyzed lignin liquefaction: mechanistic studies using TPO-MS, FT-IR, RAMAN and 1D, 2D-HSQC/NOSEY NMR, Green Chem. 18(14) (2016) 4098-4108.

[13] C. Liu, Y. Li, Y. Hou, Behavior of oxygen-containing groups in grass lignin during dissolution in basic ionic liquids, Cellulose 26(2) (2019) 737-749.

[14] M. Passiniemi, M. J Myllymaki, J. Vuokko, A. MP Koskinen, Demethylation of aromatic methyl ethers using ionic liquids under microwave irradiation, Lett. Org. Chem. 8(1) (2011) 48-52.

[15] G. J. Kemperman, T. A. Roeters, P. W. Hilberink, Cleavage of aromatic methyl ethers by chloroaluminate ionic liquid reagents, Eur. J. Org. Chem. 9 (2003) 1681-

1686.
[16] M. Thierry, A. Majira, B. Pégot, L. Cezard, F. Bourdreux, G. Clément, C. Lapierre, Imidazolium-Based Ionic Liquids as Efficient Reagents for the C-O Bond Cleavage of Lignin, ChemSusChem 11(2) (2018) 439-448.
[17] G. Corro, J. L. G. Fierro, V. C. Odilon, An XPS evidence of Pt^{4+} present on sulfated Pt/Al_2O_3 and its effect on propane combustion, Catal. Commun. 4 (2003) 371-376.
[18] K. Arata, H. Matsuhashi, M. Hino, H. Nakamura, Synthesis of solid superacids and their activities for reactions of alkanes, Cataly. Today 81(1) (2003)17-30.
[19] K. Stärk, N. Taccardi, A. Bösmann, P. Wasserscheid, Oxidative depolymerization of lignin in ionic liquids, ChemSusChem 3(6) (2010) 719-723.
[20] J. C. Araújo, D. Zanchet, R. Rinaldi, U. Schuchardt, C. E. Hori, J. L. G. Fierro, J. M. C. Bueno, The effects of La_2O_3 on the structural properties of La_2O_3–Al_2O_3 prepared by the sol–gel method and on the catalytic performance of Pt/La_2O_3–Al_2O_3 towards steam reforming and partial oxidation of methane, Appl. Catal. B 84 (2008) 552–562.
[21] V. B. Mortola, S. Damyanova, D. Zanchet, J. M. C. Bueno, Surface and structural features of Pt/CeO_2-La_2O_3-Al_2O_3 catalysts for partial oxidation and steam reforming of methane, Appl. Catal. B 107(3-4) (2011) 221-236.
[22] A. D. P. Ferreira, D. Zanchet, J. C. S. Araújo, J. W. C. Liberatori, E. F. Souza-Aguiar, F. B. Noronha, J. C. Bueno, The effects of CeO_2 on the activity and stability of Pt supported catalysts for methane reforming, as addressed by in situ temperature resolved XAFS and TEM analysis, J. Catal. 263(2) (2009) 335-344.
[23] J. C. Araújo, A. L. Pinheiro, A. C. Oliveira, M. G. Cruz, J. M., Bueno, Araujo, R. S., Lang, R. Catalytic assessment of nanostructured Pt/xLa_2O_3-Al_2O_3 oxides for hydrogen production by dry reforming of methane: Effects of the lanthana content on the catalytic activity, Catal. Today 2018.
[24] E. W. Qian, H. Tominaga, T. L. Chen, R. Isoe, Synthesis of functional ionic liquids and their application for the direct saccharification of cellulose, J. Chem. Eng. Jpn. 49(5) (2016) 466-474.
[25] S. Wang, H. Xie, Y. Lin, K. R. Poeppelmeier, T. Li, R. E. Winans, H. Zhang, High thermal stability of La_2O_3-and CeO_2-stabilized tetragonal ZrO_2, Inorg. Chem. 55(5) (2016) 2413-2420.
[26] N. Chen, Y. X. Ren, E. W. Qian, Elucidation of the active phase in PtSn/SAPO-11 for hydrodeoxygenation of methyl palmitate, J. Catal. 334 (2016) 79-88.
[27] D. Liu, G. H. Que, Z. X. Wang, Z. F. Yan, In situ FT-IR study of CO and H_2 adsorption on a Pt/Al_2O_3 catalyst, Catal. Today 68(1-3) (2001) 155-160.
[28] M. Diak, M. Klein, T. Klimczuk, W. Lisowski, H. Remita, A. Zaleska-Medynska, E. Grabowska Photoactivity of decahedral TiO_2 loaded with bimetallic nanoparticles: degradation pathway of phenol-$^{1\text{-}13}C$ and hydroxyl radical

formation, Appl. Catal. B 200 (2017) 56-71.
[29] Y., Jeon, D. H. Park, J. I. Park, S. H. Yoon, I. Mochida, J. H. Choy, Y. G. Shul, Hollow fibers networked with perovskite nanoparticles for H_2 production from heavy oil, Sci. Rep-uk. 3 (2013) 2902.
[30] Y. Yu, S. Qu, D. Zang, L. Wang, H. Wu, Fast synthesis of Pt nanocrystals and Pt/microporous La_2O_3 materials using acoustic levitation, Nanoscale Res. Lett. 13(1) (2018) 50.
[31] T. SHISHIDO, T. TANAKA, H. HATTORI, State of platinum in zirconium oxide promoted by platinum and sulfate ions, J. Catal. 172.1 (1997) 24-33.
[32] K.O. Rocha, J. B. O. Santos, D. Meira, P. S. Pizani, C. M. P. Marques, D. Zanchet, J. M. C. Bueno, Catalytic partial oxidation and steam reforming of methane on La_2O_3–Al_2O_3 supported Pt catalysts as observed by X-ray absorption spectroscopy, Appl. Catal. A 431 (2012) 79–87.
[33] R. El Hage, N. Brosse, P. Sannigrahi, A. Ragauskas, Effects of process severity on the chemical structure of Miscanthus ethanol organosolv lignin, Polym. Degrad. Stab. 95 (2010) 997-1003.
[34] M. V. Galkin, J. S. Samec, Selective route to 2-propenyl aryls directly from wood by a tandem organosolv and palladium-catalysed transfer hydrogenolysis, Chemsuschem 7(8) (2015) 2154-2158.

Chapter 5

General Conclusions

In this study, to obtain high extraction yield of lignin from red pine, different ionic liquids combined with antisolvents system were studied. The extraction yield of lignin was improved and the promising ionic liquid were chosen for the synergistic catalysis of lignin with solid acid catalysts. To further improve the catalytic performance, effects of lanthanum oxide addition to the support on the performance of Pt-La_2O_3-SO_4^{2-}/ZrO_2, where la/Pt atomic ratio was 1, 3, 6, were investigated. The detailed conclusions of this work are summarized as below:

In Chapter 2 to develop a novel process to extract lignin from biomass as the feedstock, the dissolution and extraction of lignin from lignin/cellulose/xylan mixture and red pine were evaluated with different kinds of ionic liquids and antisolvents. Comparing the catalytic activity for lignin depolymerization and the mild modification effect on the structure of alkali lignin among the used ILs, N-allyl-pyridinium chloride ([Apy]Cl) was chosen as the promising ionic liquid, moreover, methanol, water and acetonitrile were chosen as antisolvents. Extraction of lignin from red pine was successfully achieved under atmospheric pressure, with 98.7 wt. % recovery ratio at 90 ℃ for 6 h of dissolution in [Apy]Cl.

In Chapter 3 to evaluate the feasibility of IL-solid acid system, the effect of reaction temperature and the addition of platinum to the ZrO_2/SO_4^{2-} on the yields (carbon-based) of total products and phenolic compounds were studied. The results showed that the optimum reaction temperature was 210 ℃ and [Apy]Cl readily dissolved lignin and served as a medium for lignin depolymerization, which improved the reactivity of lignin. And in the case of Pt-ZrO_2/SO_4^{2-}, the yields (carbon-based) of total products and phenolic compounds reached 44.9 % and 18.7 %, higher than those of ZrO_2/SO_4^{2-}, indicating that the addition of platinum promotes the reactivity.

In Chapter 4 to further improve the catalytic performance, effects of lanthanum oxide addition to the support on the performance of Pt-La_2O_3-SO_4^{2-}/ZrO_2, where La/Pt atomic ratio was 1, 3, 6, were investigated. By adding La_2O_3 the number of Lewis acid sites increased, less Pt oxide species and better Pt dispersion on surface and/or in the mesopores of the support (La_2O_3-SO_4^{2-}/ZrO_2) especially when the La/Pt atomic ratio was 3, which showed the highest the yields of the carbon-based products and phenolic compounds of 63.9 % and 28.7 C, mol %, respectively. Simultaneously, through the study of model compounds and products distribution the depolymerization pathways of lignin in system of ionic liquids and catalysts were proposed.

List of Publications

(1) ***Xiuhui Wang***, Eika W. Qian, Extraction and Modification of Lignin from Red Pine Using Ionic Liquid, Journal of the Japan Petroleum Institute. (In press, Vol. 63 No. 3 (May issue, 2020)) (Chapter 2)

(2) ***Xiuhui Wang***, Ningning Wang, Thanh Tung Nguyen, Eika W. Qian. Catalytic depolymerization of lignin in ionic liquid using a continuous flow fixed-bed reaction system. Industrial & Engineering Chemistry Research, 2018, 57(49), 16995-17002. DOI: org/10.1021/acs.iecr.8b03939. (Chapter 3)

(3) ***Xiuhui Wang***, Yi Luo, Moriko Qian, Eika W. Qian, Catalytic depolymerization of alkali lignin in ionic liquid on Pt-supported La_2O_3-SO_4^{2-}/ZrO_2 catalysts. Sustainable Energy & Fuels. 2020,83, DOI: 10.1039/C9SE00682F. (Chapter 4)

List of Related Publications

(1) Luh Putu Pitrayani Sukma, ***Xiuhui Wang***, Sen Li, Thanh Tung Nguyen, Jianglong Pu, Eika W. Qian. Two-Step Saccharification of Rice Straw Using Solid Acid Catalysts. Industrial & Engineering Chemistry Research, 2019, 58 (14), 5686-5697.

(2) Jianglong Pu, Yi Luo, Ningning Wang, Hongxia Bao, ***Xiuhui Wang***, Eika W. Qian, Ceria-promoted Ni@Al_2O_3 core-shell catalyst for steam reforming of acetic acid with enhanced activity and coke resistance, International Journal of Hydrogen Energy, 2018, 43 (6), 3142-3153.

(3) Eika W. Qian, Hisakazu Shirai, ***Xiuhui Wang***, Kouhei Ota, Kihoon Kim, Nobuo Kasai, Rapid Analysis of Thermal Characteristics and Composition of Lignocellulosic Biomass, Journal of Analytical and Applied Pyrolysis. (**Submitted**).

(4) Hongbo Jiang, ***Xiuhui Wang***, Xiangen Shan, Kejian Li, Xuwen Zhang, Xueping Cao, and Huixin Weng, Isothermal Stage Kinetics of Direct Coal Liquefaction for Shenhua Shendong Bituminous Coal, Energy Fuels, 2015, *29* (11):7526-7531.

(5) Xiangen Shan, ***Xiuhui Wang***, Hongbo Jiang, Huixin Wong, Xuwen Zhang, Kejian Li, Correlation Models of Gas Products in Heating up Stage of Direct Coal Liquefaction Process, Chemical Reaction Engineering and Technology, 2015, 25(4): 123-128.

(6) ***Xiuhui Wang***, Hongbo Jiang, Xiangen Shan, Kejian Li, Xuwen Zhang, Kinetic Model for Isothermal Stage in Short Residence Time of Direct Liquefaction of Shenhua Shangwan Coal, Computers and Applied Chemistry, 2015,28:111-115.

List of Conference Presentations

(1) ***Xiuhui Wang,*** Yuta Yamamoto, Nguyen Thanh Tung, Eika W. Qian. Effect of pretreatment on catalytic depolymerization of lignin in ionic liquid-solvent mixture. The 63rd Lignin symposium. 2018, 11, 1. (oral presentation).

(2) ***Xiuhui Wang,*** Yuta Yamamoto, Eika W. Qian. Catalytic depolymerization of lignin in ionic liquid using a continuous fixed bed reaction system. The 48th petrochemical symposium. 2018, 10, 17. (oral presentation).

(3) Arai Kiyotaka, ***Xiuhui Wang,*** Eika W. Qian. Extraction of lignin in lignocellulosic biomass using ionic liquid. The 47th petrochemical symposium. 2017, 11, 16.

(4) Yuta Yamamoto, ***Xiuhui Wang,*** Segawa Atsushi, Thanh Tung Nguyen, Eika W. Qian. Study on solid acid catalyst for lignin depolymerization in ionic liquid. The 50th society for chemical engineer symposium, 2018, 9, 19.

(5) Yi Luo, ***Xiuhui Wang***, Eika W. Qian, Elucidation of addition effect of Nd_2O_3 to $Ni@Al_2O_3$ core-shell catalyst in steam reforming reaction, The 17th Korea-Japan symposium on catalysis, 2019, 5, 20.

Acknowledgements

The studies presented in this doctoral thesis were conducted at Department of Bio-Functions and Systems Science, Graduate School of Bio-Applications and Systems Engineering, Tokyo University of Agriculture and Technology during 2016~2019. Many thanks to this university where a pretty good research environment provided.

The author expresses his sincerest gratitude to the supervisor of this study, Professor Eika W. Qian, who provides many valuable instructions and suggestions for this research, and also gives the author plenty of knowledge in this field.

The author expresses his appreciation to Dr. Jianglong Pu, who teaches the author how to do a research. The author gives his thanks to Mr. Arai Kiyotaka, Mr. Yuta Yamamoto and all the other collaborators in this study. The author also gives his thanks to all the partners in the group of Professor Qian for their favors.

Finally, the author is pretty grateful for the love, support, and encouragement from his families. The author also expresses his genuine appreciation to Professor Hongbo Jiang, who gives many favors to the author to study in Japan.